ISBN 0-7794-7791-X

THESE TERMS GOVERN YOUR USE OF THIS DOCUMENT

Your use of this Ontario Geological Survey document (the "Content") is governed by the terms set out on this page ("Terms of Use"). By downloading this Content, you (the "User") have accepted, and have agreed to be bound by, the Terms of Use.

Content: This Content is offered by the Province of Ontario's *Ministry of Northern Development and Mines* (MNDM) as a public service, on an "as-is" basis. Recommendations and statements of opinion expressed in the Content are those of the author or authors and are not to be construed as statement of government policy. You are solely responsible for your use of the Content. You should not rely on the Content for legal advice nor as authoritative in your particular circumstances. Users should verify the accuracy and applicability of any Content before acting on it. MNDM does not guarantee, or make any warranty express or implied, that the Content is current, accurate, complete or reliable. MNDM is not responsible for any damage however caused, which results, directly or indirectly, from your use of the Content. MNDM assumes no legal liability or responsibility for the Content whatsoever.

Links to Other Web Sites: This Content may contain links, to Web sites that are not operated by MNDM. Linked Web sites may not be available in French. MNDM neither endorses nor assumes any responsibility for the safety, accuracy or availability of linked Web sites or the information contained on them. The linked Web sites, their operation and content are the responsibility of the person or entity for which they were created or maintained (the "Owner"). Both your use of a linked Web site, and your right to use or reproduce information or materials from a linked Web site, are subject to the terms of use governing that particular Web site. Any comments or inquiries regarding a linked Web site must be directed to its Owner.

Copyright: Canadian and international intellectual property laws protect the Content. Unless otherwise indicated, copyright is held by the Queen's Printer for Ontario.

It is recommended that reference to the Content be made in the following form:

Bateman, R., Ayer, J.A., Dubé, B. and Hamilton, M.A. 2005. The Timmins–Porcupine gold camp, northern Ontario: the anatomy of an Archaean greenstone belt and its gold mineralization: Discover Abitibi Initiative; Ontario Geological Survey, Open File Report 6158, 90p.

Use and Reproduction of Content: The Content may be used and reproduced only in accordance with applicable intellectual property laws. *Non-commercial* use of unsubstantial excerpts of the Content is permitted provided that appropriate credit is given and Crown copyright is acknowledged. Any substantial reproduction of the Content or any *commercial* use of all or part of the Content is prohibited without the prior written permission of MNDM. Substantial reproduction includes the reproduction of any illustration or figure, such as, but not limited to graphs, charts and maps. Commercial use includes commercial distribution of the Content, the reproduction of multiple copies of the Content for any purpose whether or not commercial, use of the Content in commercial publications, and the creation of value-added products using the Content.

Contact:

FOR FURTHER INFORMATION ON	PLEASE CONTACT:	BY TELEPHONE:	BY E-MAIL:
The Reproduction of Content	MNDM Publication Services	Local: (705) 670-5691 Toll Free: 1-888-415-9845, ext. 5691 (inside Canada, United States)	Pubsales@ndm.gov.on.ca
The Purchase of MNDM Publications	MNDM Publication Sales	Local: (705) 670-5691 Toll Free: 1-888-415-9845, ext. 5691 (inside Canada, United States)	Pubsales@ndm.gov.on.ca
Crown Copyright	Queen's Printer	Local: (416) 326-2678 Toll Free: 1-800-668-9938 (inside Canada, United States)	Copyright@gov.on.ca

Ontario

Ontario Geological Survey
Open File Report 6158

The Timmins–Porcupine Gold Camp, Northern Ontario: The Anatomy of an Archaean Greenstone Belt and its Gold Mineralization: Discover Abitibi Initiative

2005

Ontario

ONTARIO GEOLOGICAL SURVEY

Open File Report 6158

The Timmins–Porcupine Gold Camp, Northern Ontario: The Anatomy of an Archaean Greenstone Belt and its Gold Mineralization: Discover Abitibi Initiative

by

R. Bateman, J.A. Ayer, B. Dubé and M.A. Hamilton

2005

Discover Abitibi
A project of innovation, cooperation and revitalization

Découvrons l' Abitibi
Un projet d' innovation, de coopération et de renouvellement

Discover Abitibi Initiative
The Discover Abitibi Initiative is a regional, cluster economic development project based on geoscientific investigations of the western Abitibi greenstone belt. The initiative, centred on the Kirkland Lake and Timmins mining camps, will complete 19 projects developed and directed by the local stakeholders. FedNor, Northern Ontario Heritage Fund Corporation, municipalities and private sector investors have provided the funding for the initiative.

Initiative Découvrons l'Abitibi
L'initiative Découvrons l'Abitibi est un project de développment économique régional dans une grappe d'industries, projet fondé sur des études géoscientifiques de la ceinture de roches vertes de l'Abitibi occidental. Cette initiative, centrée sur les zones minières de Kirkland Lake et de Timmins, mènera à bien 19 projets élaborés et dirigés par des intervenants locaux. FedNor, la Société de gestion du Fonds du patrimoine du Nord de l'Ontario, municipalités et des investisseurs du secteur privé ont fourni les fonds de cette initiative.

FedNor
Canada

Timmins

KIRKLAND LAKE
THE RIGHT ENVIRONMENT

Ontario
Northern Ontario Heritage Fund
Fonds du patrimoine du Nord de l'Ontario

Open File Reports of the Ontario Geological Survey are available for viewing at the Mines Library in Sudbury, at the Mines and Minerals Information Centre in Toronto, and at the regional Mines and Minerals office whose district includes the area covered by the report (see below).

Copies can be purchased at Publication Sales and the office whose district includes the area covered by the report. Although a particular report may not be in stock at locations other than the Publication Sales office in Sudbury, they can generally be obtained within 3 working days. All telephone, fax, mail and e-mail orders should be directed to the Publication Sales office in Sudbury. Use of VISA or MasterCard ensures the fastest possible service. Cheques or money orders should be made payable to the *Minister of Finance.*

Mines and Minerals Information Centre (MMIC) Macdonald Block, Room M2-17 900 Bay St. Toronto, Ontario M7A 1C3	Tel:	(416) 314-3800
Mines Library 933 Ramsey Lake Road, Level A3 Sudbury, Ontario P3E 6B5	Tel:	(705) 670-5615
Publication Sales 933 Ramsey Lake Rd., Level A3 Sudbury, Ontario P3E 6B5	Tel: Fax: E-mail:	(705) 670-5691(local) 1-888-415-9845(toll-free) (705) 670-5770 pubsales@ndm.gov.on.ca

Regional Mines and Minerals Offices:

Kenora - Suite 104, 810 Robertson St., Kenora P9N 4J2

Kirkland Lake - 10 Government Rd. E., Kirkland Lake P2N 1A8

Red Lake - Box 324, Ontario Government Building, Red Lake P0V 2M0

Sault Ste. Marie - 70 Foster Dr., Ste. 200, Sault Ste. Marie P6A 6V8

Southern Ontario - P.O. Bag Service 43, 126 Old Troy Rd., Tweed K0K 3J0

Sudbury - Level B3, 933 Ramsey Lake Rd., Sudbury P3E 6B5

Thunder Bay - Suite B002, 435 James St. S., Thunder Bay P7E 6S7

Timmins - Ontario Government Complex, P.O. Bag 3060, Hwy. 101 East, South Porcupine P0N 1H0

Toronto - MMIC, Macdonald Block, Room M2-17, 900 Bay St., Toronto M7A 1C3

Cette publication est disponible en anglais seulement.

Parts of this report may be quoted if credit is given. It is recommended that reference be made in the following form:

Bateman, R., Ayer, J.A., Dubé, B. and Hamilton, M.A. 2005. The Timmins–Porcupine gold camp, northern Ontario: the anatomy of an Archaean greenstone belt and its gold mineralization: Discover Abitibi Initiative; Ontario Geological Survey, Open File Report 6158, 90p.

Contents

FIGURES

PHOTOS

TABLES

GEOLOGIC MAPS

Abstract

Mapping of foliations in the Timmins–Porcupine gold camp, in the Abitibi greenstone subprovince of northern Ontario, has systematically identified 3 foliations in Tisdale and Porcupine assemblage rocks, 2 of these in younger Timiskaming assemblage sediments, plus 2 minor late crenulations. Previously, a maximum of 2 important foliations had been recognized, both post-Timiskaming. While pre-Timiskaming folding has long been recognized in Tisdale assemblage rocks, no foliations had been attributed to these events. Penetrative foliation in all rocks is still attributed to post-Timiskaming deformation. The new data and interpretations refine the structural history of the gold camp by more precisely defining the generations, timings and effects of deformation phases. Examination of diamond drill core through 3 profiles across the Porcupine–Destor deformation zone has also given new timing and kinematic data.

Initial deformation was a regional uplift-extension event, producing a low-angle unconformity between Tisdale and Porcupine assemblages, with partial excision of upper Tisdale stratigraphy. An early D2 dip-slip, south-over-north thrusting event imbricated a set of south-over-north thrust sheets. These root into the Porcupine–Destor deformation zone. The opening of the Timmins Timiskaming basin is interpreted in terms of syntectonic opening of a transtensional basin in the curvilinear trace of the Porcupine–Destor deformation zone. The Dome fault may represent the normal-faulted margin of a half-graben. D3 folds along the northern flank of the Porcupine–Destor deformation zone can be interpreted as a set of en echelon folds resulting from left-lateral strike-slip movement along this zone continuing from before to after Timiskaming sedimentation. The S4 foliation formed during right-lateral strike-slip movement and folding of S3 foliation. Intense constrictional strain deformed D4 lineations, and may be related to right-lateral movement, making a compressional jog in the trace of the Porcupine–Destor deformation zone of the previously dilatational jog that hosts Timiskaming assemblage sediments. These D3-D4 phases represent an overall transpressional regime.

There were several phases of gold mineralization in the Timmins–Porcupine gold camp. Gold-bearing ankerite clasts in Timiskaming assemblage conglomerate attest to early mineralization. Gold mineralization in early ankerite veins at Dome and McIntyre mines may predate Timiskaming sedimentation. However, the important gold-depositional phases postdate Timiskaming sedimentation, as S2 foliation is overprinted by alteration. S3 foliation crosscuts early ankerite veining and alteration and some quartz veining, as at Vedron. Sequences of quartz-carbonate-tourmaline-gold veins (Hollinger-McIntyre, Hoyle Pond, Dome, Aunor-Delnite mines) also formed within Timiskaming assemblage and adjacent Tisdale assemblage rocks (Hollinger-McIntyre mine). These gold deposits developed largely as oblique-slip and extensional vein arrays formed during north-south shortening and local strike-slip faulting. Younger deposits (Pamour mine) formed with dip-slip faulting, and are weakly deformed in late D4. They have all been post-dated by constrictional strain and minor veining that was probably not associated with much additional gold.

A protracted history of orogenesis and gold mineralization demonstrates a long-lived or multi-phase gold-bearing hydrothermal system, and indicates a plumbing system geometrically stable enough, and for long enough, to feed gold into a relatively small volume throughout a period of transpressional deformation. This work also suggests that Timiskaming assemblage sediments may be more widespread than previously believed, and so the area of interest for exploration expands into areas previously not considered very prospective.

The Timmins–Porcupine Gold Camp, Northern Ontario: The Anatomy of an Archaean Greenstone Belt and its Gold Mineralization: Discover Abitibi Initiative

R. Bateman[1], J.A. Ayer[2], B. Dubé[3] and M.A. Hamilton[4]
Laurentian University, Sudbury, Ontario
Open File Report 6158

2005

[1]Post-doctoral fellow, Mineral Exploration Research Centre, Department of Earth Sciences, Laurentian University, Willett Green Miller Centre, 933 Ramsey Lake Rd., Sudbury, Ontario, P3E 6B5, Canada
rbateman@laurentian.ca

[2]Ontario Geological Survey, Precambrian Geoscience Section, Willett Green Miller Centre, 933 Ramsey Lake Rd., Sudbury, Ontario, P3E 6B5, Canada
john.ayer@ndm.gov.on.ca

[3]Geological Survey of Canada Quebec, 880 Chemin Sainte-Foy, C.P. 7500, Sainte-Foy, Quebec, G1V 4C7, Canada
bdube@nrcan.gc.ca

[4]Jack Satterley Geochronology Laboratory, University of Toronto, Toronto, Ontario, M5S 3BI, Canada
mahamilton@geology.utoronto.ca

Introduction

The Timmins–Porcupine gold camp of northern Ontario is one of the most important gold camps hosted in Archaean greenstone belts in the world, together with Kalgoorlie (southwestern Australia). The Timmins–Kirkland Lake region of the Abitibi greenstone belt also contains major Cu-Zn and Ni-Cu-PGE mineralization. Most of these deposits were found by prospecting or investigating near-surface geophysical anomalies. Although data on the geology of the Abitibi greenstone belt is good at the mine and regional scales, the understanding of the geology at the sub-regional and district scales is less clear, because of complex stratigraphic variations and complex metamorphic and structural overprints.

The next generation of deposits may be found beneath the extensive overburden that covers much of the Abitibi greenstone belt. Thus, future exploration will require more detailed understanding of the geological characteristics of the existing deposits, the stratigraphic and structural architecture of the region, and will rely on geophysical and geochemical techniques, tested by diamond drilling. The Greenstone Architecture Project was one of 19 projects of the Discover Abitibi Initiative, managed by the Timmins Economic Development Corporation. The project was focussed on improving knowledge of the stratigraphy, volcanology, geochemistry, metamorphic petrology, and structural geology of selected mineralized and barren areas. The objective was to better understand the geological architecture of the belt, to increase knowledge of the complex interactions of stratigraphic, lithological, structural, alteration, geochemical, and metamorphic controls on the localization and genesis of Cu-Zn, Ni-Cu-PGE and Au deposits, and to aid in the development of new concepts for discovering deposits. This contribution presents results of Discover Abitibi Initiative research in the Timmins–Porcupine gold camp, and has focussed on transects through the Pamour-Hoyle Pond and Dome-Buffalo, Ankerite-Hollinger-McIntyre mines areas. This work around Timmins has been greatly aided by cooperation with the Porcupine Joint Venture, which manages current mining operations at the Hoyle Pond, Dome and Pamour mines in the Timmins area. The Porcupine Joint Venture has provided a wide variety of confidential data that has been used in this project. Some interpretations presented here are partly based on data, confidential to the corporate owners of the data, which themselves cannot be reported.

The first geological report preceded discovery (Parks 1900). Gold was discovered in 1909 by J.S. Wilson (Dome mine) and B. Hollinger and A. Gillies (Hollinger mine). Dome mine has been one of the largest producers in this camp, and has been in continuous production since the earliest days. The earliest reports and maps were published at this time (Burrows 1911, 1912, 1915, 1924). Early work was consolidated in a benchmark report (Ferguson et al. 1968). Since then, a great diversity of research projects have been carried out on the Timmins camp, making this one of the best-studied gold camps and the largest Archaean greenstone deposit in the Canadian Superior Province.

General Geology of the Abitibi Subprovince

The Timmins–Porcupine gold camp lies within the Abitibi Subprovince (Figure 1), Superior Archaean craton of eastern Canada. A particularly important recent contribution (Ayer et al. 2002) to Abitibi tectonics and consequently Timmins stratigraphy describes the stratigraphic constitution of the southern Abitibi Subprovince in terms of autochthonous volcanic construction comprising 9 supracrustal assemblages, rather than an amalgamation of numerous allochthonous terranes (Dimroth et al. 1983; Jackson 1994; Daigneault, Mueller and Chown 2002). In this autochthonous model, there is a repetition of similar volcano-sedimentary successions throughout the Abitibi and spanning 75 Ma (2750-2675 Ma). Each assemblage is laterally extensive, stacked, with conformable, unconformable or disconformable

contacts (Figures 1, 2). The Timmins–Porcupine gold camp lies on the northern flank of the Porcupine–Destor deformation zone (Figure 1). This deformation zone, and the Larder Lake–Cadillac deformation zone, are the most important deformation zones within the Abitibi Subprovince in terms of both structural effect and gold production.

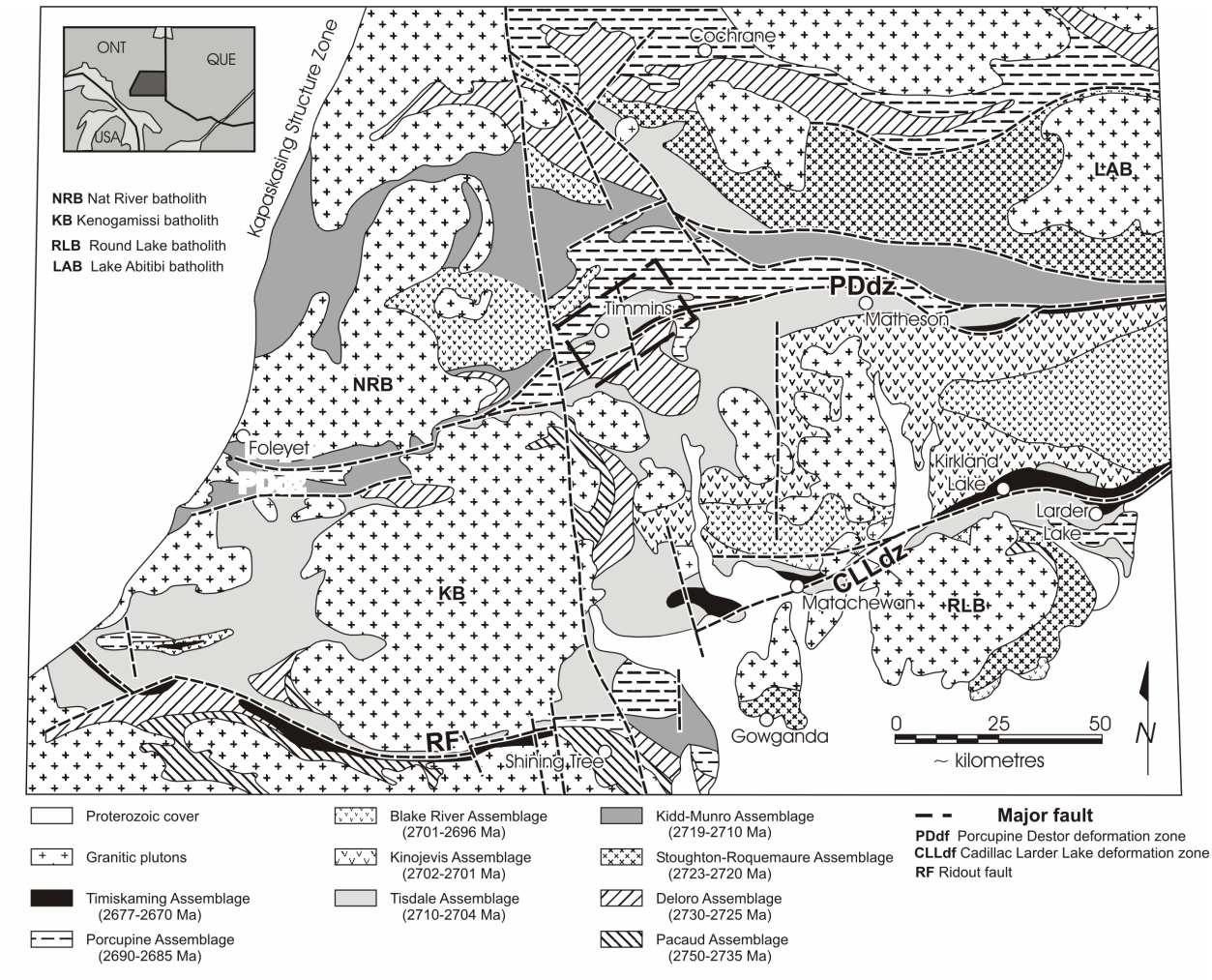

Figure 1. Map of the Abitibi Subprovince showing the distribution of assemblages (Ayer et al. 2002). The box around Timmins shows this study's field area.

TIMMINS AREA LITHOLOGY, STRATIGRAPHY AND GEOCHRONOLOGY

A variety of division names have been used for the supracrustal assemblages of the Timmins district (Figures 1, 3), but the scheme of lithologies and geochronological data used here (Ayer et al. 2002; Ayer, Ketchum and Trowell 2002; Ayer et al. 2003) is summarized in Table 1, together with the subdivisions of the Timiskaming and Porcupine assemblages (Born 1995) and the Tisdale assemblage (Mason and Melnik 1986).

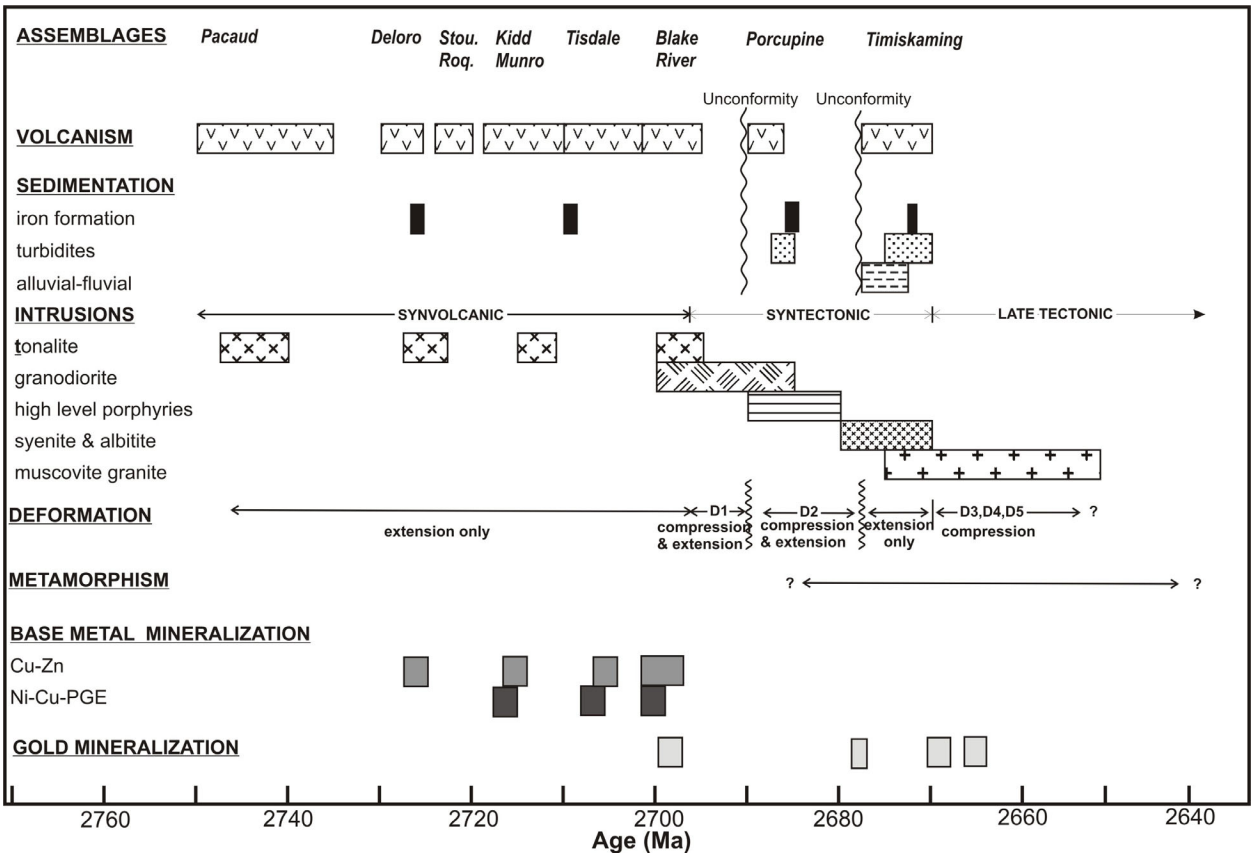

Figure 2. Timeline for the evolution of southern Abitibi greenstone belt including the volcanic and sedimentary assemblages, intrusions, deformation, metamorphism and mineralization episodes. Geochronological data are from several sources (Ayer, Trowell and Josey 2004; Corfu 1993; Mortensen 1993; Powell, Carmichael and Hodgson 1995; Bleeker, Parrish and Sager-Kinsman 1999; Davis et al. 2000; Heather 2001; Ayer et al. 2002; Ayer, Ketchum and Trowell 2002; Ayer et al. 2003; Dubé et al. 2004; Ayer et al. 2005).

Table 1. Tectonostratigraphic, lithological and geochronological summary for rocks of the Timmins gold camp.

Assemblage	Formation	Flow	Lithology
	Dykes		Pamour porphyry 2677±1 Ma; albitites 2673±6/-2 Ma and 2676±2 Ma (Corfu et al. 1989; Ayer et al. 2005)
Albitites cut quartz-feldspar porphyries (Mason and Melnik 1986) and Timiskaming assemblage (Ayer et al. 2005)			
Timiskaming	Three Nations		Interbedded sandstone, pebbly sandstone, conglomerate, shale; 2669±1 Ma (Bleeker, Parrish and Sager-Kinsman 1999)
	Dome		Greywacke, sandstone, conglomerate Post 2679 Ma (Ayer et al. 2003)
angular unconformity			
Porcupine	Beatty		Sandstone, greywacke, shale
	Krist		Felsic volcaniclastic breccia, heterolithic tuff, shale ~2690 Ma (Bleeker 1999; Ayer et al. 2003; Bateman et al. 2004)
	graphitic phyllite		Carbonaceous shale, typically well deformed
disconformity (and shear zone?)			
	Dykes		Quartz-feldspar porphyries ~2690 Ma (Corfu et al. 1989)
intrusive into Tisdale Formation, not known within Porcupine or Timiskaming at Timmins			
Tisdale	Gold Centre	V11	Massive and pillowed lava
	Vipond	V10	Massive and variolitic lavas
		V9	Carbonaceous shale
		V8	Variolitic and pillowed lavas
		V7	Carbonaceous shale
		99	Massive lava, ankerite-sericite alteration 2707±3 Ma (Ayer et al. 2002)
	Central	C17	Carbonaceous shale
		C16	Amygdaloidal lava
		C15	Pillow lava, flow breccia
		C14	Massive lava
		C12	Variolitic lava
		55	Massive lava
		95	Massive, amygdaloidal, variolitic, pillowed, hyaloclastic lavas, carbonaceous shale
	Northern	63	Massive, amygdaloidal, polygonal jointed lava, carbonaceous shale
		51	Massive, amygdaloidal lava
	Hersey Lake		Mafic and komatiitic lavas
unconformable contact (Ayer et al. 2004) and Porcupine–Destor deformation zone			
Deloro 2724 - 2730 Ma (Ayer et al. 2002)			Mafic and ultramafic lavas
			Iron formation
			Felsic volcanics and volcaniclastic rocks
disconformity (Ayer et al. 2002)			

A detailed report of the geochronological work done for the Greenstone Architecture Project is reported elsewhere (Ayer et al. 2005), but a summary of the new results on samples from the Timmins area are reported below. The oldest assemblage within the camp is the Deloro assemblage. It consists predominantly of pillowed calc-alkaline mafic volcanic rocks with lesser amounts of intermediate to felsic volcanics and iron formations. It occurs within the central part of the Shaw antiformal structure, south of the Porcupine–Destor deformation zone (Figure 3). A new geochronological sample from felsic volcanics immediately underlying the iron formations in northeastern Shaw Township have yielded zircons with an age of 2727 Ma confirming the presence of the Deloro assemblage in this area (Ayer et al. 2005). Geochronological analysis was carried out on a felsic volcanic sample intercalated with komatiites south of the Porcupine–Destor deformation zone (PDDZ) in Deloro Township (Figure 3, location 1). From this sample, data for 5 single-grain zircon fractions regress to yield an upper intercept age of

2724.1 ± 3.7 Ma (this and all following age errors quoted at 2σ level of uncertainty). Although this result is consistent with a Deloro age, the sample also contains a subpopulation of less well preserved rounded and pitted zircons (as yet unanalysed), suggesting sedimentary recycling or transport. This indicates that the sample is likely epiclastic and may be part of the Deloro tectonically interleaved with Tisdale assemblage komatiites, or be part of the Tisdale assemblage with the above analysed zircons possibly being xenocrysts derived from either erosion or entrainment of underlying Deloro assemblage material.

The Tisdale assemblage overlies the Deloro assemblage with a disconformity which may locally be an angular unconformity (Ayer et al. 2004). It occurs around the margin of the Shaw antiformal structure and north of the PDDZ, where the lowermost horizon of the Tisdale assemblage consists of komatiites and basaltic komatiites of the Hersey Lake formation (~600 m thick). These are dark green to black rocks in flows 1-4 m thick, massive, with chilled margins, spinifex textures in upper parts, and common polysuturing. They comprise serpentine, tremolite, chlorite, talc, carbonate, and some relict olivine, plus chromite and magnetite. Tisdale komatiites are mostly Al-undepleted komatiites derived late in an evolving mantle plume, with minor crustal contamination (Lahaye et al. 2001; Sproule et al. 2002). The upper Tisdale assemblage consists of the Central formation (450 m thick), the Vipond formation (200-300 m) and the Gold Centre formation (800 m). These formations are comprised of a variety of essentially tholeiitic lavas together with subordinate ultramafic lavas, and minor carbonaceous shale interflow sediments. Basalts are variously pillowed (1-2<5 m), massive or hyaloclastic in flows 10-150 m thick. Petrographically, they consist of actinolite-tremolite, plagioclase, trace quartz, and titanite. The more Fe-rich tholeiites are darker in colour, contain magnetite and more pleochroic actinolite and higher contents of quartz. Some Vipond formation Fe-rich lavas are very distinctive in their intensely variolitic texture (<3cm), and these serve as marker horizons, and are a feature of well-mineralized rocks (Jones 1992). Tisdale lavas are similar in Th-Nb-LREE to ocean plateau or ocean island basalts erupted above a plume in a subduction zone (Kerrich, Polat et al. 1999). Crustal contamination of these rocks has been ruled out by some workers (Fan and Kerrich 1997; Kerrich, Wyman et al. 1999; Ayer et al. 2003). Published geochronology from the Tisdale has given an age of 2707 ± 3 Ma from the 99 Flow of the Vipond formation west of the Dome mine in Tisdale Township, and an age of 2708 ± 2 Ma from the southeastern margin of the Shaw antiformal structure in Langmuir Township (Ayer et al. 2002).

The base of the Porcupine assemblage varies from disconformable to an angular disconformity (Buffam 1948). At the base is a discontinuous horizon of carbonaceous sedimentary rocks (up to 100 m), separating the underlying Tisdale assemblage mafic lavas from the Krist formation. The Krist formation is a calc-alkaline pyroclastic deposit, locally up to 500 m in thickness, with an age ranging from 2690 to 2688 Ma (Ayer, Ketchum and Trowell 2002; Ayer et al. 2003). It is poorly sorted and bedded, with angular clasts of 1 to 25 cm across, consisting of feldspar (± sparse quartz)-phyric rhyodacite, chert, and minor but ubiquitous fuchsite-bearing chips of ultramafic rock. The fine-grained matrix to the clasts is also feldspar-bearing. Greywackes, siltstone and mudstone (~1000 m) overlie the Krist pyroclastic formation, in places unconformably (Ferguson et al. 1968). Elsewhere the Krist formation is absent and the greywackes of the Beatty formation (Porcupine assemblage) directly overlie Tisdale assemblage lavas with an unconformable or faulted contact. The sediments are fine- to medium-grained, well-bedded or laminated arkosic-lithic turbidites with scour and flute marks and crossbedding. Lithic fragments are principally volcanics in an extremely fine-grained quartz-feldspar-sericite matrix.

The Hoyle formation is an extensive part of the Porcupine assemblage lying to the east, north and west of the Timmins camp (see Figure 1). The youngest zircon derived from volcaniclastic arenites within the Hoyle formation south of the Kidd Creek mine provides a maximum age for deposition of 2684.7 ± 6.3 Ma (Bleeker, Parrish and Sager-Kinsman 1999). Analysis of detrital zircons from sandstones in Mountjoy Township (Figure 3, location 2) yielded ages ranging from about 2705 Ma to 2691.3 ± 1.5 Ma, the latter indicating a maximum depositional age of the unit (Bleeker 1999). A third Hoyle formation sandstone sample was collected from diamond drill core intersecting the septum of Porcupine

sedimentary rocks northeast of the McIntyre mine in central Tisdale Township (Figure 3, location 3). Four single zircon grains have been analyzed - 2 were large, slightly elongate colourless subhedral prisms, which gave concordant ages at 2690.9 ± 2.5 and 2699.4 ± 3.8 Ma. One was a smaller brown prism that is slightly discordant (0.8%) at 2692.3 ± 1.4 Ma, while the fourth was a small elongate prism or needle, concordant at 2695.8 ± 2.8 Ma. Hence, the maximum age of deposition for this sample is constrained to be <2690.9 ± 2.5 Ma. A fourth Hoyle formation sandstone sample was collected from diamond drill core in Hoyle Township (Figure 3, location 4). This sample yielded detrital zircons ID-TIMS (isotope dilution-thermal ionization mass spectrometry) ages of ca. 2725 Ma, 2713 Ma, 2711 Ma, 2704 Ma, 2690.4 Ma, and 2688.2 Ma. SHRIMP (sensitive high-resolution ion microprobe) data on a larger group of detrital zircons from the same sample indicate an older grain at ca. 2756 Ma but with the bulk of the zircon detritus having ages clustering near 2690 Ma.

The Beatty formation is located in the core of the Porcupine syncline. A sample of Beatty formation sandstone immediately underlying the Timiskaming angular unconformity in Tisdale Township (Figure 3, location 5) contains detrital zircons with ID-TIMS ages of ca. 2726 Ma, 2720 Ma, 2708 Ma, 2692 Ma, and 2687 Ma. By comparison, SHRIMP data on a larger group of detrital grains from this sample indicate zircon ages ranging from about 2760 Ma to 2680 Ma, with the bulk of the youngest zircon detritus ages clustering near 2690 Ma. The combined geochronological data from the Porcupine sandstone samples indicates that the Hoyle and Beatty formations are correlative and that detritus constituting these sedimentary units was derived from a source region (or regions) of diverse ages, and included material derived from all older Abitibi assemblages and/or their intrusive equivalents. The results thus confirm a period of significant uplift, erosion and unconformity occurred leading up to deposition of the Porcupine assemblage (see Figure 2).

Overlying the Porcupine assemblage with angular unconformity (Ferguson et al. 1968) is the Timiskaming assemblage (~ 900 m thick). In the Dome formation, basal conglomerate of up to 50 m contains abundant angular mafic and ultramafic rock clasts, among other rock types, from the underlying Tisdale rocks. The Dome formation contains 2 other cobble conglomerate horizons. Greywacke consist of alternating shale (5-20 cm) and sandstone (10-50 cm). P. Born (Ayer et al. 1999) interprets the lower Dome formation as a sequence of turbiditic fan sediments. Two samples from the Dome formation at the Dome mine were analysed using the ID-TIMS method (Ayer et al. 2003): wacke from the basal part of the Dome formation in the Greenstone Nose (Figure 3, location 6) contains detrital zircons with ages ranging from 2710 Ma to 2679 ± 4 Ma, whereas conglomerate in the “sedimentary trough” yielded a broader spectrum of detrital zircon ages ranging from 2814 Ma to 2674 ± 2 Ma. Less precise but more comprehensive SHRIMP results from these 2 samples reveal bimodal age distributions with a significant pre-Abitibi population ranging in age from 2820 to 2780 Ma and an Abitibi-aged population ranging from 2730 Ma to approximately 2660 Ma.

Stratigraphically overlying the Dome formation, the Three Nations formation consist of quartz-lithic sandstones, with angular grains, in festoon-crossbedded beds on the scale of 25-100 cm. Conglomerate beds contain rounded clasts (1 to 25 cm) of siltstone, felsic volcanics, ultramafic rock, and vein quartz. The Three Nations formation is interpreted as deltaic-fluvial deposits (Ayer et al. 1999) with mixed felsic-lesser mafic provenance (Feng and Kerrich 1990). Detrital zircons from the upper part of the Three Nations formation provide a maximum depositional age of 2669 Ma (Bleeker, Parrish and Sager-Kinsman 1999; Ayer et al. 2003). As-yet unassigned Timiskaming assemblage-aged sedimentary units with maximum depositional ages of 2674 Ma occur as tectonically interleaved slivers within Tisdale assemblage volcanics proximal to the Porcupine–Destor deformation zone at the Buffalo Ankerite and Naybob mines (Ayer et al. 2003). In addition, recent diamond drilling by the Porcupine Joint Venture has indicated the presence of more extensive Timiskaming assemblage units further to the west in Ogden Township consisting of jasper-bearing conglomerate, sandstone and siltstone in faulted contact with ultramafic volcanics to the south.

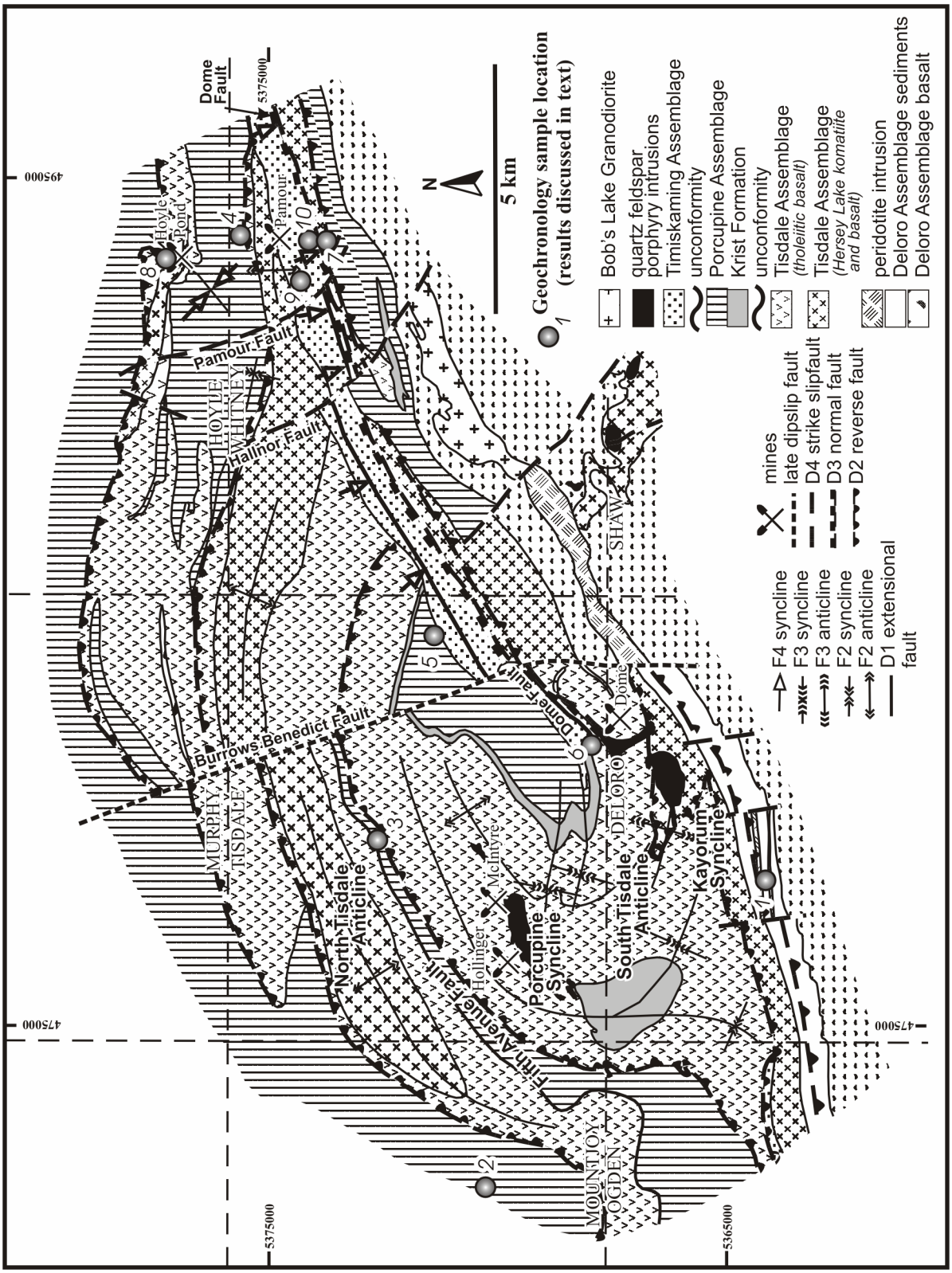

Figure 3. A generalized map of the Timmins–Porcupine gold camp, covering Tisdale, Deloro, Mountjoy, Ogden, Whitney and Hoyle townships. Location of cross-sections in Figures 13, 14, 24 are shown as straight broken lines. This map is a summary of the 2 maps in the back pocket of this report, geochronology and previous work (Carlson 1967; Ferguson et al. 1968; Piroschco and Kettles 1991; Brisbin 1997; Berger 1998; Hall and Smith 2002).

Timiskaming-aged units also occur south of where they have been previously indicated in Whitney Township. For example, a sample of sandstone interbedded with conglomerate from a unit previously considered to be part of the Porcupine assemblage (Figure 3, location 7) contains detrital zircons with ID-TIMS ages of 2726 Ma, 2723 Ma, 2692 Ma, 2689.9 ± 1.2 Ma and 2690 Ma. SHRIMP data from a larger population of detrital zircons from the same sample show that the zircons define a spectrum of ages between approximately 2750 and 2670 Ma. The younger ages indicate that the unit is likely part of the Timiskaming assemblage and thus extends the known distribution of this assemblage further to the south in Whitney Township.

Porphyry stocks (up to 1200 by 400 m) and dyke swarms intrude the Tisdale assemblage lavas, but are not known to intrude Porcupine or Timiskaming assemblage sediments (Holmes 1944; Brisbin 1997; Bateman et al. 2004): dykes are truncated at the Timiskaming unconformity surface; porphyry clasts occur in the overlying conglomerates; and so these porphyry bodies are typically older (2691-2687 Ma) than the ages given for the overlying sediments. The porphyries consist of plagioclase (30-60%, 1-5 mm) and quartz (5%, 1-5 mm) phenocrysts in a fine groundmass of feldspar and quartz with sericite and chlorite in foliation, plus carbonate, leucoxene, apatite and actinolite (Pyke 1982). Geochemically, the porphyries are identical to the Krist pyroclastics (unpublished Porcupine Joint Venture data). Geochronological work was carried out on 2 felsic units found within the south volcanic package at the Hoyle Pond mine (Figure 3, location 8): a quartz porphyritic sericite schist and a quartz-albite porphyry (QFP) (Dinel and Fowler 2004). In contrast to the quartz feldspar porphyries, the quartz porphyritic sericite schist is strongly foliated and sericitized and appears to be conformable with the adjacent mafic and ultramafic volcanic units over 200 m (horizontal and vertical). Because of its conformable relationship and embayed quartz phenocrysts, a dissolution texture common in volcanic rocks, the unit was sampled to attempt to date the Tisdale stratigraphy in the mine area. Four single-grain zircon analyses from this unit define a primary age of crystallization of 2687.6 ± 2.2 Ma. This age is within error of most of the other porphyry intrusion ages in the Timmins camp (MacDonald, Piercey and Hamilton 2005). On the basis of this new geochronological data, the unit is best interpreted as a quartz porphyritic intrusion emplaced into the Tisdale assemblage volcanic units. The other quartz-feldspar porphyry is trachytic in texture, composed of quartz and albite phenocrysts with a preferential alignment in a groundmass of microlites. The dominant tectonic fabric is S2 and it appears to have been intruded into a dilation zone during D2 (E. Dinel, personal communication, 2004). The best age estimate for this porphyry is provided by 3 concordant and near-concordant single-zircon analyses, which yield a weighted mean age of 2684.4 ± 1.9 Ma. Minor inheritance is indicated at about 2695 Ma. The crystallization age of the quartz-feldspar porphyry is slightly younger than, but within the error of, most of the early porphyries in the Timmins gold camp (MacDonald, Piercey and Hamilton 2005), which suggests that its age of emplacement may in fact provide an absolute constraint on the timing of D2, which is considered to be pre-Timiskaming assemblage (see “Metamorphism, Structure, Tectonics” section, below).

The Pamour porphyry is a recently recognized intrusion southwest of Pamour mine. The intrusion is not exposed at surface, but recent diamond drilling by the Porcupine Joint Venture indicate it is an elongate body up to several hundred metres in length (MacDonald, Piercey and Hamilton 2005). It consists of 1-5 mm quartz-feldspar porphyritic crystals, with accessory biotite-chlorite-pyrite. Clots of mafic minerals occur, up to 1 cm long. It truncates foliation in the host ultramafic rocks of the Porcupine–Destor deformation zone. The foliation in the porphyry is defined by flakes of mafic minerals, by foliation within the clots, and by the shape orientation of the clots. This foliation lies at an angle to that in the host rocks, and may be an igneous foliation. These relationships also suggest that foliation development postdates major movement (D2 – see below) on the Porcupine–Destor deformation zone. Conventional ID-TIMS zircon dating of the Pamour porphyry is complicated by the combined effects of inheritance and Pb-loss. At present, the best constraint on the age of intrusion is provided by a near-concordant, single grain analysis at 2677.5 ± 2.0 Ma. Additional zircon analyses at 2690 Ma and 2703 Ma clearly define xenocryst ages. The age of intrusion is apparently younger than most other porphyries in the camp (see above) and its age constrains D2 as occurring before this time.

Albitite dykes (Ferguson et al. 1968), up to maximum dimensions of 5 x 1000 m, are known from underground at the Hollinger and McIntyre mines. The dykes consist largely of feldspar, with very minor quartz, biotite/chlorite, plus sericite, carbonate, amphiboles, tourmaline and epidote. Albitite dykes are crosscut by gold-bearing veins and alteration in Hollinger-McIntyre mine (Burrows et al. 1993). Zircons from this dyke yielded an age of 2673 +6/-2 Ma (Corfu et al. 1989). Three additional single-grain fractions were analysed from this sample (SM85-60**)** to better constrain its age. One shows definite signs of inheritance with a Pb^{207}/Pb^{206} age of 2694.4 ± 1.8 Ma; however two others are concordant and overlapping and alone would suggest an age of 2672.7 ± 1.2 Ma. These points are identical to the most precise earlier analyses, which all together give an age of 2672.8 ± 1.1 Ma. This dyke age gives a maximum age for vein quartz gold mineralization at the Hollinger-McIntyre mines. Albitite dykes were also observed in diamond drill core intruding the Timiskaming assemblage conglomerates and ultramafic volcanic rocks proximal to the Porcupine–Destor deformation zone in Whitney township (E. Barr, personal communication, 2004). An 8 m wide dyke cutting ultramafic volcanics in this area (Figure 3, location 9) was sampled for precise U-Pb geochronology. Four abraded zircon fractions from this transgressive unit yield a tightly collinear regression with a concordia upper intercept age of 2677.0 ± 2.2 Ma, interpreted to represent the primary age of crystallization of the albitite dyke. This age is within error of the McIntyre albitite dyke and the Pamour porphyry, indicating that post D2 magmatism is more widespread in the Timmins camp than was previously recognized.

TTG (trondhjemite-tonalite-granodiorite) granitoid plutonism, in particular tonalite, in the Abitibi Subprovince is associated with all mafic-ultramafic volcanic episodes and with all deformation periods (Chown, Harrap and Mouksil 2002). Granitoids are closely related to felsic volcanism, and may form subvolcanic complexes. Chown, Harrap and Mouksil (2002) related this granitoid plutonism to extensional phases of subduction- and plume-related tectonics. The Kenogamissi Batholith lies southwest of the camp (see Figure 1) and is a multiphased body consisting of foliated to gneissic synvolcanic hornblende- and biotite-tonalite ranging in age from 2745 to 2713 Ma, moderately to weakly foliated syntectonic biotite- and hornblende-granodiorite and hornblende-diorite ranging from 2700 to 2680 Ma, and massive biotite-granite with an age of ca. 2670 Ma (Heather and van Breeman 1994; Bleeker, Parrish and Sager-Kinsman 1999; Becker and Benn 2003). The Adams pluton (Pyke 1982) consists of weakly foliated granodiorite with an age of 2685 ± 3 Ma intruded into Tisdale assemblage rocks southwest of the Shaw antiform. Bob's Lake granodiorite is a fine- to medium-grained, locally foliated pink to light grey granodiorite.

Post-Archaean rocks in the Timmins area include the Proterozoic diabase dyke suites. The Matachewan dykes strike north-northwest, the Abitibi dyke set strikes east-northeast, and other strike sets are discussed in some detail elsewhere (Pyke 1982). The north or north-northwest dykes consist of quartz- and olivine-bearing variants with plagioclase phenocrysts, dated at 2454 ± 2 Ma (Heaman 1988). The east-northeast Abitibi set consist of 2 large olivine diabase dykes dated at 1140.6 ± 2 Ma (Krogh et al. 1987): these are very similar to another set of less common northwest-trending dykes.

METAMORPHISM, STRUCTURE, TECTONICS

Metamorphism is recorded in all Archaean rocks, and reached lower to middle greenschist grade (only local biotite) in the Timmins area (Thompson 2003). Occurrences of biotite may be attributable to contact metamorphism around porphyry intrusions and/or to potassic metasomatism associated with gold mineralization. An estimate of the age of metamorphism is between 2677 and 2643 Ma, based on overprinting relationships (Powell, Carmichael and Hodgson 1995). Much younger ages (Powell et al. 1995) of 2421, 2543 and 2578 Ma suggest multiple and very young metamorphic events. While the multiple foliations recorded in the Timmins area (described and discussed below) require multiple episodes of metamorphism, sufficient data to date have not been acquired to allow assignment of different

grades to different structural/foliation/mineral growth stages and hence to define a P-T trend through a significant period of time. Pressures of metamorphism of ~200 MPa measured on both sides of the Porcupine–Destor deformation zone (Powell, Carmichael and Hodgson 1995) set a limit to vertical offset along this shear zone.

Deformation history in the Abitibi Subprovince and the Timmins area specifically remains a subject for controversy. Regional deformation episodes have been identified based on overprinting relationships of folds and faults with the earliest compressional regime constrained by cessation of Blake River assemblage volcanism at 2696 Ma and onset of the deposition of the Porcupine assemblage at 2690 Ma, synchronous with emplacement of a suite of syn-tectonic granitic plutons (Corfu 1993; Bleeker 1999; Heather 2001; Ayer et al. 2002). These early folds are commonly refolded and transposed by later deformation events and it is therefore often difficult to determine their original orientation. A series of folds and 1 or 2 foliations have been identified (Ferguson et al. 1968; Piroschco and Kettles 1991). The Porcupine syncline (traditionally no related foliation) has been recognized as being early, predating both the Timiskaming unconformity and the foliations in Timiskaming assemblage rocks (Burrows 1915; Hodgson 1983). Folds predating the Porcupine syncline, also traditionally with no foliation, are implied (Hodgson 1983; Piroschco and Kettles 1991), but not discussed in unambiguous terms. These 2 early fold sets dominate the map-scale geometries of the Timmins area. Two foliations have been noted (Brisbin 1997) but they are not attributed to distinct fold sets. In addition to the foliations, an extremely strong lineation (extreme prolate strain in pillow lavas and vesicles, in Krist clasts, and in Timiskaming pebbles) plunges moderately to the east. This is best developed in the western half of the area, along the north side Porcupine–Destor deformation zone. The Dome fault cuts the southern margin of the Timiskaming assemblage trough. Late northwest (right lateral) and northeast (left lateral) trending faults crosscut the sequence and all folds and foliations and earlier faults. It has been proposed that the presence of auriferous clasts within the basal Timiskaming conglomerate proves the existence of pre-Timiskaming gold concentrations (Gray and Hutchinson 2001), whereas others have proposed a magmatic hydrothermal intrusion-related model for gold mineralization in the Timmins district (Mason and Melnik 1986; Brisbin 1997). However, overall, mineralization has generally been recognized as occurring late in this history (Hodgson 1983; Hodgson, Hamilton and Piroschco 1990; Piroschco and Kettles 1991; Robert and Poulsen 1997).

Movement along the Porcupine–Destor deformation zone within the Duparquet Basin (Québec) is constrained to 2700-2680 Ma (Mueller et al. 1996), with a change at 2690 Ma (about Porcupine assemblage age) from thrusting to right-lateral transpression. Thrusting was along a shallowly north-dipping zone (Hodgson 1983; Calvert and Ludden 1999; Daigneault, Mueller and Chown 2002). Left-lateral strike-slip motion has also been described (Hodgson 1983). These structural histories are broadly similar in kinematics. Along the Larder Lake–Cadillac deformation zone (see Figure 3), deformation started with coaxial shortening with south-over-north thrusting on a south-dipping (Wilkinson, Cruden and Krogh 1999), or north-over-south movement on a north-dipping (Wilkinson, Cruden and Krogh 1999; Neumayr, Hagemann and Couture 2000) surface. Dip-slip movement is followed by left- and then right-lateral non-coaxial strain, and ages for strike-slip movement along the Larder Lake–Cadillac deformation zone – post-2675 Ma and post-2669 Ma, respectively (Wilkinson, Cruden and Krogh 1999) – are younger than those for the Porcupine–Destor deformation zone. In the Timmins area, the abundance of higher stratigraphic units in the northern block suggests south block up. In detail, the Porcupine–Destor deformation zone has not been adequately identified, located, defined or described in the Timmins camp. Past work has not described any strain gradient across this zone, and in fact the most obvious gradient is *along* strike.

Tectonically, discussion has been dominated by the “oceanic island arc subduction zone” model (Jackson and Fyon 1991; Kerrich, Wyman et al. 1999; Wyman and Kerrich 2002; Ayer et al. 2002; Wyman, Kerrich and Polat 2002). This depends on the presence of oceanic crust beneath the mafic

volcanic centres. In contrast, juvenile crustal material detected in geochemical and geochronological studies (Lahaye et al. 2001; Thurston 2002; Sproule et al. 2002) and seismic data (Calvert and Ludden 1999) indicates a continental substrate to some of these volcanics, and hence gives strong support to the model of (para)autochthonous terrane development (Thurston 2002; Ayer et al. 2002).

GOLD MINERALIZATION IN THE TIMMINS–PORCUPINE CAMP

Two recent reviews have given good overviews of gold mineralization in the Abitibi Subprovince (Robert and Poulsen 1997; Hagemann and Cassidy 2000). The Timmins–Porcupine gold camp is one of the great gold camps of the world, with total historic plus modern production and resources totalling 2350 tonnes of gold (Rhys 2003). In addition to the major mines (Dome, Pamour and Hollinger-McIntyre), there are numerous other deposits over 35 km of strike including Hoyle Pond and Aunor-Delnite mines, which have produced nearly 140 tonnes or 4.5 M oz of gold (Rhys 2003). Geologically, the gold deposits of the Timmins camp can be divided into several categories according to relationships between vein parageneses, metal inventory, proximity to the Porcupine–Destor deformation zone, host rock (Timiskaming sediments, Tisdale basalts, felsic porphyry intrusive stocks), geometry and kinematics of vein opening, and chronology of the mineralization relative to the different phases or increments of deformations.

The McIntyre Cu-Au-Ag-Mo porphyry-style ore body hosted by the Pearl Lake porphyry at depth in the McIntyre mine, and the entire Hollinger-McIntyre deposit, have been interpreted as a porphyry-type hydrothermal system with a porphyry Cu-Mo stockwork surrounded by a peripheral zone of auriferous quartz-carbonate veins (Mason and Melnik 1986). Spatially, it is closely related to quartz-feldspar porphyry intrusive rocks. The Hollinger mine consists of extensional quartz-ankerite vein arrays centred on tholeiites and felsic porphyries. Alteration haloes consist of zoned chlorite-calcite-sericite to ankerite (Burrows et al. 1993). Pyrite within host rocks is the main sulphide, and minor components include scheelite, albite, tourmaline, and Ag, W, As, Te, Bi. Mineralization is spatially related to the Pearl Lake porphyry and to the Hollinger Main Fault, which is a high-strain zone of lineation and constrictional strain development with no identified offsets. Fluids for the Hollinger and McIntyre mines were similar (Spooner et al. 1987). Pressure of mineralization were interpreted at 100-260 MPa, depending on the occurrence of phase immiscibility (Spooner et al. 1987; Hagemann and Brown 1996). Despite the spatial relationships between gold mineralization and the intrusive centre, presence of auriferous quartz-carbonate veins that cut the 2673 Ma albitite dike at the McIntyre mine (Marmont and Corfu 1989) clearly indicate that the mineralization is much younger than the 2690 Ma porphyry and postdates albitite magmatism. Recent radiometric dating of mineralization at 2672 ± 7 Ma (Bateman et al. 2004) indicate that there is about a 20 M.y. (minimum) time gap between the quartz-feldspar porphyries (~2690 Ma) and mineralization. Alteration consists of sericite-chalcopyrite-pyrite-albite-hematite-anhydrite-Ag-Cu-Mo-Te. Cu-Au mineralization is cut by main-stage quartz veins, so there was a protracted period of mineralization, but there is disagreement on whether McIntyre is pretectonic (Robert and Poulsen 1997) or syntectonic (Rhys 2003).

The Dome mine is the second largest deposit of the district. Different styles of mineralization are exploited at Dome including 1) concordant ankerite interflow veins cut by gold-bearing extensional quartz veins and confined within Fe-tholeiitic basalt, and 2) carbonate and quartz-fuchsite-tourmaline veins hosted by a variety of rock types: basaltic and komatiitic rocks of the Tisdale Group, sediments of the Timiskaming Group, and the altered Preston and Paymaster quartz-feldspar porphyries (Rogers 1986; Proudlove and Hutchinson 1989; Moritz and Crocket 1990). The deposit is centred on the folded Timiskaming unconformity and it is next to the Dome fault. Syntectonic veins (Moritz and Crocket 1990) consist of quartz-ankerite (+fuchsite in ultramafic rocks), some in extensional arrays, some conformable and some discordant (Proudlove and Hutchinson 1989). Disseminated pyrite and pyrrhotite are the

principal sulphides. Elemental enrichment includes Ag, Zn, B. Mineralization post-dated Timiskaming sedimentation at 2670 ± 10 Ma (Bateman et al. 2004). At Dome, there has been argument over the role of a component of syngenetic mineralization (Proudlove and Hutchinson 1989).

Pamour mine is the principle example of gold mineralization type that extends along the Timiskaming assemblage unconformity in the Timmins–Porcupine gold camp. It consists of quartz-ankerite-albite vein arrays that are hosted mainly in Timiskaming conglomerates, and to a lesser extent in underlying Tisdale (ultra)mafic lavas. Mineralization consists of shear-related east-west-striking sets of fault-fill veins, and sheeted east-dipping extensional arrays (Duff 1986; Aitken 1990). Sericite alteration is relatively weak. Disseminated pyrite, pyrrhotite, sphalerite and arsenopyrite are the sulphide minerals. Metals include Ag, Zn, As, Pb. Mineralization post-dated Timiskaming sedimentation at 2673 Ma (Ayer et al. 2003).

Lithogeochemistry and Basalt Stratigraphy

In order to help define the stratigraphy and to use it to resolve structural complexities and timing relationships, a set of discriminants (elemental abundance and ratios) have been determined for the various Tisdale assemblage basalt rock units (Table 2) based on geochemical binary plots derived from the Discover Abitibi Initiative sampling (Appendix 1). TiO_2, Zr, V, Ni and Cr proved to be the most useful, similar to Kalgoorlie (Bateman, Costa et al. 2001). These discriminants are also similar to those used by the Porcupine Joint Venture (confidential data) in a modern, large and comprehensive (62 elements) data set that includes all Tisdale volcanic rocks (basalts and ultramafic), intrusive rocks (porphyry and albitite dykes) and sedimentary rocks (Timiskaming and Porcupine assemblages). These data enormously expand on early data (Fan and Kerrich 1997).

Discover Abitibi Initiative analytical work distinguished 3 subgroups within the Central formation, and 2 within the Hersey Lake formation. Porcupine Joint Venture work did not identify these subgroups, but did distinguish 2 subgroups in the Gold Centre formation and 2 subgroups in the Vipond formation (V vs. TiO_2: Figure 4). Figure 4 shows variation of TiO_2 vs. V. Subgroups of Hersey Lake and Central formations form 2 relatively distinct arrays with slightly different slopes. This bimodality is less obvious on other diagrams (Figure 5: TiO_2 vs. Zr). The third Central formation group is an isolated cluster in TiO_2-Zr (Figure 5), but otherwise is broadly coincident with the trends for both the other 2 Central formation subgroups and Hersey Lake subgroups (Figures 4 and 5). In TiO_2-V, Gold Centre, Vipond and Central formation subgroups form distinct arrays, and only Central and Hersey Lake formations are collinear. On a Al_2O_3-Fe_{total}-MgO ternary diagram (not shown), Central formation rocks plot as Mg tholeiites, and Gold Centre and Vipond formations plot as Fe tholeiites. None are calc-alkaline basalts. They have generally higher Zr and TiO_2 than Hersey Lake-Central formations, and on Figures 5 and 6 plot on inflections in the Hersey Lake-Central formation trend. In Ni-Cr, the 2 subgroups of Hersey Lake formation (Figure 7) and the corresponding 2 Central formation subgroups (Figure 8) are not distinguishable, and form an array up to high values for both elements. The third Central formation subgroup, Vipond and Gold Centre are all restricted to lower and diminishing Cr-Ni values (in that order).

Table 2. Geochemical criteria used to discriminate between the formations of the Tisdale assemblage volcanic rocks. These discriminants are based on Discover Abitibi Initiative geochemical data and on unpublished work of Porcupine Joint Venture and PlacerDome (CLA). Primitive mantle (p.m.) is used for normalization of trace elements (Sun and McDonough 1989).

	Ni	Cr	Cr/Ni	V	Y	Zr	V/TiO_2	V/Zr	Zr/TiO_2	V/Y	Fet/MgO	Th/ TiO_2	Th	Ce
Timiskaming assemblage	Argillite-greywacke sediments of Timiskaming and Porcupine assemblages are not distinguished													
Porcupine assemblage												>8	>5	>40
Krist formation												<8	<5	<40
Tisdale assemblage	Ni	Cr	Cr/Ni	V	Y	Zr	V/TiO_2	V/Zr	Zr/TiO_2	V/Y	Fet/MgO	REE	normalized trace elements	anomalies
Gold Centre 2 groups	<125	<250	1-4	<150	>30	>125	20; 80	<1	100-150	<3	>3; MgO<5%	flat REE @ 40-50 times chondrite	10-15 times p.m.; flat	Ni, Cr very depleted; mostly negative Eu anomalies
Vipond 2 groups	10-150	<250	1-4	<150	<25	<150	150; 250	1-4	50-300	3-10	>2; MgO<7%	flat REE @ 15-30 times chondrite	3-10 times p.m.; flat	Ni, Cr very depleted; negative P, Ti, Nb; mostly negative Eu anomalies
Central 3 groups	25-250	<400	1-4	>150	10-30	<100	>250	>4	40; 75; 60	>10	1-3; MgO>3%	flat REE @ 7-20 times chondrite; one group with positive slope in HREE to 10-15	1-10 times p.m.; flat	Ni, Cr depleted; negative Ti, P, Nb; mostly negative but some positive Eu anomalies
Hersey Lake 3 groups	>250	>700	<4	<225	<15	<50	>250	10; 6.5; 4.5	40; 55; 65	>10	4; MgO>5%	flat REE @ 2-7 times chondrite; depleted LREE	1-5 (p.m.) flat	Negative P; some negative Eu anomalies

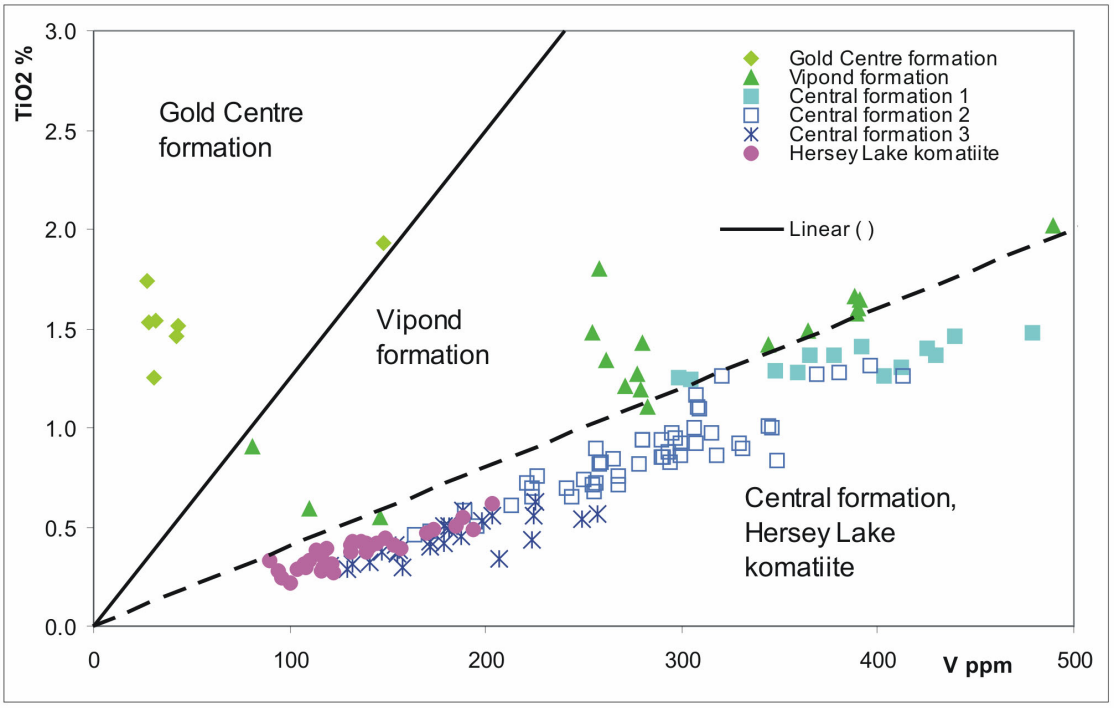

Figure 4. Plot of V vs. TiO_2 for Tisdale assemblage mafic and ultramafic lavas. Lines mark off arrays of Gold Centre and Vipond formation, based on discriminants in Table 2. Numbers refer to subgroups defined by trace element discriminant work. Other Ontario Geological Survey data included (Pressacco 1999).

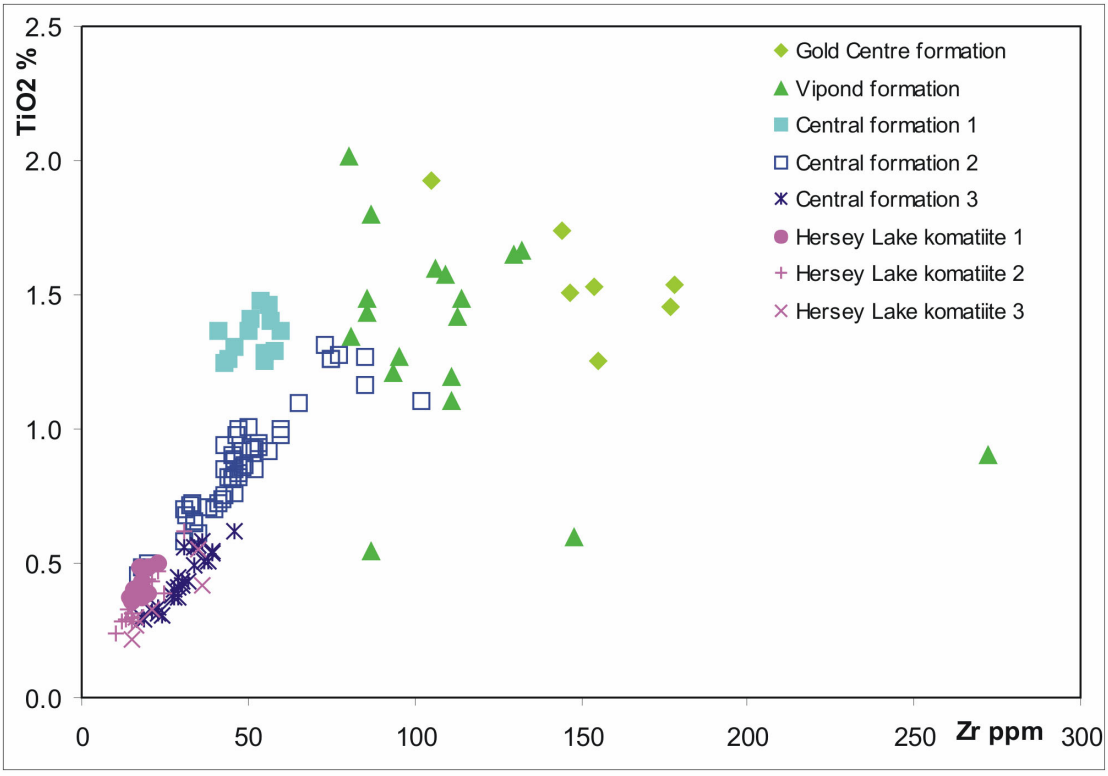

Figure 5. Plot of Zr vs. TiO_2 for Tisdale assemblage mafic and ultramafic lavas. Numbers refer to subgroups defined by trace element discriminant work. Some data from Ontario Geological Survey data (Pressacco 1999).

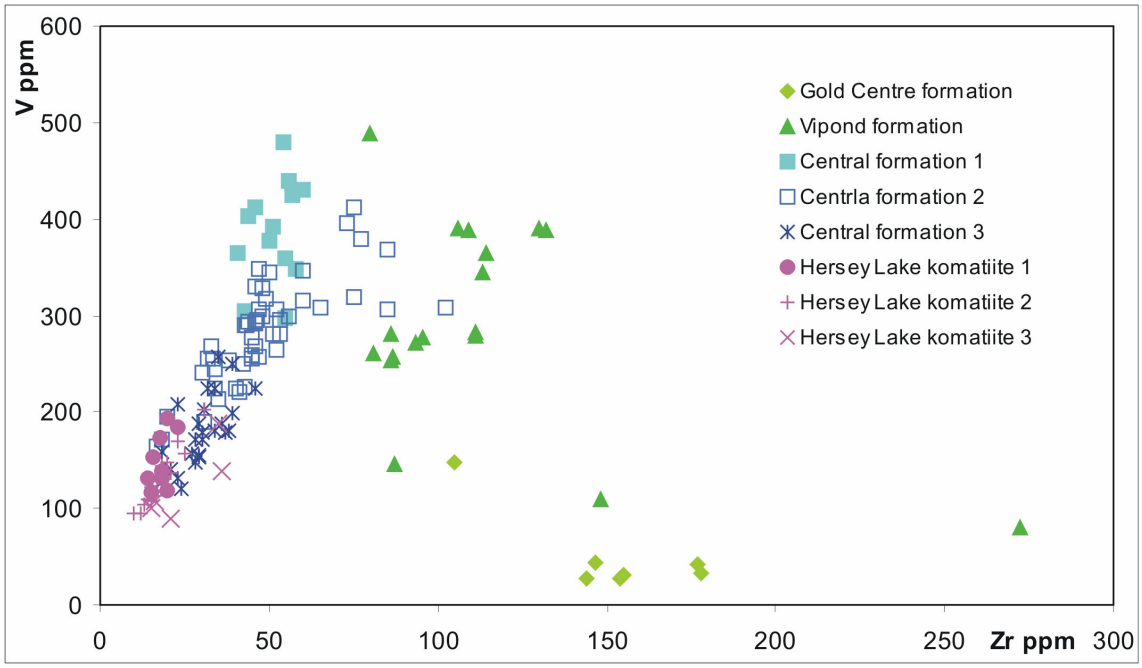

Figure 6. Plot of V vs. Zr for Tisdale assemblage mafic and ultramafic lavas. Numbers after formation name refer to subgroups defined by trace element discriminant work. Some data from Ontario Geological Survey data (Pressacco 1999).

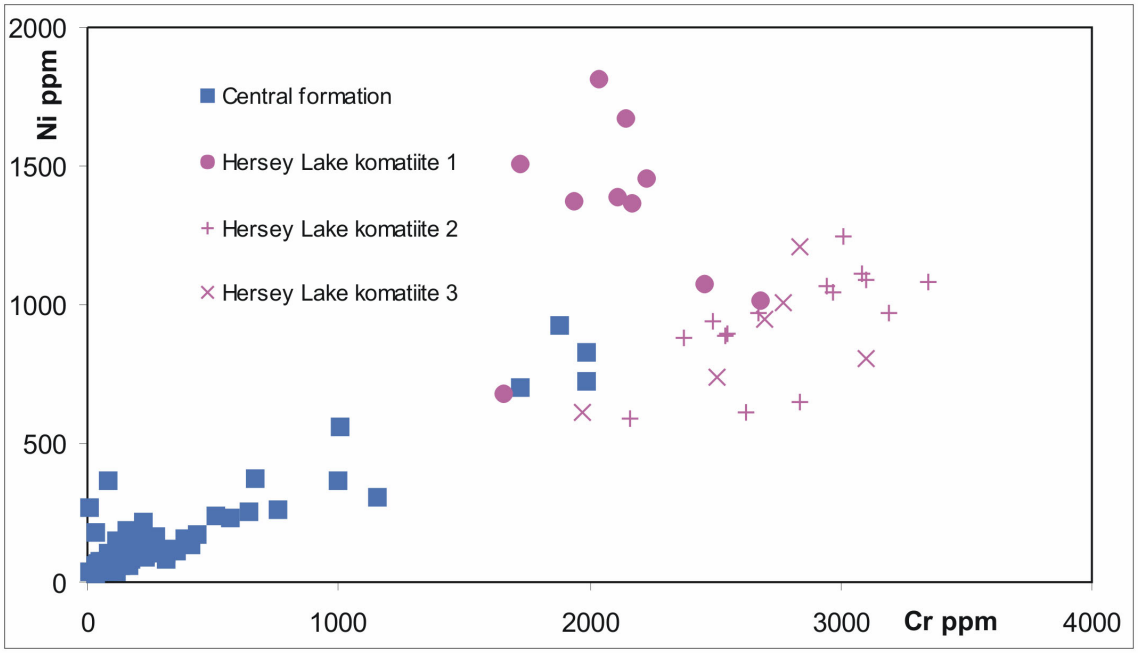

Figure 7. Plot of Cr vs. Ni for Central formation (Tisdale assemblage) mafic lavas and Hersey Lake ultramafic lava subgroups. Numbers after formation name refer to subgroups defined by trace element discriminant work. Some data from Ontario Geological Survey data (Pressacco 1999).

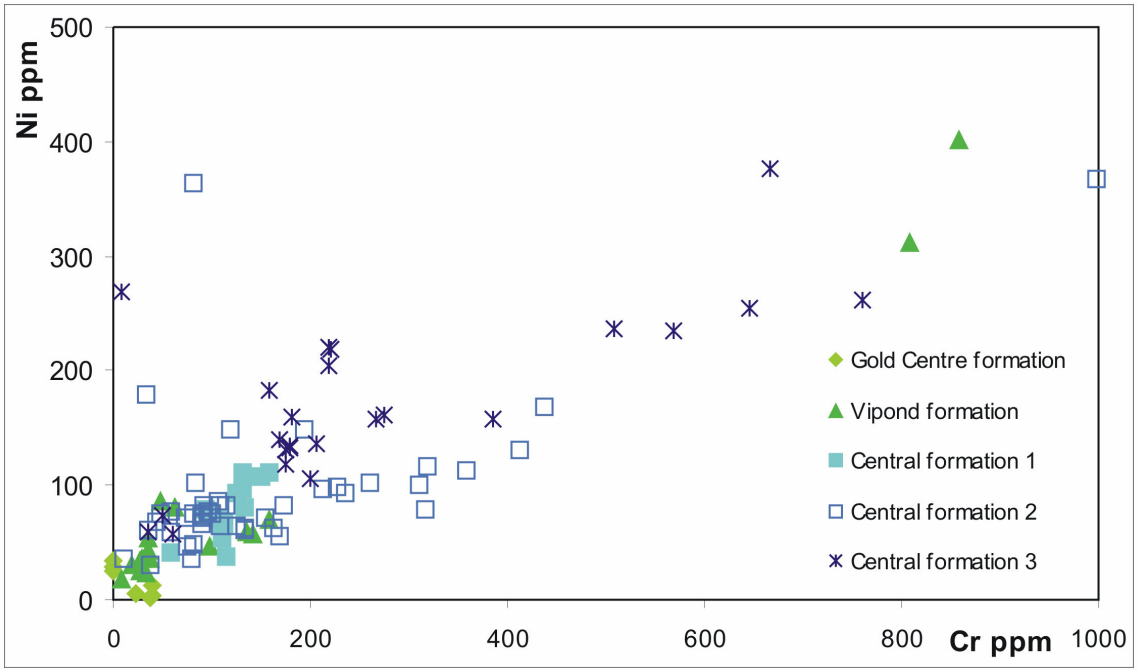

Figure 8. Plot of Cr vs. Ni for Gold Centre, Vipond and Central formation (Tisdale assemblage) mafic lavas and their subgroups. Numbers after formation name refer to subgroups defined by trace element discriminant work. Some data from Ontario Geological Survey data (Pressacco 1999). This is an enlargement of part of Figure 7.

In rare earth elements (Figure 9), a distinctive feature is evident among the subgroup 3 samples of the Central formation rocks. Most groups (Gold Centre formation, Vipond formation, Central formation subgroups 1 and 2) show flat patterns with modest Eu anomalies (positive and negative) and very slight LREE depletion. The Hersey Lake komatiites show marked LREE depletion.

Central formation subgroup 3, however, show quite unique patterns, most notably in HREE enrichment (Figure 9), with a positive slope in Gd to Lu. This, together with moderately elevated MgO (to 12 wt %), Ni (to 376 ppm), Cr (to 760 ppm), high Al_2O_3 (up to 19.38 wt %), low TiO_2 (below 0.62 wt %), low Zr (below 46 ppm), and negative Nb (normalized) and V (normalized) anomalies indicate that these rocks are boninitic in affinity (Kerrich, Wyman et al. 1999). Few boninitic rocks have been recognized in Archaean greenstone belts (Manikyamba et al. 2005). Their interpretation of this identification is that these magmas were the product of plume-subduction zone interaction.

The multi-element plot of Figure 10 shows generally flat trends at enrichments between 1 and 10 times primitive mantle. Notable are weak and variable, yet discernible, negative anomalies in Nb and Ti, and above all in P, suggesting a weak crustal input into these lavas. Nd isotope data (Ayer et al. 2002; Sproule et al. 2003) are interpreted to indicate a lack of significant crustal contamination. Nd model ages are very close to their eruption ages, indicating that any contaminant had separated from the mantle just before (<250 Ma) incorporation in the volcanics. Ba shows moderately strong enrichment, as do the few data for Rb, and this is most likely in large measure an affect of alteration accompanying gold mineralization. However, these are not the elements that are most enriched: W, K, Ag, As, Sb, Li and CO_2 show the most intense increases that can be attributed to alteration (Figure 11).

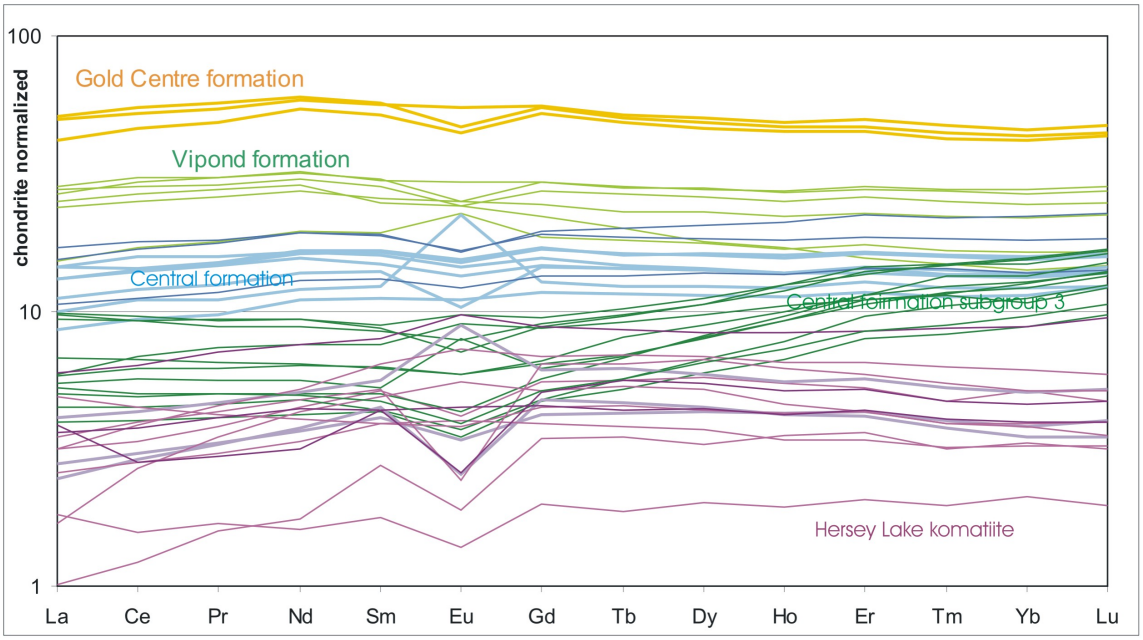

Figure 9. Plot of rare earth elements in selected samples of the Tisdale assemblage mafic lavas and their subgroups. Normalized to chondrite (Sun and McDonough 1989).

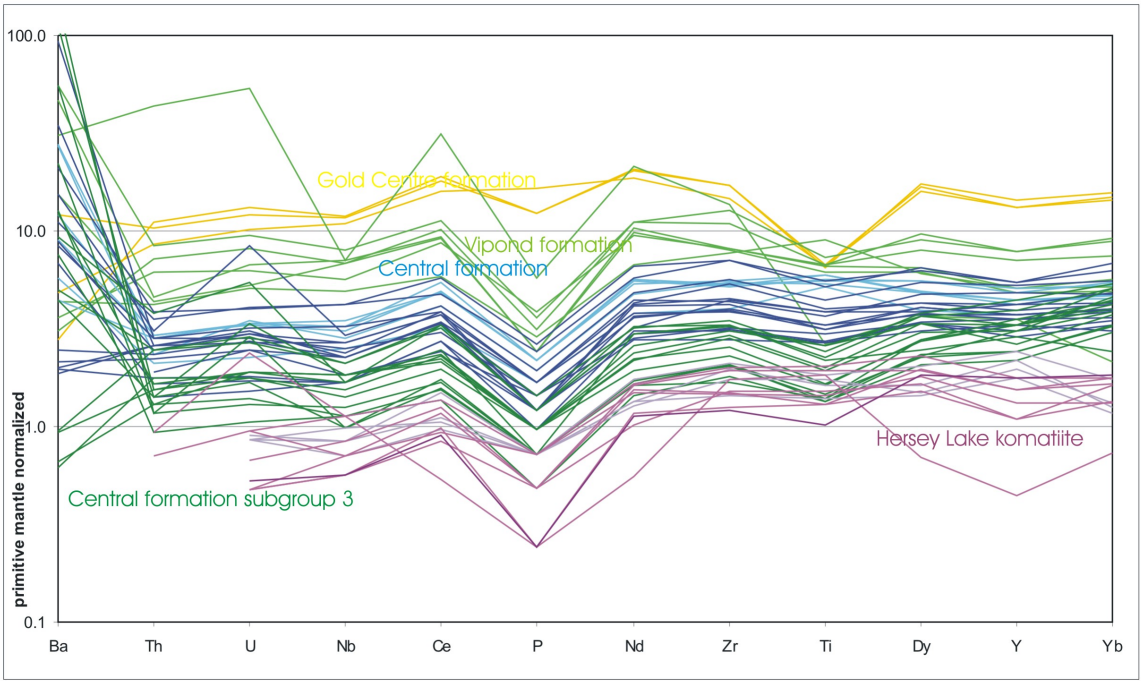

Figure 10. Plot of trace elements in samples of the Tisdale assemblage mafic lavas and their subgroups. Normalized to primitive mantle (Sun and McDonough 1989).

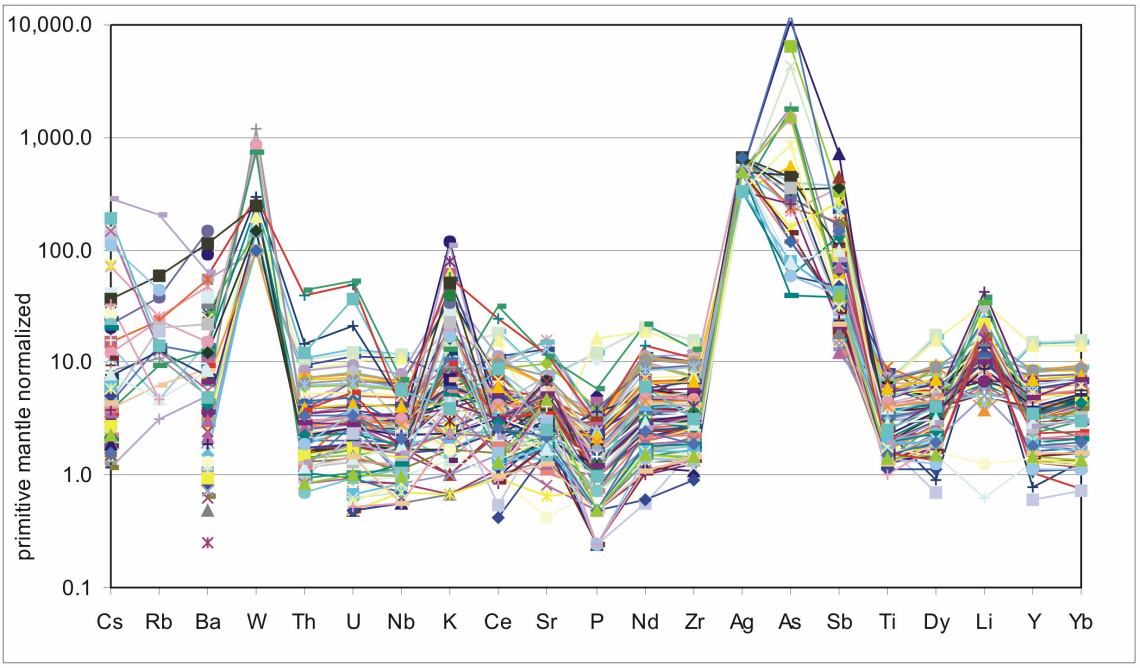

Figure 11. Plot of trace elements including those typically enriched around gold mineralization in samples of the Tisdale assemblage mafic lavas and their subgroups. Normalized to primitive mantle (Sun and McDonough 1989).

Thus, 2 major groupings of Tisdale mafic lavas can be made: [1] 2 subgroups of both Central and Hersey Lake formation form 2 slightly different collinear arrays; [2] the third Central formation subgroup appears to be more closely related to the Vipond and Gold Centre formations, which are themselves divided into distinct, non-collinear arrays. The subgroups in Hersey Lake komatiites are defined by sampling in drill core, and these subgroups alternate along the core, indicating that the subgroups coexisted spatially and are purely geochemical groups and do not represent stratigraphic-time units. For the other subgroup, the data do not permit distinctions between simple geochemical or stratigraphic groupings. On Figure 12, basalts in close spatial association with Hersey Lake komatiites are shown as magnesian basalts, although geochemically they appear as Group 3 of the Central formation (see Figures 4, 5, 6, 8).

On the basis of lithogeochemistry, the Gold Centre, Vipond and Central formations do appear to be true stratigraphic units since they display systematic map patterns. The geochemical work reported here is the basis of the formation divisions shown for Timmins on Figure 12 and Map P.3555 (back pocket). However, geochemical groupings as formations are not entirely mutually exclusive. Geochemically, Hersey Lake komatiite and Central formation rocks are closely related and commonly collinear on discrimination diagrams. While the Central formation (as defined geochemically) is largely restricted to the lowest horizon of the Tisdale assemblage, Vipond and Gold Centre geochemical groups are geochemically quite distinct but are interleaved. The boundaries drawn on Map P.3555 separate zones dominated by one group or the other, rather than delimit "geochemically pure" zones. At the top of the stratigraphic pile of Tisdale assemblage basalts, immediately below the graphitic phyllites at the base of the Porcupine assemblage are basalts that show a geochemical affinity to Central or Vipond formations. This occurs all around both the Porcupine syncline and the Kayorum syncline, rather than Gold Centre geochemical-type basalts that might be expected from the established stratigraphic column (see Table 1). Gold Centre formation rocks are never immediately adjacent to the contact. This means either that there is an unrecognized geochemical group at the top of the Tisdale assemblage that may warrant formation

status, or that an anticlinal crest (presumptively of D2 age), exposing deeper stratigraphic levels, that is not indicated by any structural data parallels the Porcupine assemblage contact.

This uppermost geochemical group disappears to the northeastern part of Figure 12 with Vipond and Central formations occurring adjacent to the Porcupine assemblage contact. Similarly, to the north around the North Tisdale anticline, Central formation rocks are in direct contact with the sediments of the Porcupine assemblage. This implies that the upper parts of the Tisdale assemblage has been excised at the base of the Porcupine assemblage, and that the base of the Porcupine assemblage may be either an unconformity, a major fault, or both.

Structure of the Timmins–Porcupine Gold Camp

Over the years, considerable work on the structure of Timmins has been done, yet a clear understanding of which phase of deformation is responsible for which structures remains elusive. The idea that the Timiskaming assemblage, itself folded, postdates the Porcupine syncline and other early folding was adopted early (Ferguson et al. 1968; Roberts 1981). Reasons for these difficulties in interpretation are that foliation has not hitherto been recognized as part of the earlier phases of folding (Ferguson et al. 1968; Brisbin 1997), and that systematic variations in bedding dips cannot be defined in the pillow basalts because flattening accompanying foliation forms the observable layering. This fact prevents the use of bedding-foliation vergences in identifying such features as antiformal synclines. Moreover, folding episodes cannot be discriminated on the scale of outcrops. Figure 3 shows a general geology map of the study area, and maps P.3555 and P.3547–Revised (back pocket) show fuller details.

One major innovation of the work reported here is the recognition and systematic mapping of S2 foliation restricted to the Tisdale assemblage, in addition to the previously recognized S3 and S4 foliations found in the Timiskaming assemblage. While D1 is a recognized deformation event, it is interpreted here as an extensional event and no S1 foliation has been ascribed to it. In general, as described below, D2 and post-Timiskaming D3, D4 and constrictional strain occur in the Tisdale and Porcupine assemblages, whereas S3 and S4 foliation are the principal fabrics found in the Timiskaming assemblage. The foliations tend to occur in pairs (S2-S3, and S3-S4), and S4 is only locally recognized in Tisdale assemblage rocks adjacent to the Porcupine–Destor deformation zone. The criteria used to distinguish the foliations are: [1] S4 foliation has a regular orientation striking west or west-southwest nearly parallel to the strike of bedding in Timiskaming assemblage sediments; [2] locally within the Tisdale assemblage basalts, a foliation with typical S4 orientation crosscuts S2 and S3; [3] the foliation enumerated S3 has a regular strike generally west to northwest, distinct from S4, and parallel to the axial surfaces of parts of the Porcupine syncline, and oblique to the Timiskaming unconformity; [4] within S3 crenulations, a foliation enumerated S2 is recognized within Tisdale and Porcupine assemblages, and this is in places parallel to the North Tisdale anticline axial surface that has been refolded by F3 folds; and [5] Tisdale assemblage rocks show S2 trends and basalt pillow facings together with formation distribution that are interpreted as F2 folds refolded by the F3 Porcupine syncline (Map P.3555). These distinctions are central to this study and underpin the structural interpretations. Another innovation is a reinterpretation of pre-Timiskaming deformation: here, D1 is interpreted as extensional-uplift, and D2 a fold-and-thrust event. The large-scale Porcupine syncline is not interpreted as the result of 2 pre-Timiskaming folding events, but as a result of overprinting of a pre-Timiskaming folding event by a post-Timiskaming folding event.

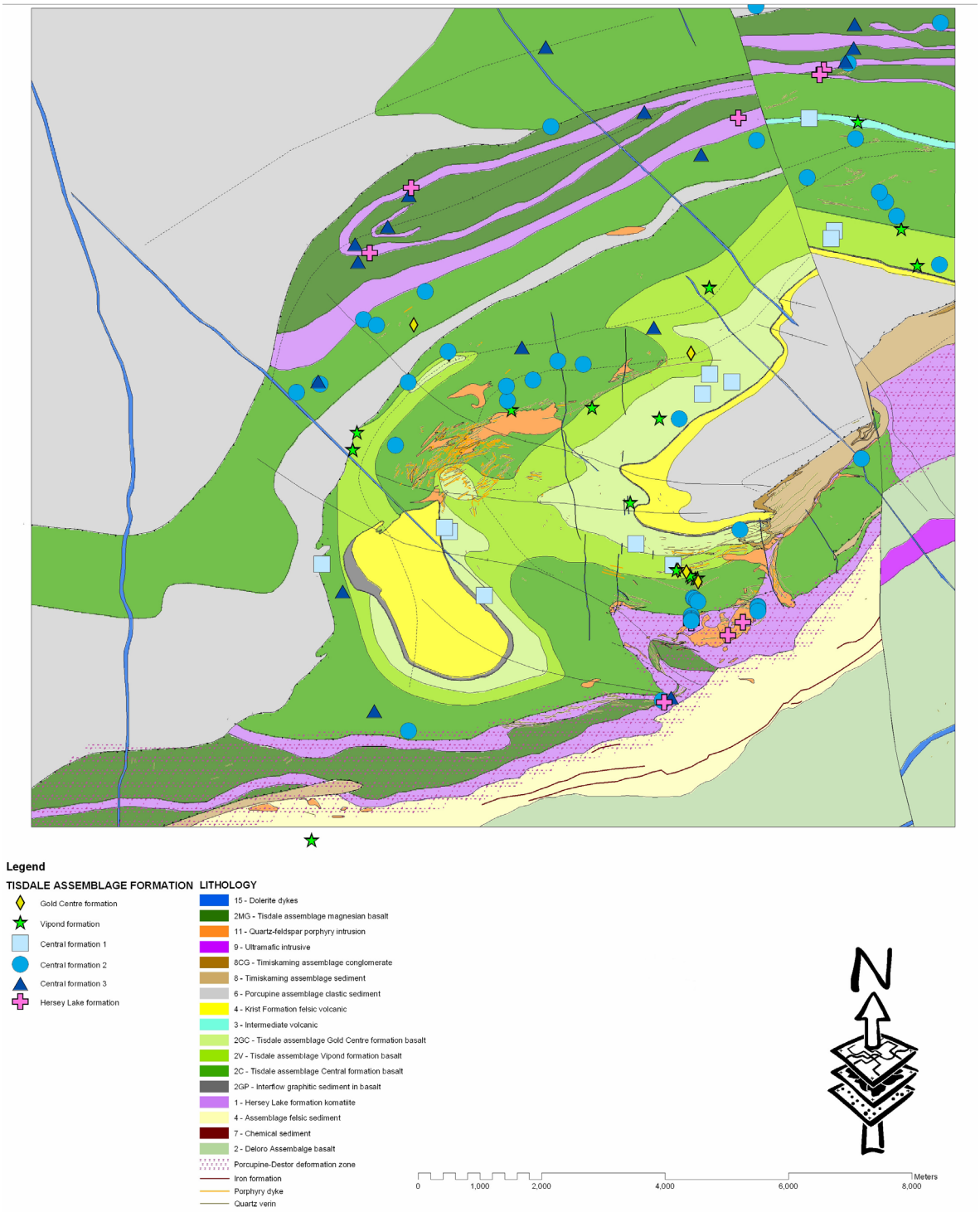

Figure 12. Map of the Timmins camp area, the same as in Map P.3555 (back pocket), with the locations of Discover Abitibi Initiative geochemical samples classified by TiO_2-Zr-V-Ni-Cr into Tisdale assemblage basalt formations. The stratigraphic subdivisions are based on these plus a large number of geochemical samples that are confidential and are not shown here. This figure is a summary of the 2 maps in the back pocket of this report, and previous work (Carlson 1967; Ferguson et al. 1968; Piroschco and Kettles 1991; Berger 1998; Hall and Smith 2002). A larger, full-colour version of this figure is included in the back pocket of this report.

UPLIFT, EXTENSION AND EXCISION OF STRATIGRAPHY D1

On a regional scale, there is evidence for deformation predating deposition of the Porcupine assemblage. Regional deformation episodes have been identified based on overprinting relationships of folds and faults with the earliest compressional regime constrained by cessation of Blake River assemblage volcanism at 2696 Ma and onset of the deposition of the Porcupine assemblage at 2690 Ma, synchronous with emplacement of a suite of syn-tectonic granitic plutons (see Figure 2). In the Timmins camp, there is an age difference of about 15 Ma between cessation of Tisdale assemblage volcanism and deposition of the overlying Porcupine assemblage (see Table 1). The base of the Porcupine assemblage has been interpreted as an unconformity or disconformity on a regional scale (Bleeker, Parrish and Sager-Kinsman 1999) and this is clearly supported by the new geochronological data presented in the Timmins area stratigraphy and lithology section. The Porcupine–Tisdale contact may be better interpreted in terms of uplift and extension, with or without folding. There is the possibility of a folding event predating the deposition of Porcupine assemblage rocks, to wit the interpretation above (from basalt geochemistry) suggesting that an anticline within Tisdale assemblage volcanics has been truncated at the base of the Porcupine assemblage.

There is local evidence for a deformation only affecting Tisdale assemblage rocks and an unconformity predating the Porcupine assemblage. Along the southern margin of the North Tisdale anticline, there is an abbreviated Tisdale assemblage section, with a very narrow sequence of basalts north of a narrow septum of Porcupine assemblage sediments (see Figures 1, 3, Map P.3555). Geochemically (TiO_2, Zr, V, Ni, Cr – see "Lithogeochemistry and Basalt Stratigraphy" section above), these basalts can all be defined as Central formation (see Figures 4, 5, 6, 7, 8), particularly further east around Pamour mine where there is greater density of sampling. Thus, it appears that both the Vipond and Gold Centre formations are missing. The northern contact of the sediment septum is not exposed or available for examination in drill core, and may be either a fault or an intact stratigraphic contact. This contact is folded by F2 and F3, and hence dates from a very early stage.

Further east, the contact between Tisdale assemblage volcanics and Porcupine assemblage rocks in the vicinity of Hoyle Pond mine is also a shear zone (Bateman, Ayer and Dubé 2003) marking a zone of excised stratigraphy, where the trends of the mafic-ultramafic volcanic units are also truncated against this contact (Map P.3547–Revised). The volcanic-sediment contacts are characteristically marked by several metres of graphitic schists (Map P.3547–Revised), which are typically strongly deformed and foliated (Photo 1). This zone of graphitic schist lies on both the northern and southern sides of the Hoyle Pond mafic-ultramafic belt. In the vicinity of Owl Creek, the zone of graphitic schist diverges from the mafic-sediment contact where the contact rolls over to a more flat-lying orientation: the graphitic schists continue in a steeply dipping zone entirely within the sedimentary rocks. This indicates that this shearing episode post-dated the juxtaposition – D1 along the North Tisdale anticline – of the 2 rock packages (volcanic and sedimentary). Most drill core is not oriented, so it is not possible to determine foliation orientation or to interpret kinematic microstructures. These graphitic shears most likely are late (D4?) overprints of these early D1 (extensional?) structures.

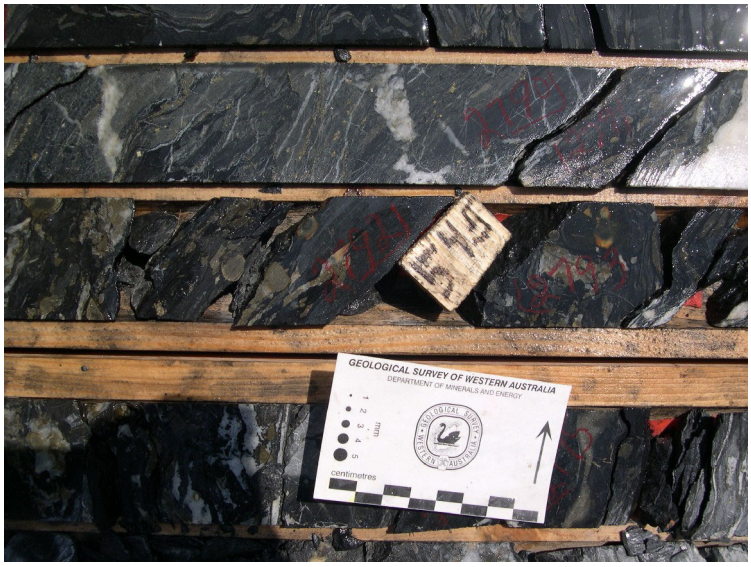

Photo 1. Graphitic phyllite with intense foliation and deformed pyrite lenses lie along the contact at the base of the Krist formation volcaniclastic and Tisdale assemblage basalts in the Kayorum syncline. This may mark the locus of early faulting. Drill hole KAY99-09, 647 m (Moneta Mines Inc.).

South of Porcupine–Destor deformation zone, along a powerline traverse across the Deloro–Tisdale–Porcupine assemblage contacts south of Timmins, there is also an abbreviated interval of basalts lying between ultramafic spinifex-textured lavas (assumed to be the Hersey Lake komatiite of the Tisdale assemblage) and felsic volcaniclastic rocks of the Krist formation. Thus, there is a significant interval of Tisdale assemblage rocks missing along both the northern and southern flanks of the Porcupine gold camp, with a thick succession in the middle. This may be interpreted in several ways: [1] in these northern and southern areas, the upper Tisdale assemblage basalts were never erupted, and the central basin of thicker basalt sequence may have been flanked by syn-volcanic faults; [2] there was a more or less uniform sequence of basalts, but some were structurally excised before F2 folding. This may have been caused by extensional faulting, which, given the apparent symmetry, implies north-south extension along east-west-striking faults. The base of the Krist formation is marked by several metres of deformed graphitic phyllite in both the Kayorum and Porcupine synclines, which has been subsequently folded in all folding events. This contact may represent a shear zone with significant displacement in some areas, but in the Kayorum syncline the Gold Centre formation of the uppermost Tisdale assemblage basalts has been identified geochemically; or [3] in some cases such as around Hoyle Pond-Owl Creek properties, late faulting may have contributed, at least in part, to the excision of stratigraphy. This may have been in D3 or D4, during deformation accompanying gold mineralization.

Along the base of the Krist formation in the Porcupine syncline, an unconformity has been identified (Buffam 1948) on the basis of locally truncated folds. Around the northern flank of the Porcupine syncline, the geochemical classification of Tisdale assemblage basalts (Map P.3555) indicates that, further east, progressively lower stratigraphic level basalts are exposed along the Tisdale–Krist contact. This implies that the contact (unconformity or fault) progressively cuts down section further east, but above all cuts down section in the north and probably the south. Given the inferences of D2 thrusting discussed below, reconstruction of thrust slices suggests that the contact between Tisdale and Porcupine assemblages cuts down section toward the north, because the thrust slice with the most complete Tisdale stratigraphic section may have been derived from furthest south. The Tisdale–Krist contact is marked on Map P.3555 as an extensional fault and unconformity attributed to D1 uplift and extension.

DEFORMATION D2

D2 is the earliest folding phase that can be identified in the field. F2 folding is most clearly defined in the North Tisdale anticline that strikes from the northwestern part of the gold camp eastward to the north of the Pamour open pit. The trends of layering of mafic and ultramafic lavas at Pamour are well defined by abundant drilling data in 3 dimensions. In plan view, opposed facings in pillows over a wide area (Map P.3547–Revised) indicate an anticlinal fold closure, and this fold closure is also well defined in cross sectional view (Figure 13). F2 folds consists of north-dipping recumbent isoclinal folds that plunge eastward at a shallow angle. The axial surface dips to the north-northeast at 40°, but is somewhat irregular in dip, presumably due to later folding. In cross-section at Pamour mine, the drilling data is sufficient to demonstrate the mafic-ultramafic stratigraphy in the North Tisdale anticline is truncated against the contact with the Porcupine assemblage sediments to the north (Figure 13) along the northern flank of the eastern end of the North Tisdale anticline.

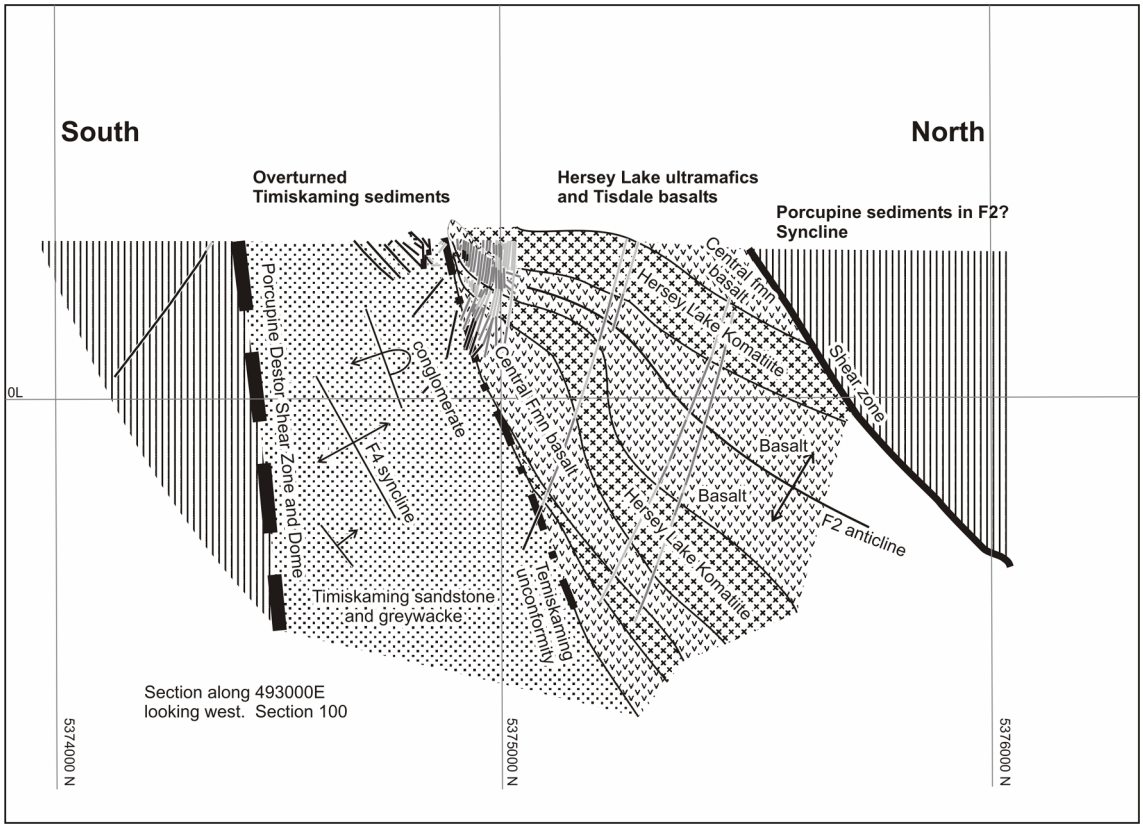

Figure 13. Cross-section through the eastern continuation of the North Tisdale anticline, to the north of the Pamour open pit. Location of section shown in Figure 3. The section shows the recumbent F2 anticlinal hinge with the Timiskaming unconformity to the south (left) and a shear zone contact truncating Tisdale assemblage volcanics and juxtaposing them against Porcupine assemblage sediments to the north (right).

North and northwest of Timmins, the S2 foliation parallels the axial surface of the F2 North Tisdale anticline. This fold is defined by outward facing of basalt pillows and by the trends of distinctive units, which are best shown by aeromagnetic images. This F2 fold plunges west and southwest, with a moderately to steeply south-dipping axial surface. The ultramafic stratigraphy north of Timmins is best defined by aeromagnetic data and is truncated against the contacts with the sediments further north (Map

P.3555; Figure 14). This may be interpreted as a hanging-wall syncline related to the Fifth Avenue thrust (discussed below). On the scale of the entire gold camp, this North Tisdale–Pamour fold is a doubly plunging non-cylindrical anticline.

A syncline-anticline pair of folds have been defined in the large, central block of Tisdale assemblage basalts by pillow facings in the basalts and by S2 trends (Map P.3555). The syncline is well defined by facing of pillows and by stratigraphy. It lies immediately to the south of the septum of Porcupine assemblage sediments to the north, and may be correlated with the Kayorum syncline (Map P.3555). The southwestern end of this syncline is not well defined, and may be truncated against the fault marking the northern edge of the main southern trend of Hersey Lake komatiites. S2 trends closely parallel the contact between the Tisdale assemblage and Porcupine assemblage rocks. Similarly, an F2 anticline, refolded around the F3 components of the Porcupine syncline, is defined by pillow facings and lies parallel to, and to the southeast of the F2 syncline. It is referred to as the Central Tisdale Anticline, but it does not closely correspond with the previously defined Central Tisdale anticline (Ferguson et al. 1968). Northwest of Timmins, the ultramafic stratigraphy is best defined by aeromagnetic data, and is truncated against the contacts with the sediments further north (Map P.3555).This may also be interpreted as a hanging-wall syncline related to the Fifth Avenue thrust.

On a previous map (Ferguson et al. 1968) the Porcupine assemblage sediment septum along the south flank of the North Tisdale anticline was shown within a synclinal closure, but facing is uniformly southward within both the sediments and the adjacent basalts, showing that it is not a fold. For stratigraphic reasons – incomplete stratigraphic sequence – a fault must be inferred. Two cross sections have been drawn across the southern contact of this septum, using drill hole data, and the sections show both south- and north-dipping contacts (Figure 14). Along the southern contact of this septum of Porcupine assemblage sediments with the Tisdale assemblage volcanics to the south are horizons of deformed graphitic schists (Photo 2). This contact is best interpreted as a D2 thrust fault zone, here termed the Fifth Avenue thrust (Figures 3, 14). It probably extends into Whitney Township across the Burrows–Benedict fault, but has not been identified, as the sediment septum does not appear to extend to the east.

Three other D2 thrust faults are inferred. The North Tisdale anticline is interpreted as a hanging-wall anticline, with the corresponding thrust surface along its northern contact, herein named the North Tisdale thrust. This fold and thrust extends into Whitney Township, immediately north of Pamour mine. The thrust follows along the northern contact of the North Tisdale anticline in Whitney Township at Pamour and dips to the north, with truncated volcanic stratigraphy abutting Porcupine assemblage sediments (see Figure 13). A third D2 thrust is interpreted along the northern contact of the belt of Tisdale assemblage volcanics in southern Hoyle Township that contain the Hoyle Pond mine. This fault also truncates the stratigraphy internal to this belt of volcanic rocks (Map P.3547–Revised), which extends west into northernmost Tisdale Township. The wide belt of Porcupine assemblage sediments along the Whitney–Hoyle townships boundary (Map P.3547–Revised) dips and faces southward, except for a narrow selvedge at the southern flank, immediately below the North Tisdale thrust. A fourth D2 thrust fault marks the boundary between Central formation basalts and Hersey Lake ultramafic rocks north of the Porcupine–Destor deformation zone (Map P.3555; Figure 3). The Central Tisdale anticline here strikes nearly north-south (not readily distinguishable from the D3 South Tisdale anticline – see “Deformation D3”, below), and appears to be truncated by this fault. The fault is a locus of intense ankerite alteration, and has been folded in D3. It also appears to be truncated by the Fifth Avenue thrust to the west, and so it appears to have been formed slightly earlier in D2 during imbrication of a series of thrust slices. No Porcupine assemblage sediments are involved at the present level of exposure, unlike the more northerly thrusts, and no anticline has been defined in the ultramafic rocks south of this fault.

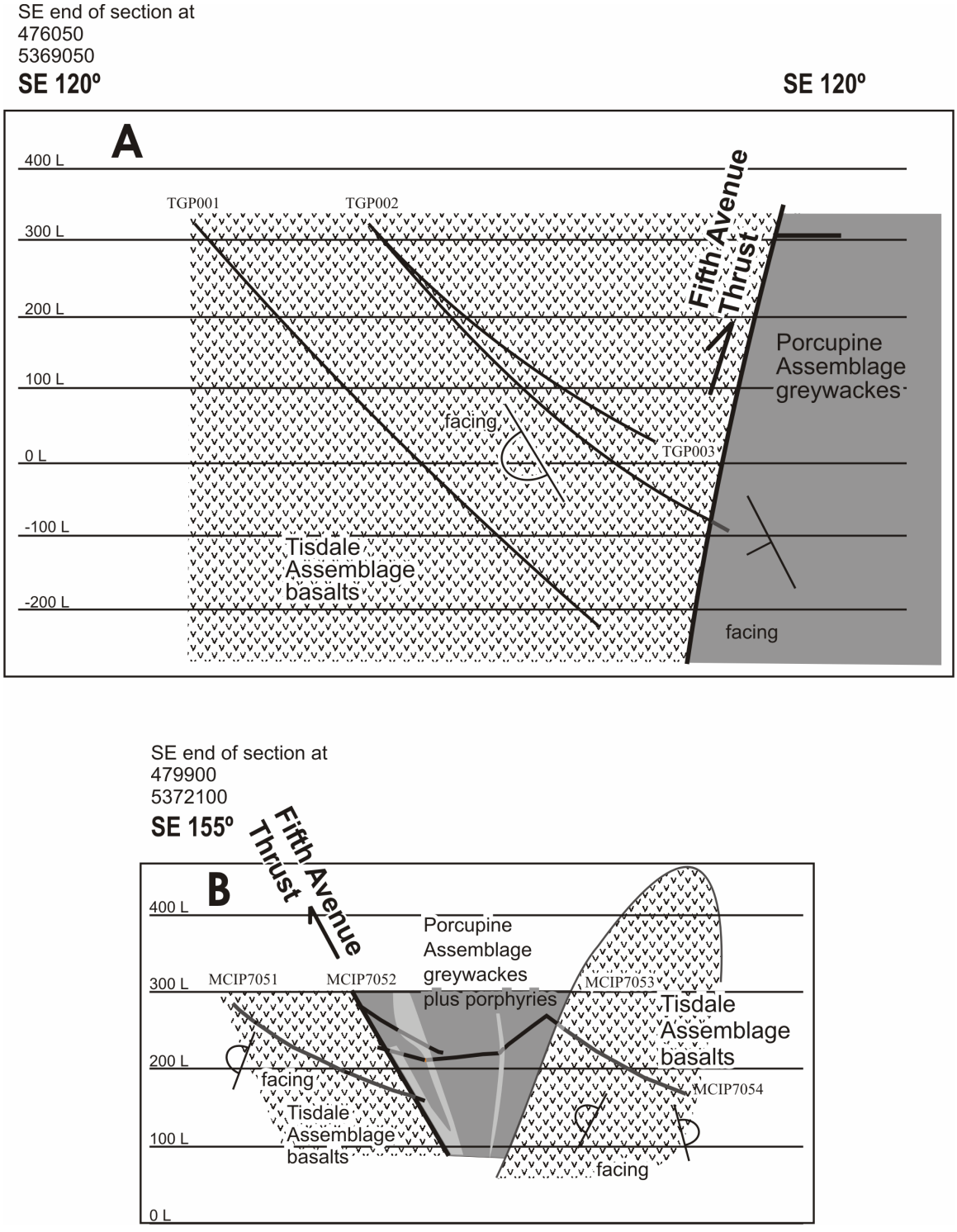

Figure 14. Two cross-sections through the D2 Fifth Avenue thrust, constructed from diamond drill hole profiles. Location of section shown in Figure 3. Locations and dips of the fault in each profile are well constrained, so the variable dip of the fault is correct.

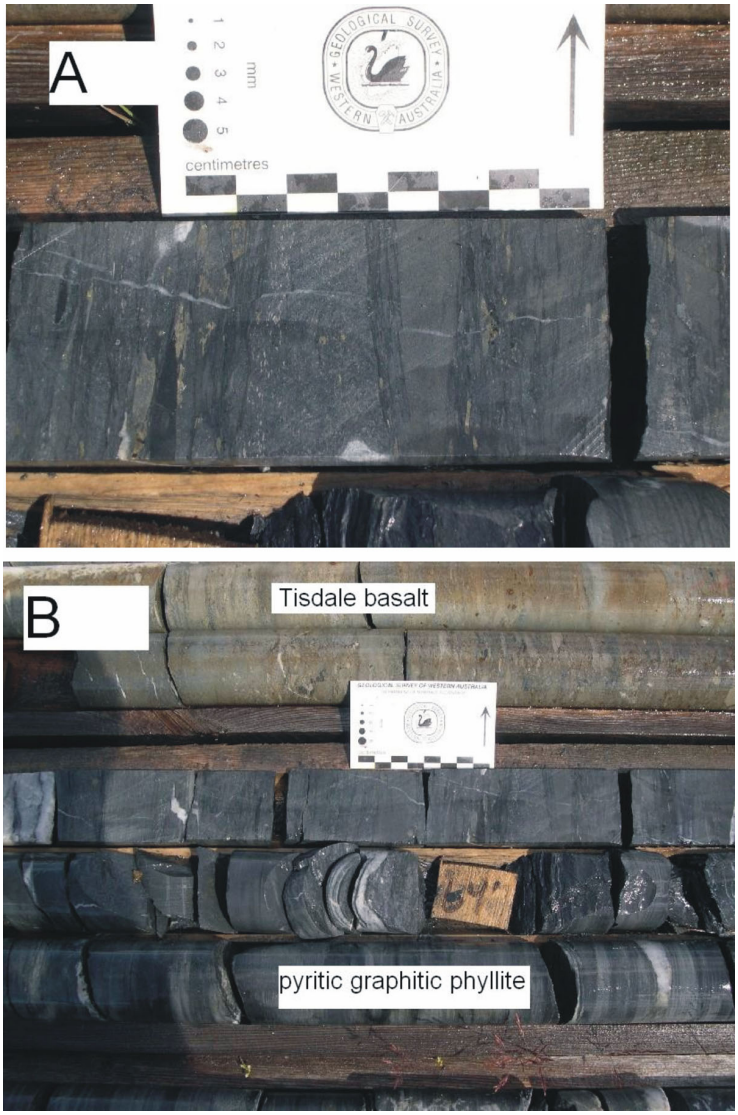

Photo 2. Graphitic phyllite, intense foliation, deformed pyrite lenses (A) and later brittle fractures and veins mark the southern contact (B) of a belt of Porcupine assemblage sediments and an extensive belt of Tisdale assemblage basalts. This probably marks the locus of D2 thrusting. Drill hole TGP002, 647 m (Timginn Property) near Timmins railway station.

These 3 basalt-sediment contacts along the northern edges of (ultra)mafic volcanic rocks may be 3 imbricate D2 thrusts, with a hanging-wall anticline defined in one. The southernmost contact (see Figure 14) has been informally referred to as the Fifth Avenue thrust due to its location in Timmins city. Here, the thrust is marked in drill core by a narrow (less than 1 m: Photo 2) of highly deformed and foliated sulphidic graphitic schist. The geometries of truncated volcanic stratigraphy implies south-over-north D2 thrusting, which is most probably rooted in the Porcupine–Destor deformation zone. The thrusts appear to dip both north and south, and it is assumed here that these variable dips are the result of later deformation. The Fifth Avenue thrust and others disappear below the Timiskaming assemblage rocks. Based on relative chronology, D2 folding and thrusting dates from some time between the end of Porcupine assemblage deposition (ca 2685 Ma) and the beginning of Timiskaming assemblage deposition after 2679 Ma (Bleeker, Parrish and Sager-Kinsman 1999; Ayer et al. 2003).

Since the F2 North Tisdale anticline affects Porcupine assemblage rocks, it is to be expected that rocks within the Porcupine syncline should also exhibit F2 folds. Outcrop and facing data are sparse amongst the Beatty formation sediments of the Porcupine syncline, but F2 folding can be inferred by a line of symmetry that strikes east-northeast parallel to the flank of the Porcupine syncline (seen on the large-scale on Map P.3555, back pocket), yet at an angle to the trend of the crosscutting S3 foliation, dividing east- (inward) dipping, south-dipping and north-dipping beds. This is interpreted as an F2 syncline, refolded in F3. Thus, the Porcupine syncline is mainly an F2 syncline, parallel to F2 folding in the Tisdale assemblage basalts to the north. A stereoplot (Figure 15) of S2 foliations shows the wide range of orientations, reflecting subsequent deformation. The calculated beta axis is close to the constrictional lineation (see below).

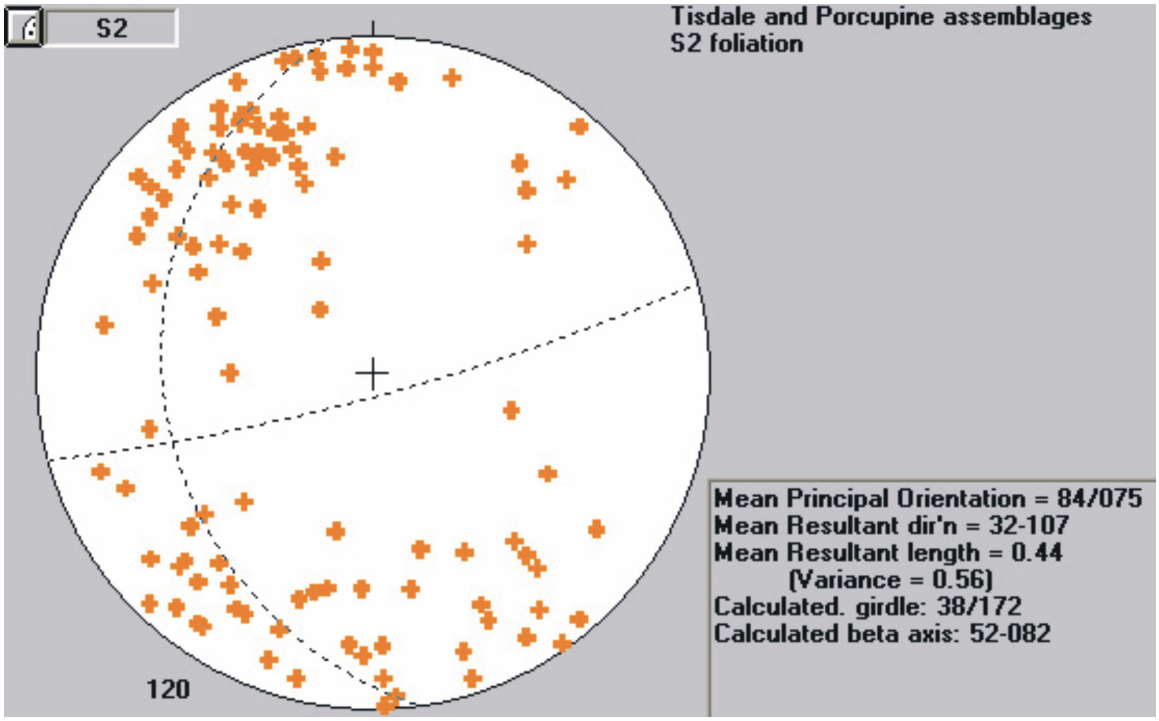

Figure 15. Stereoplot of poles to S2 foliations, mainly from Tisdale Township. Average S2 dips 84°, strike (RHR) 075°.

An inferred D2 anticline south of the Porcupine–Destor deformation zone is shown in the southwestern corner of Map P.3547–Revised. Its axial trace is undulatory, strikes east-west, and dips north at a moderate angle. It is cut at its eastern end by a fault that terminates against the Porcupine–Destor deformation zone, and at the western end by a fault that also terminates against a faulted contact. Hence the fold is early. The rocks involved in the fold include chemical sediments (iron formation and chert), and most likely belong to upper parts of the Deloro assemblage. A fault to the north of this anticline has been named the Whitney thrust (Piroschco and Kettles 1991), and hence the implication is south-over-north movement, toward the Porcupine–Destor deformation zone. No further data is available to better interpret these faults. It may be a pre-Tisdale structure, or part of the thrusts described above.

DEFORMATION D3

The trends of S3 are relatively regular within the Tisdale assemblage basalts (Map P.3555), with an average strike of 281° and a dip of 77° to the northeast (Figure 16). This is the main foliation that is recognized in the Timmins camp, forming the obvious, spaced to near-penetrative foliation in the basalts, and a penetrative fabric that is folded in D4 crenulations in Timiskaming assemblage rocks. Hence, D3 deformation postdates Timiskaming sedimentation. Further to the north, the strike of S3 foliation swings slightly to a more westerly trend. Trends become much more irregular in the vicinity of the Timiskaming trough where D4 deformation is more intense, and is responsible for folding of S3 by F4 folds. This S3 foliation is axial plane to both the South Tisdale anticline (Photo 3) and to subordinate F3 folds overprinting the mainly F2 Porcupine syncline. The fact that the South Tisdale anticline and the Porcupine syncline fold axes plunge in different directions (northwest and east, respectively) shows that they cannot be wholly the product of the same generation of folds, if the two areas have undergone the same styles of deformation prior to F3. The Kayorum syncline is also probably an F3 fold, but it has an odd geometry that is interpreted here as a combination of F2 and F3 folding. S3 is also axial surface to folded trends of S2 (Map P.3555). The F3 South Tisdale anticline appears to terminate against the Porcupine–Destor deformation zone, and does not extend to the southern side of the deformation zone. These F3 folds also become less well defined to the northwest, with tight fold hinges becoming broad warps further northwest from the Porcupine–Destor deformation zone. These features may be interpreted to indicate that F3 folding was a result of oblique-slip movement along the major deformation zone, forming en echelon fold arrays. S2-S3 intersection lineations (L^2_3) generally plunge east (Figure 17), and this most likely reflects the effects of later deformation, in particular the strong constrictional strain affecting the Timiskaming assemblage.

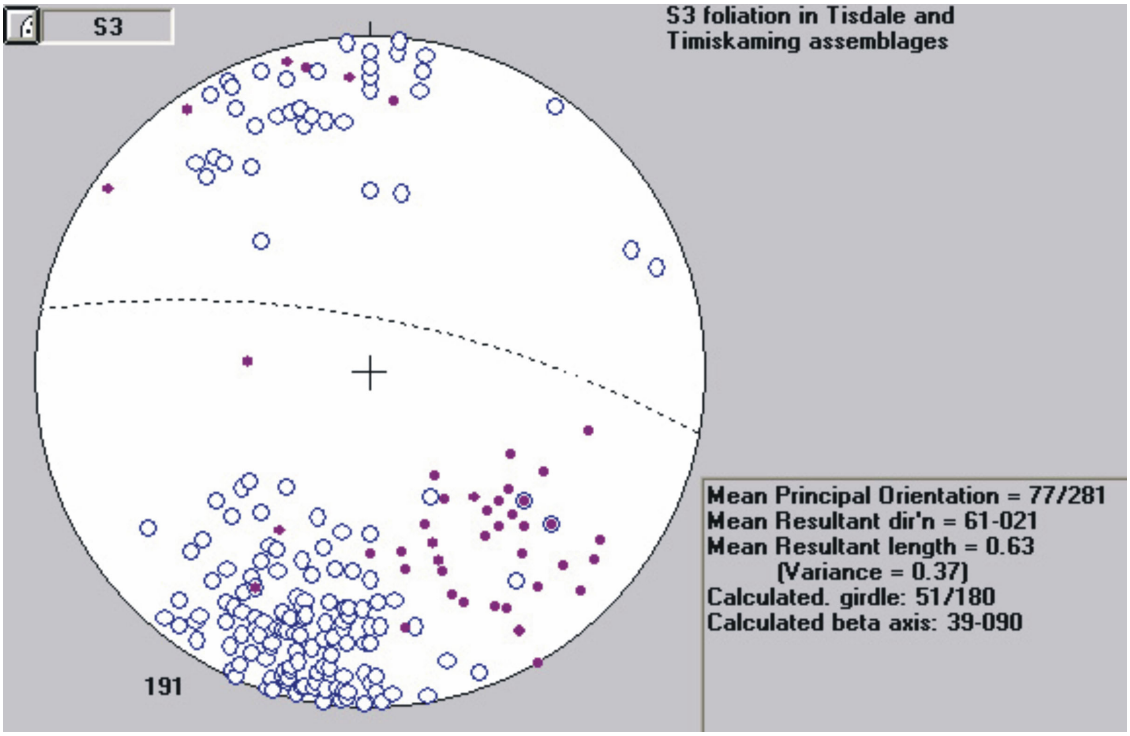

Figure 16. Stereoplot of poles to S3 foliations, circles represent Tisdale assemblage basalts and dots represent Timiskaming assemblage sediments. Average S3 dips 77°, strike (RHR) 281°.

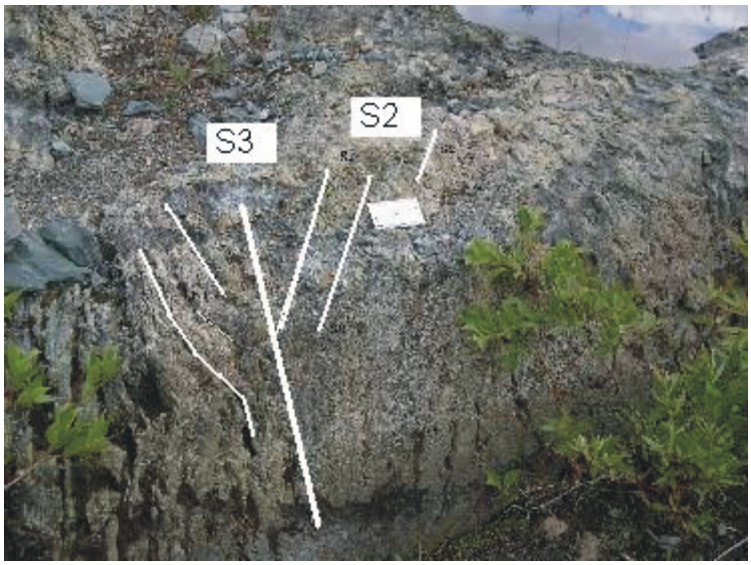

Photo 3. Intensely deformed Tisdale assemblage basalts, foliated in S2 and crenulated in S3. S3 is axial surface to the South Tisdale anticline. Location 04RJB0467, Vedron property, southeast of Timmins.

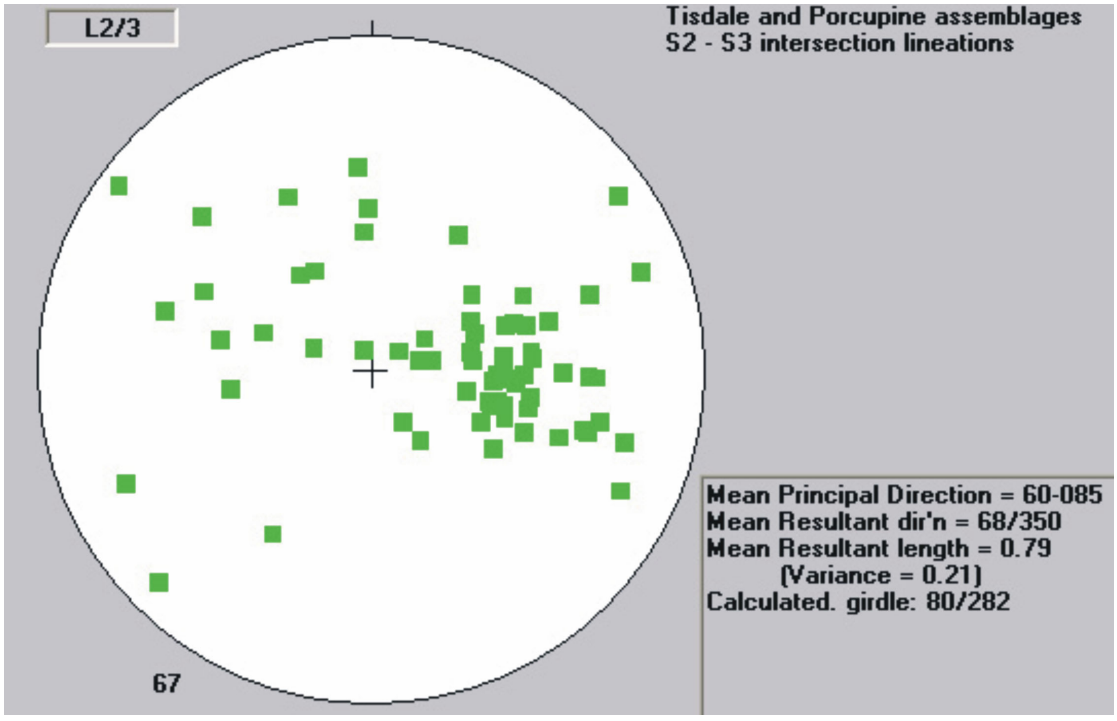

Figure 17. Stereoplot of S2-S3 intersection lineations, in Tisdale and Porcupine assemblage rocks in Tisdale Township.

S3 foliation cuts ankerite alteration in Tisdale assemblage basalts near Vedron mine (Photo 4), and quartz veins at Vedron within the South Tisdale anticline hinge are tightly folded with S3 along the axial surface (Photo 5). Thus, Vedron mineralization appears to be pre- to early-D3 deformation. In Whitney Township, S3 is recognized within S4 crenulations, where it is a penetrative foliation dipping moderately to steeply to the northwest within sedimentary rocks of the Timiskaming assemblage. Here, S3 commonly strikes more southwesterly (dip of 58° toward 328°, see Figure 16) than the overprinting west-southwesterly striking S4 foliation. S3 is present in Timiskaming assemblage rocks and so D3 is younger than 2679 Ma.

An important fact is that, while major F3 folds affect Tisdale and Porcupine assemblage rocks, rocks in the Timiskaming assemblage trough show only relatively local-scale F3 folding. An exception is the F3 folding (South Tisdale anticline) of the sliver of Timiskaming assemblage conglomerates at the Buffalo-Ankerite mine (Kinkel 1948). There is no clear evidence for map-scale F3 folding of the unconformity surface, except east of Pamour mine (Map P.3555) (Price and Bray 1948). At Dome mine, the sedimentary trough is considered to be primarily a feature of palaeotopography on the unconformity surface (E. Barr, personal communication, 2004), although this ancient ravine may have been appressed during D3 strain.

Bedding-S3 foliation intersection lineations, mainly in Timiskaming assemblage rocks (Figure 18), have variable fold plunges that lie along a girdle, which suggest that these folds have been refolded with a northwest-southeast trend.

Photo 4. Tisdale assemblage basalts, foliated in S3. S3 crosscuts and encloses lenses of pre-S2 ankerite alteration. Location 04RJB0342, near Vedron property.

Photo 5. Tisdale assemblage basalts, foliated in S3. S3 folds quartz veins. Location 04RJB0465, Vedron property.

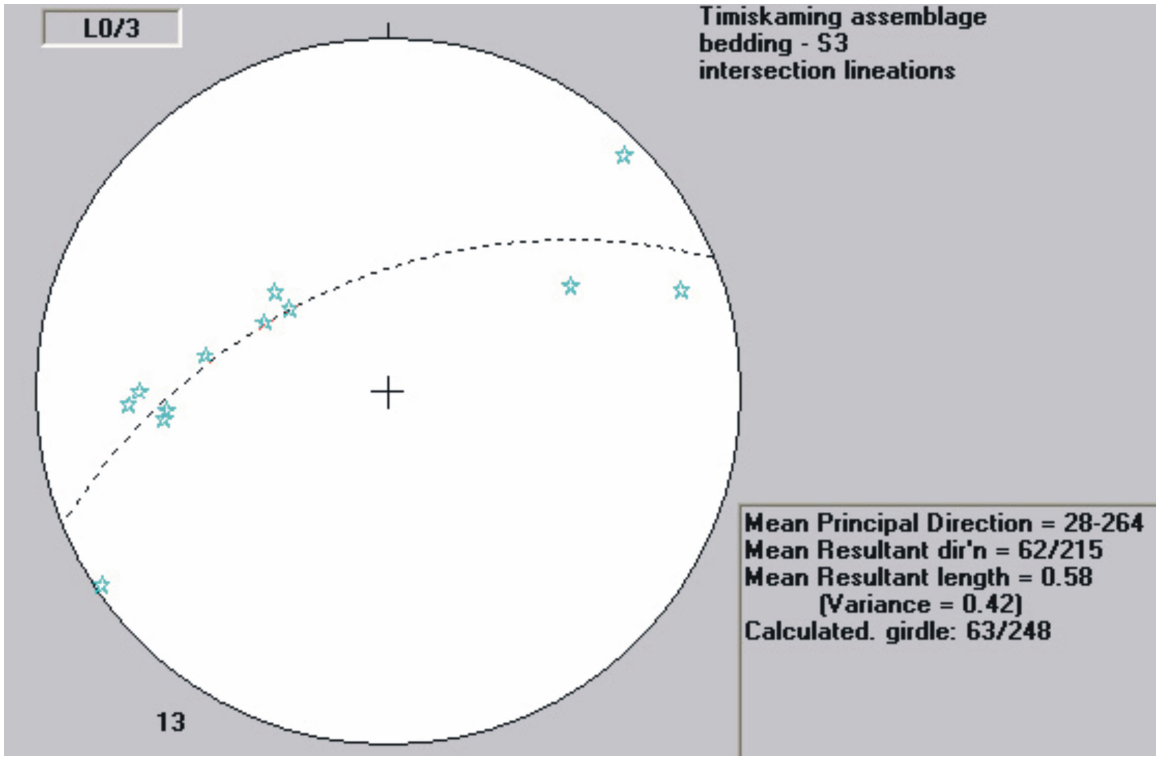

Figure 18. Stereoplot of bedding-S3 intersection lineations, mainly in Timiskaming assemblage rocks in Whitney Township.

DOME FAULT

Brittle faulting (Photo 6) forms a later stage of movement along the Porcupine–Destor deformation zone postdating thrusting, and is not directly related to ductile shearing. In most locations, the southern edge of the Timiskaming sediments is marked by a brittle fault which is interpreted as the eastward continuation of the Dome fault (Davies 1977), which is defined around Dome mine west of the Burrows–Benedict fault (see Figure 3). This fault is narrow, typically characterized by brittle features including veining and brecciation. Carbonate alteration and S3 and S4 foliation all overprint the fault zone. The Dome fault approximately parallels the unconformity along the southern limb of the D4 syncline hosting Timiskaming assemblage sediments, but in places the north-facing unconformity between the Tisdale and Timiskaming assemblages is intact. Three-dimensional information derived from a number of scissor diamond drill holes indicates that this faulted contact dips steeply north (Figure 19). At the Dome mine, it dips south near the surface and to the north at depth (Brisbin 1997). It cuts folding of undetermined generation: in most cases bedding in Timiskaming assemblage sediments faces away from the fault, but in some cases facing is down toward the fault. Therefore there are folds that are older than the fault, and the Dome fault is younger than the first phase of post-Timiskaming folding, F3. Data from drill holes are insufficient to identify folding of this fault. Commonly, the zone across this fault is not marked by strong ductile foliation, and there is also an angular discordance in pre-Timiskaming foliation across it. One possible interpretation of the curve of the fault trace from a west-southwest strike to a south strike in the vicinity of Dome mine in Tisdale Township is that it has been rotated by left-lateral strike-slip motion along the Porcupine–Destor deformation zone, just as F3 folds and S3 have slightly curvilinear trends.

Photo 6. There is an angular discordance in foliation across the Timiskaming–Tisdale contact in places within the Porcupine–Destor deformation zone. The sediments are much less deformed than the volcanics. Drill hole 18964, south of Pamour pit, Whitney Township (Porcupine Joint Venture).

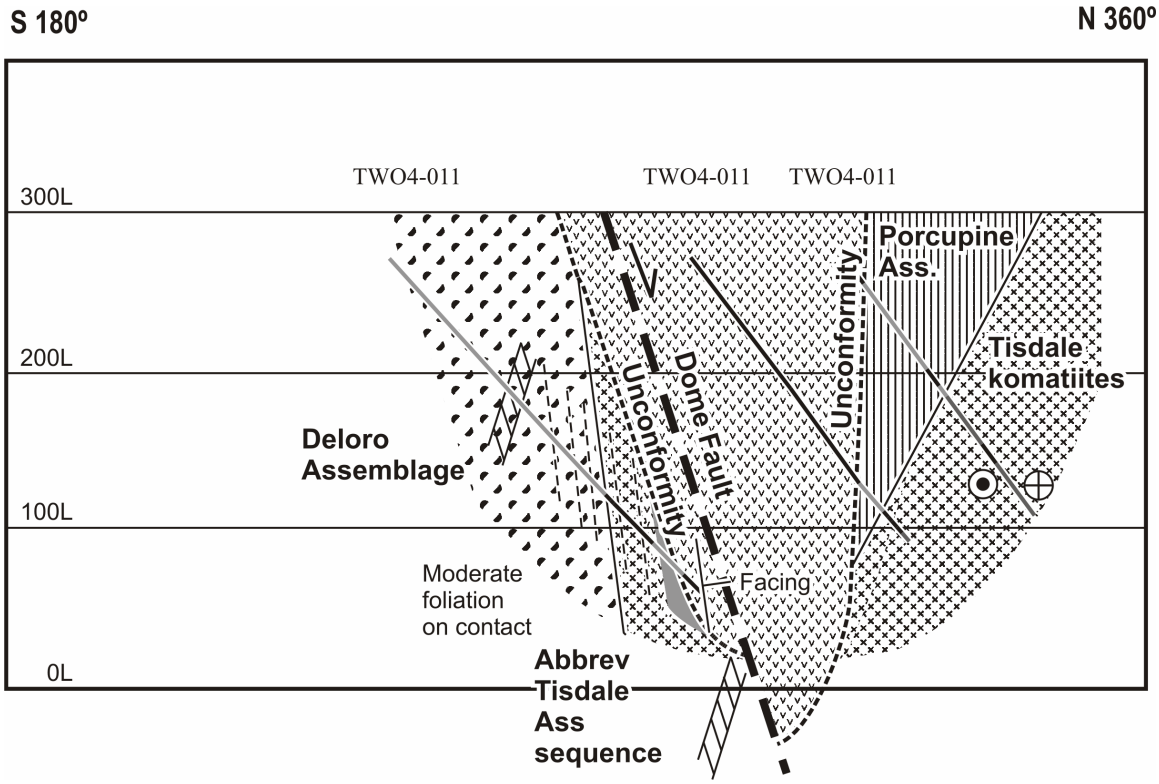

Figure 19. Cross section through the Dome fault in the western part of the area, along easting 472500.

There are inconsistencies in timing of the Dome fault and folding of Timiskaming assemblage sediments. The fault cuts minor folds, likely to be F3 since small F4 are less common. However, foliations postdate the fault, yet F3 folds do not seem to have affected the broad outline of the syncline, in particular the trend of the unconformity, even though S3 is imposed on both Timiskaming and older assemblages. This may be interpreted to indicate that sedimentation was synchronous with D3 deformation, and hence that D3 generated the Timiskaming assemblage basin. The Dome fault may have formed as a fault during transtensional D3 deformation, with left-lateral strike-slip motion along an anticlockwise curve in the trend of the Porcupine–Destor deformation zone opening the basin. The Dome fault may be the structure marking the faulted southern edge of a syn-D3 half-graben hosting Timiskaming sediments.

At the Dome Mine, the Dome fault is occupied by a melange of altered porphyry intrusions, carbonatized serpentinites, talc-chlorite schists and Timiskaming sedimentary rocks (Holmes 1968; Brisbin 1997). High-grade quartz-fuchsite and quartz-tourmaline auriferous veins are hosted by highly carbonatized and sericitized rocks within or in the vicinity of the Dome fault (Holmes 1968; Moritz and Crocket 1990). South of the Pamour mine, the Dome fault is overprinted by S4 foliation and carbonate alteration. Quartz-tourmaline veins crosscut the fault, and so it predates mineralization in the Timiskaming sediments and some of the deformation. Gold mineralization is associated with strike-slip D3 faulting and dip-slip reverse D4 faulting.

DEFORMATION D4

The major effects of D4 are mostly recorded in the eastern part of the study area (Map P.3547–Revised), where S4 is subparallel to the axial plane of the long trough containing the Timiskaming assemblage. S4 is a strong crenulation cleavage with a foliation spacing of 2-5 mm, overprinting S3. Its average strike is 254°, and dip is 70° to the north (Figure 20). The D4 deformation phase resulted in the formation of the syncline in which the Timiskaming assemblage rocks are preserved, and the S4 foliation is axial plane to this syncline. The syncline is asymmetrical, with a north-dipping, overturned northern limb. The southern limb is commonly cut off by the Dome fault, although restricted occurrences of north-facing sediments have been found: the Dome fault is broadly parallel to the syncline's southern limb. In general, the southern edge of Timiskaming sediments are not everywhere intensely deformed, and along its southern margin the Dome fault appears to be a brittle-ductile structure, and is likely a manifestation of Porcupine–Destor deformation zone activity, postdating ductile D2 strain. Remnants of Timiskaming sediments at the Buffalo-Ankerite pits and at Naybob mine site in Ogden Township (Ayer et al. 2003) also have S4 foliation. The Buffalo-Ankerite Timiskaming assemblage remnants appear folded by the large F3 South Tisdale anticline (Kinkel 1948). D4 strain seems to be oblate in the east (Photo 7), whereas intense prolate strain is recorded in Tisdale Township, which is attributed to the D5 phase of deformation (see below). The age of D4 is post Timiskaming (Ayer et al. 2003).

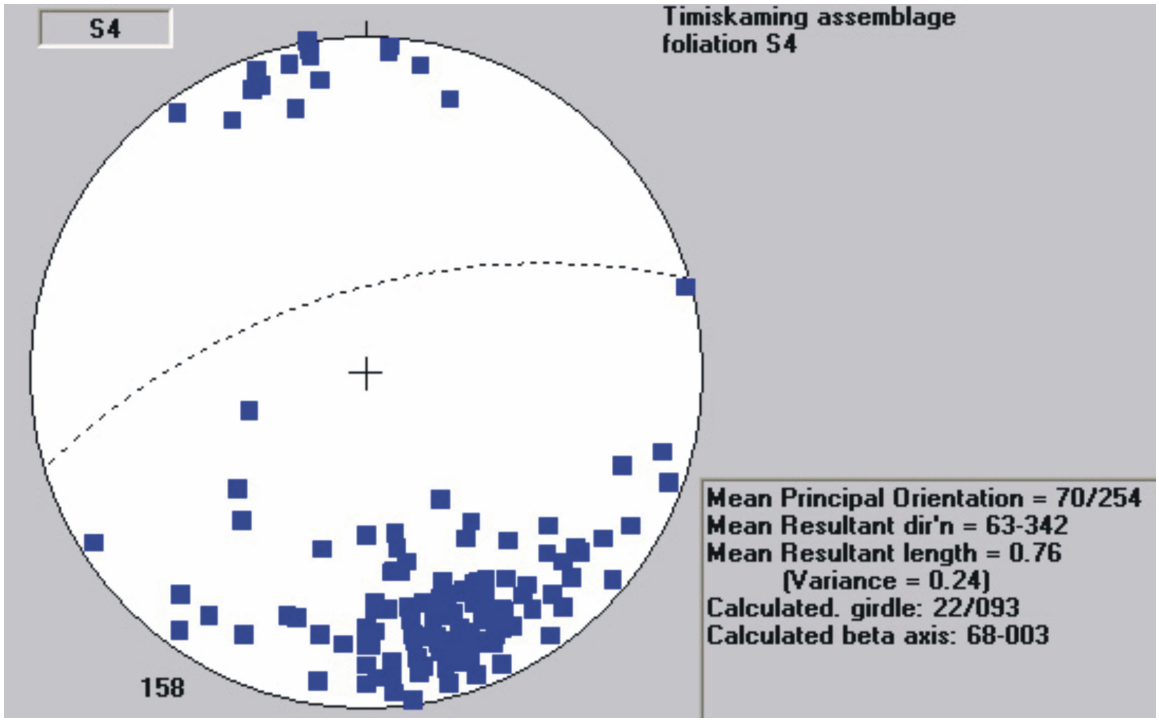

Figure 20. Stereoplot of poles to S4 foliation, mainly in Timiskaming assemblage rocks in Whitney Township. Average S4 dips 70°, strike (RHR) 254°.

Photo 7. Underside of bedding in Dome conglomerate in Timiskaming assemblage rocks, showing characteristic D4 flattening strain in pebbles (~10 cm across). No stretching is evident. Station 03RJB0057, Hoyle pit.

S4 foliation and deformation are not recorded in the Kidd Creek area (Bleeker 1999), so this event does not appear to have been regional in the Timmins district. Thus, S4 foliation is not widespread, and is largely restricted to the Timiskaming syncline along the Porcupine–Destor deformation zone. It is recognisable in the Tisdale assemblage lavas only as relatively weak and broad crenulations in the periphery of the Timiskaming trough. A number of minor folds (Z asymmetry, 1-100 m in amplitude) within the Timiskaming trough and between Pamour pit and the Hallnor fault (Photo 8) can be attributed to this event. Characteristically, these folds can not be followed far along the trend of the axial surfaces. These small folds mimic the Z asymmetry in S3 folded in F4 seen at the larger scale of the entire camp. The F4 fold axes, L^0_4 intersection lineations (bedding-S4: Figure 21) and L^3_4 intersection lineations (S3-S4: Figure 22) are very variable in plunge and lie on girdles identical to that for L^0_3 intersection lineations (bedding-S3). The intense constrictional strain best seen in Tisdale assemblage basalts and locally in Timiskaming pebbles evidently postdated S4 and these girdles are most likely the result of constriction and stretching superimposed on F4 axes. A major map-scale F4 fold with a southwest-trending axial surface is at the Hoyle Pond mine (southeast Hoyle Township). In this Z-asymmetry kink in the trend of the Hoyle Pond-Owl Creek volcanic belt, S4 is axial plane to these folds. Hoyle Pond quartz veins are also folded in F3 (Rhys 1999).

Quartz-albite-carbonate veins at Pamour mine within Timiskaming assemblage sediments formed late to post-S4. They are mostly straight and crosscut foliation, but some are weakly folded and are crosscut by S4 foliation and pressure-solved against it (Photo 9). In relative chronology, these veins are late to post D4 in timing. This contrasts with pre- or early-S3 veins elsewhere in the camp.

Photo 8. Greywacke in the Timiskaming assemblage, showing S4 foliation strain in pebbles (~10 cm across) and shallow-dipping extensional quartz-carbonate veins at high angle to the foliation. No stretching is evident. Station 03RJB022, Hoyle pit.

Photo 9. Minor folds in Timiskaming sediments are likely F3 folds. Looking east, location 04RJB01, north of South Porcupine townsite.

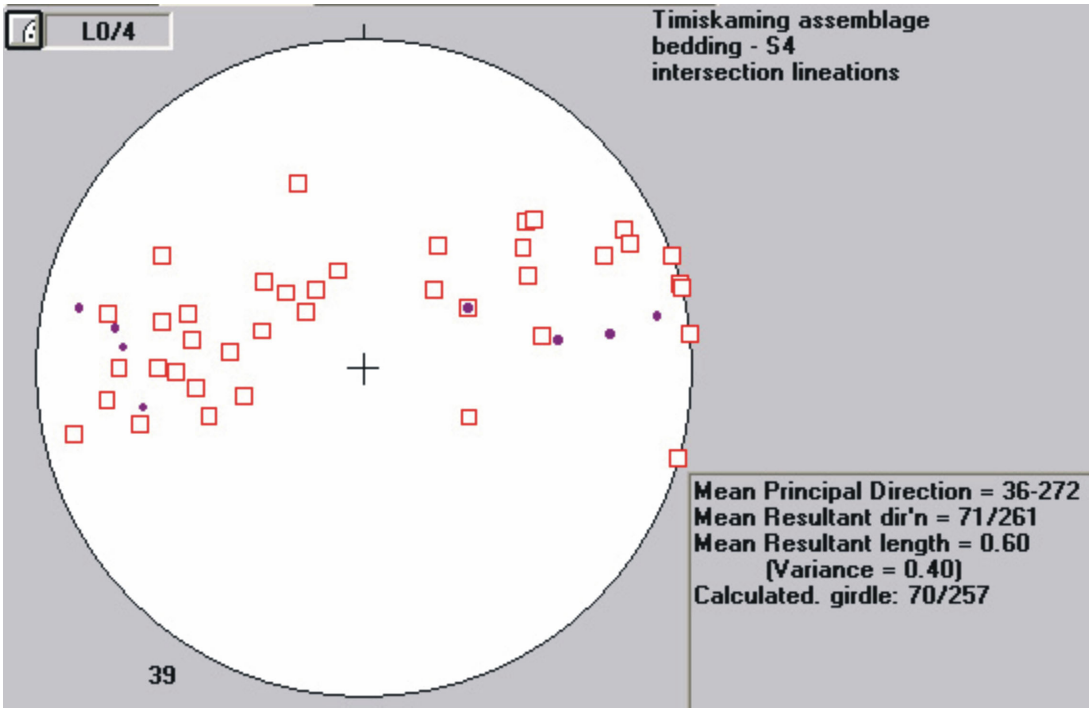

Figure 21. Stereoplot of bedding-S4 (L^0_4) intersection lineations (squares) and F4 fold axes (dots), mainly in Timiskaming assemblage rocks in Whitney Township.

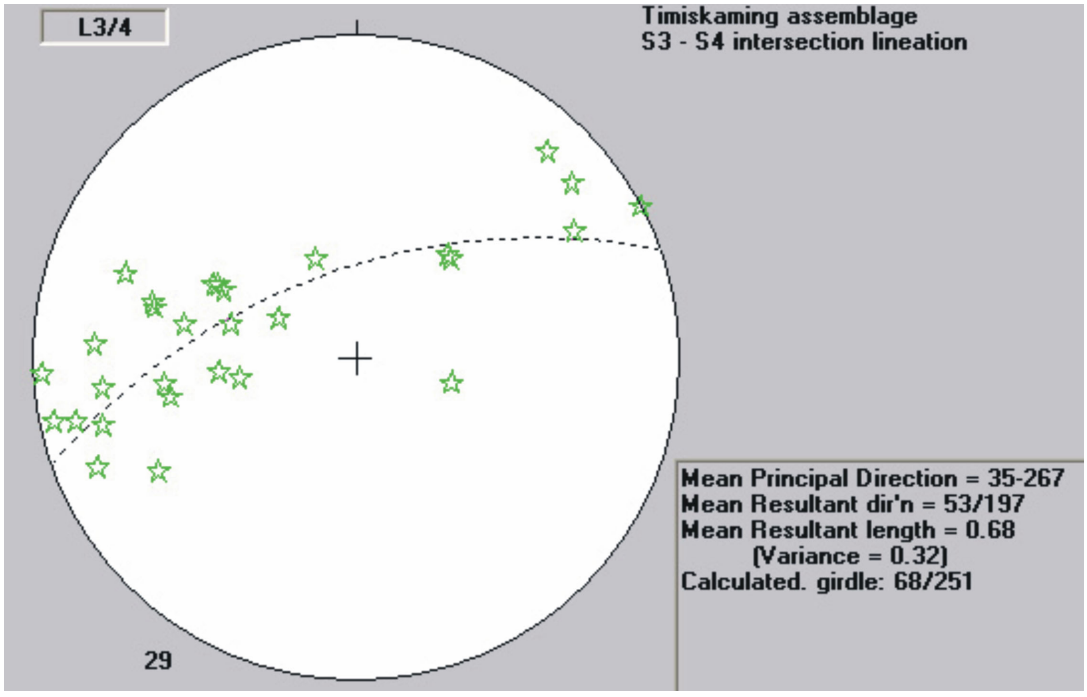

Figure 22. Stereoplot of S3-S4 (L^3_4) intersection lineations, mainly in Timiskaming assemblage rocks in Whitney Township.

The generation of S3-S4 foliation may be related to movement along the Porcupine–Destor deformation zone. On the regional scale, this area of occurrence of S4 lies along the Porcupine–Destor deformation zone and diminishes in intensity further away from the deformation zone, and so shows a strain gradient across the deformation zone. It may be related to basin inversion postdating Timiskaming sedimentation. Below, under discussion of the kinematics of the Porcupine–Destor deformation zone, right-lateral strike-slip movement is inferred, which would have converted a dilatation pull-apart basin that received Timiskaming assemblage sediments into a compressional jog.

D4 Dip Slip Faults

A number of faults have been identified in both the Pamour and Hoyle pit areas, some dipping moderately to the north and others dipping steeply south, with a reverse sense of movement (Aitken 1990). These structures host the 51, 62 and Three Nations fault-fill veins. Offsets can be seen in the open pit (Photo 10) that give north-over-south movement. Major faults can also be identified along the flanks of the mafic-ultramafic belts in the eastern half of the gold camp, where the volcanic-sediment contact is almost invariably marked by intensely deformed graphitic schists. Kinematic indicators are not available in the drill core where these shears have been identified, so movement could only be inferred from map-scale patterns. The fault along the northern edge of the Hoyle Pond volcanic belt is interpreted to be a F2 thrust, but otherwise the faults between Hoyle Pond and Pamour are interpreted as D4 reverse faults. These are particularly closely related to Pamour syn- to late-D4 mineralization (Aitken 1990), where fault-fill veins were emplaced along steeply dipping faults. Accompanying these are shallowly dipping sheeted arrays of extension veins (Photo 11).

CONSTRICTIONAL STRAIN D5

Deformation in southern Tisdale Township is characterized by locally intense constrictional strain (distinguished from intersection lineations and other weaker mineral stretching lineations), which produced very strongly stretched pillows (Photo 12), amygdales and variolites in Tisdale assemblage basalts and stretched lapilli in Krist formation volcaniclastic rocks over a large area (Map P.3555) of Tisdale Township, concentrated in an east-west-trending zone west of the Porcupine syncline. This constrictional strain is most prominent in the vicinity of the deviation of the Porcupine–Destor deformation zone from an east-northeast trend to the more northeast trend around Dome mine. Intense constriction is also found locally in pebbles in the Timiskaming assemblage sedimentary rocks at Buffalo-Ankerite and Dome mines. Strain is almost pure constriction (prolate ellipsoid), with ellipse ratios of up to 1:1:10. The constrictional lineation has a regular orientation: it plunges eastward at an angle of about 55° and is always slightly more shallow than the intersection lineation of S2 and S3, which plunges eastward at an angle of about 65° (Figure 17). Shallowly dipping thin quartz veins that indicate moderately steep extension crosscut ankerite alteration and are interpreted as contemporaneous with the D5 constrictional strain event (Photo 13).

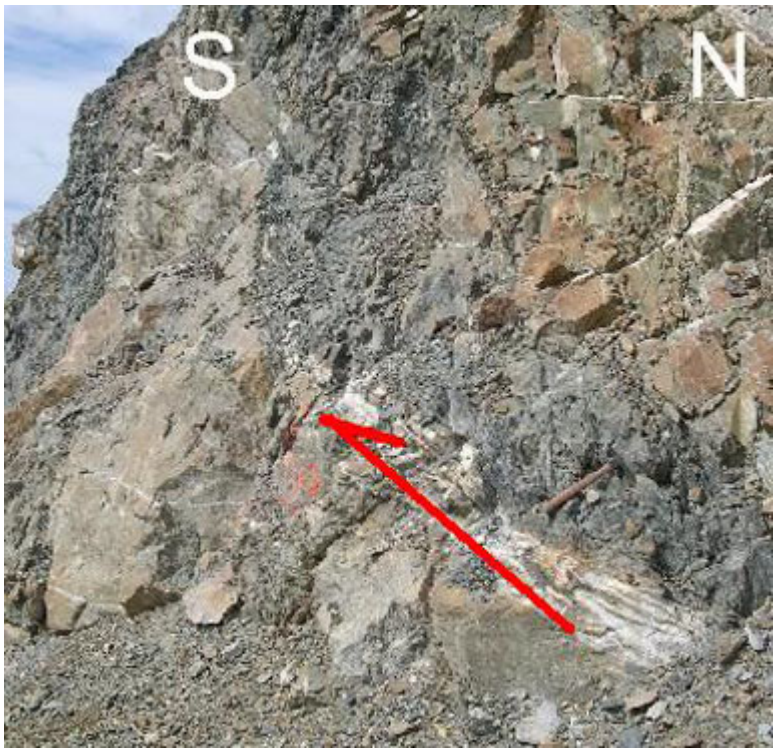

Photo 10. In northern Pamour pit, laminated fault-fill veins with associated extension quartz vein arrays indicate reverse north (right) block up during vein growth. Other quartz veins grew as extensional arrays.

Photo 11. South wall of Pamour pit in Three Nations formation, Timiskaming assemblage. Major veins dip east/left with a subordinate set in en echelon arrangement dipping more shallowly eastward. Location 03RJB0025.

Photo 12. Strongly stretched pillows deformed in intense constrictional strain formed cigar-shaped structures. Station 04RJB0471, Tisdale basalts, Maclean Street, north of Timmins

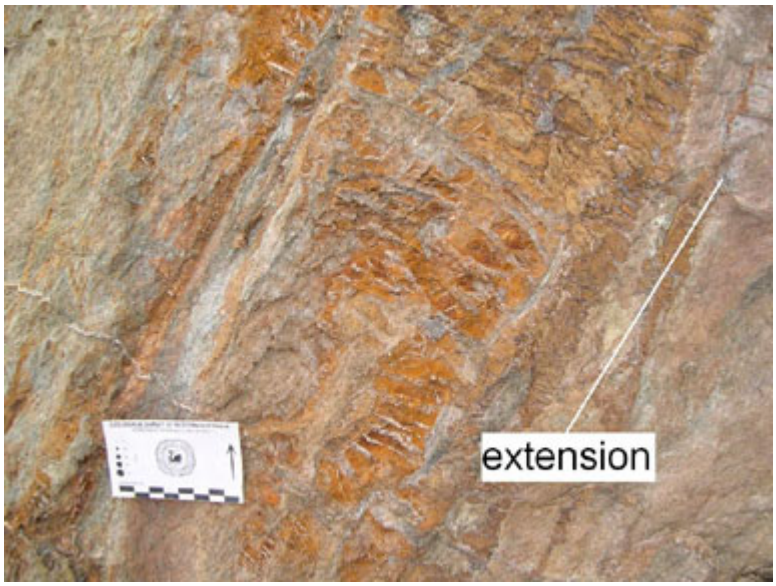

Photo 13. Blocks or lenses of early ankeritic alteration are cut by ladder quartz veins that are continuations of larger scale veins. The ladder veins are perpendicular to regional constrictional strain, and were opened during this event. Station 04RJB0331, on Highway 101 east of Timmins and south of McIntyre headframe.

The event to which this constriction can be assigned is not wholly clear, but enumerating it as an additional event makes most sense. Overprinting criteria are not useful as constriction postdating a foliation does not produce the same overprinting relationships as does one foliation overprinting another (Mason and Melnik 1986; Burrows et al. 1993). The constrictional lineation does not lie within the plane of S3, even after any hypothetical effects of D4 folding have been removed. Its orientation is at right angles to the intersection lineation L^3_4 in the plane of S4 (Figures 22 and 23). This lineation lies more closely to, but not exactly within, the plane of S4, between S3 and S4. It is sub-parallel to the S2-S3 intersection lineations (see Figure 17). Constriction and S4 foliation appear to be mutually exclusive, so one hypothesis is that this constrictional lineation is a late deformation increment of D4 strain. Constrictional strain does not appear to be consistent with F4, as the D4 fold axes have a variable plunge, and because most D4 strain in Whitney Township appears to be typically pure flattening (see Photo 8), not stretching. The variable L^0_3, L^3_4 and L^0_4 intersection lineations described above lie on very similar girdles, and are best interpreted as being due to this constrictional strain, postdating D3 and D4 deformation, and hence it is distinguished here as a later, D5 phase.

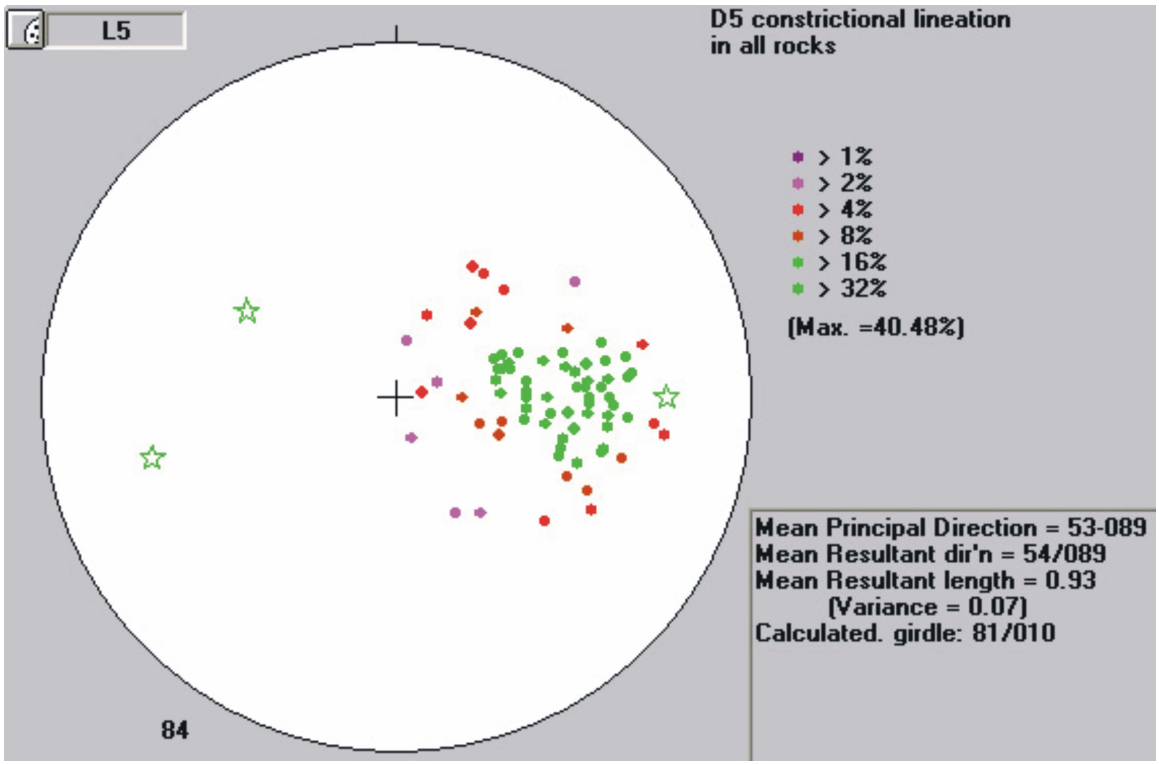

Figure 23. Stereoplot of D5 constrictional lineation, mainly in Tisdale assemblage basalts in Tisdale Township.

PORCUPINE–DESTOR DEFORMATION ZONE

The Porcupine–Destor deformation zone has long been recognized as the major structure of the area (Hurst 1936; Pyke 1982). It is generally described as a poorly exposed regionally extensive fault, approximately 150 m wide and characterized by steeply dipping penetrative foliations and talc-chlorite schists and serpentinite (Pyke 1982). The fault has been described (Bleeker 1997) as a steeply dipping, long-lived strike-slip structure, more than 450 km long, active between ca. 2680-2600 Ma with no significant difference in crustal level on either side and consequently negligible net dip-slip component

but with a minimum lateral offset of several kilometres. However, interpretations concerning the Porcupine–Destor deformation zone lack data, detail and clarity because of its poor exposure. Various previous maps of the area show the fault as a discrete surface rather than a zone, and in a variety of locations (Hodgson, Hamilton and Piroschco 1990; Piroschco and Kettles 1991). The general strain gradient is generally moderate across zones to the north of the Porcupine–Destor deformation zone, whereas the strain gradient along the strike of the deformation zone is important, where the intensity of the constrictional strain vs. flattening strain is considered. Diamond drilling indicates that the ductile component of the Porcupine–Destor deformation zone is a zone some hundreds of metres across consisting of anastomosing zones of high strain enclosing lower strain lozenges. The deformation zone occurs principally in ultramafic volcanic rocks of the Tisdale assemblage, but S4-foliated rocks of the younger Timiskaming assemblage also record considerable strain locally. There is no major contrast in metamorphic grade across the deformation zone (Bleeker 1997), and Tisdale assemblage rocks are exposed on both sides, so while it is difficult to estimate dip-slip offset, it cannot be extreme. In this work, 12 unoriented diamond drill cores were examined from 3 areas along its length within the map area (Figures 3, 24). Orientations can generally be deduced from unoriented core in isolated holes based on the assumption that foliations dip steeply and not subhorizontally, but a few scissor holes allow for less ambiguous interpretations.

A multi-stage, prolonged kinematic history is proposed for the deformation zone. Diamond drill cores display C-S structures in which the S foliation dips steeply north and the C planes dip south, with a mineral stretching lineation at a high angle to the C-S intersection, indicating dip-slip movement with south block up displacement along south dipping shears (Photos 14, 15). These are the dominant structure within the eastern drill holes. The ultramafic volcanic rocks are variably deformed, with alternating low-strain and high-strain intervals. This first phase of multi-stage deformation is concordant with D2 thrusting, and the Porcupine–Destor deformation zone is interpreted here as the root thrust from which the Fifth Avenue and other thrusts splay toward the north.

Photo 14. C-S fabric in intensely deformed Hersey Lake komatiites within the Porcupine–Destor deformation zone. These structures indicate dip-slip movement on a south-dipping zone of high strain. Drill core, hole 18986, from near Pamour mine (Porcupine Joint Venture).

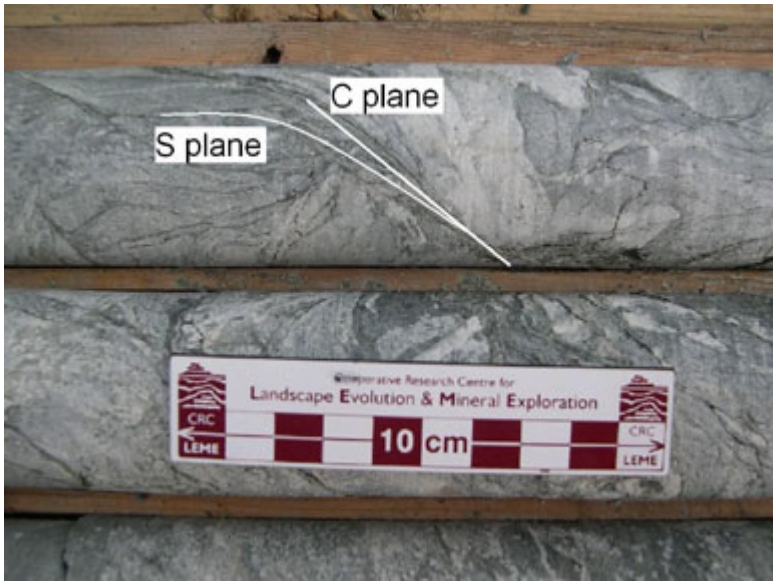

Photo 15. Deflection of S planes near parallel to core axis into C shear planes oblique to core in komatiite. Drill core, hole 18986, from near Pamour mine (Porcupine Joint Venture).

Granitoid dykes in the Porcupine–Destor deformation zone in southeastern Denton Township, 40 km southwest of the Timmins gold camp, have provided an age of 2689.3 ± 4.5 Ma (Hall and Smith 2002). These dykes are syn-tectonic with respect to right lateral strike slip movement of D2 age (Hall and Smith 2002) as indicated by the fact that the dykes crosscut the mylonite foliation yet are boundinaged within it, and folded (Photo 16). The dyke age is within error of the age of the Krist formation and the quartz-feldspar porphyry intrusive rocks, implying that D2 ductile movement in this zone had largely finished before Timiskaming sedimentation, and was related to the D2 thrusting event. The Timiskaming assemblage sedimentary rocks did not record this early thrusting strain. Moreover, in places there is an angular discordance in foliation orientation between Timiskaming assemblage rocks and ultramafic Tisdale assemblage rocks (Figure 24C), and so Timiskaming deposition appears to coincide with the change from dip-slip movement to D3 transpressional strike slip motion along the Porcupine–Destor deformation zone (Bleeker 1995).

D3 folds such as the South Tisdale anticline and elements of the Porcupine syncline are interpreted above as an en echelon array of folds formed during strike-slip movement, possibly related to the opening of the Timiskaming assemblage trough in a left-lateral dilatational jog along the Porcupine–Destor deformation zone. Poorly preserved, strike-slip C-S structures found in one hole in the west may record this second phase of strike-slip movement. The Timiskaming assemblage sedimentary rocks generally show lower strain than the Tisdale assemblage ultramafic rocks, which may suggest that the bulk of Porcupine–Destor deformation zone strain predated Timiskaming sedimentation (although sedimentary rocks and ultramafic lavas have very different competencies). In places, ultramafic volcanic rocks adjacent to the contact with Timiskaming assemblage rocks have a relatively low strain state compared with those further from the contact (Photo 17), indicating the ductile deformation zone was not likely responsible for juxtaposition of the Timiskaming assemblage against the older Tisdale assemblage rocks.

Photo 16. Syntectonic granodiorite dykes with an age of 2689.3 ± 4.5 Ma cutting mylonitized mafic metavolcanic rocks and folded by steeply plunging F2 folds (Hall and Smith 2002) (axial surface marked) within the Porcupine–Destor deformation zone along the Tatachikapika River in southeast Denton Township (NAD 83 UTM 453686E, 5350395N).

Photo 17. Brecciation and veining marks the contact between Timiskaming sediments and Hersey Lake komatiites within the Porcupine–Destor deformation zone. The ultramafic rocks are not highly deformed adjacent to the contact, but become more deformed further from the contact. The sediments are much less deformed than the volcanics. Drill hole 18964, south of Pamour pit, Whitney Township (Porcupine Joint Venture).

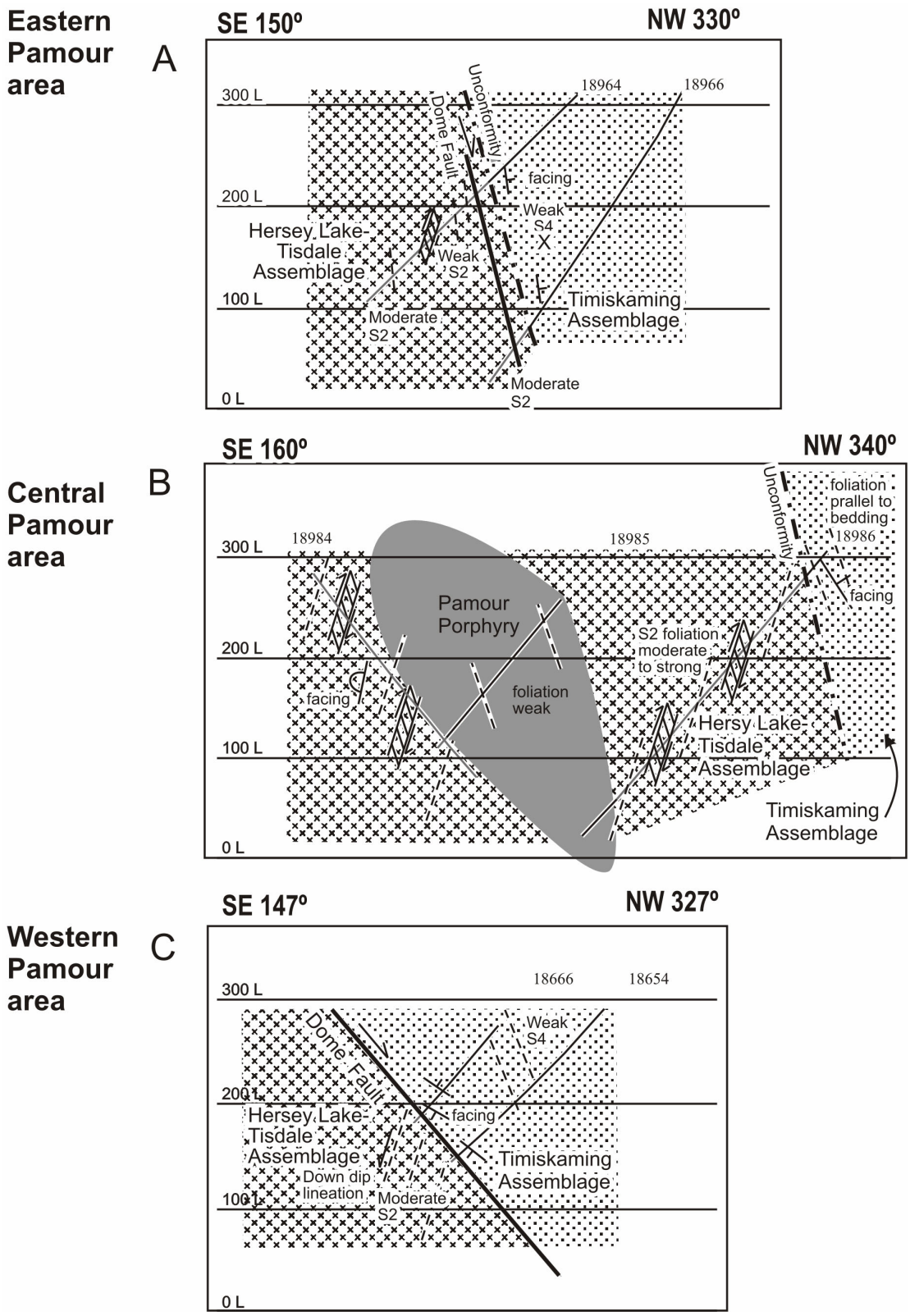

Figure 24. Three cross-sections through the Porcupine–Destor deformation zone, as mapped in diamond drill holes. Location of section shown in Figure 3.

The relationship between S3 and S4 foliations within Timiskaming assemblage rocks (plunge of intersection lineation, foliation vergence) can be interpreted as indicating oblique right lateral strike-slip movement. In Photo 18, S4 foliation in Timiskaming assemblage sediments crosscuts S3, which itself cuts quartz veining. The lower-strain lens of S3 foliation and deformed vein is deformed and wrapped by S4, very different to the D4 crenulations that typically deform S3 and are seen elsewhere in Photo 18, can be interpreted as indicating D4 right lateral movement. On the regional scale (Tisdale and Whitney townships), S3 foliation strikes northwest, but within the Timiskaming rocks where S4 is best developed, S3 commonly strikes northeast as a result of D4 folding in the F4 syncline holding Timiskaming assemblage sediments. Thus, S3 shows Z asymmetry with respect to S4. This suggests D4 deformation as part of late Porcupine–Destor deformation zone, similar to interpretations of the Larder Lake–Cadillac deformation zone (Wilkinson, Cruden and Krogh 1999). D5 constrictional strain is intense in a belt parallel to the Porcupine–Destor deformation zone adjacent to the inflection in its trend. This inflection would be compressional with right-lateral movement. D5 constriction is thus interpreted here as the result of strain in such a compressional jog during right-lateral transpression.

Photo 18. Highly strained and foliated Timiskaming assemblage sediments. Foliation S3 cuts early quartz veins, and is preserved within low-strain S4 pods. Asymmetry implies right-lateral movement during S4 formation. Hammer handle points north. Field station 03RJB08, Highway 101, 10 km east of Timmins, Whitney Township.

Tisdale and Porcupine assemblage rocks are identified on both sides of the deformation zone. On the south side of the Porcupine–Destor deformation zone, the structural history appears to be partly similar to that to the north. An early recumbent isoclinal fold involves chert and banded iron formation of the upper Deloro assemblage (southwest corner of Map P.3547–Revised). These folds are akin to those recognized as F2 thrust hanging-wall anticlines on the north side. Major folds in Whitney Township south of the Porcupine–Destor deformation zone with a east-northeast strike (subparallel to the Timiskaming trough) may be F4 folds, and map patterns (non-parallel limbs) suggest a significant northeast plunge for the fold axes. However, a northwest-striking major fault of unknown generation separates the 2 very distinct zones just described (with F2 and with F4 folds). Geologically and aeromagnetically, this inferred fault clearly terminates against the Porcupine–Destor deformation zone, and hence predates it.

DEFORMATION D6

The sixth deformation phase identified in the Timmins camp consists of flat-lying crenulations with relatively coarse microlithons up to 1 cm, that may be a product of late extensional collapse (Bleeker 1999), following D4-D5 basin inversion. D6 was a very minor deformation phase and generated no map- or outcrop-scale structures of any importance relative to gold mineralization.

DEFORMATION D7

The D7 deformation phase also appears to be a geometrically minor event with no F7 folds recognized at the map scale, and only a few structures at the outcrop scale. It consists of sporadic kinks and chevron folds (Photo 19) that strike north or north-northeast, and a steep axial surface and steep kink hinges. Z asymmetries are most common, and conjugate sets also occur. They are typically discontinuous and F7 affected zones have not been traced over any distance. Its effects are widespread, and have been noted by others (Bleeker 1999; Hall and Smith 2002). In particularly well-foliated rocks, such as around the Porcupine–Destor deformation zone, chevron-style folds are developed (Photo 19).

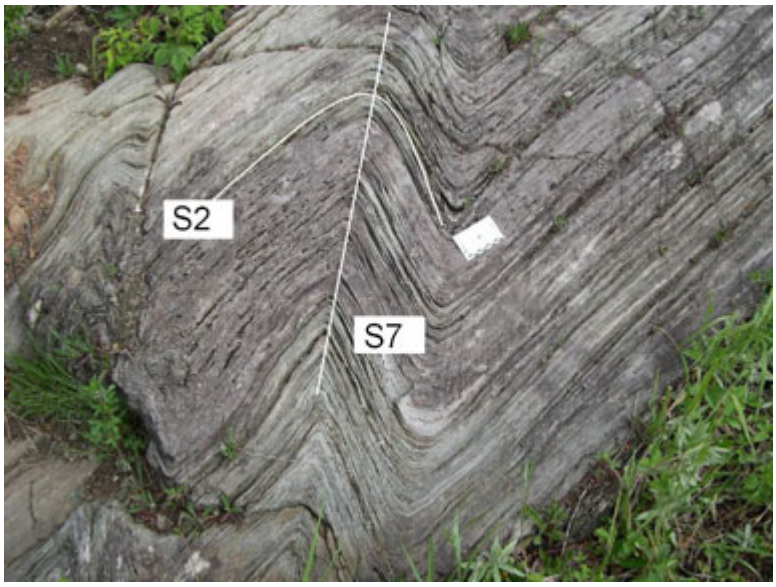

Photo 19. Schistose basalts in the Porcupine–Destor deformation zone. These have been strongly folded into chevron F7 folds. Location 04RJB240, powerline south of Timmins.

Some local geometrical features may be attributed to this event. In Broulan and Pamour pits, quartz veins normally occur as simple veins in swarms. Toward the tips of some, the veins break down into an array of en echelon veins (Photo 20). These arrays are parallel to the major single veins, but the arrays can also be interpreted as either rock bridges (Robert, Poulsen and Dubé 1994) or as a the product of east-over-west reverse movement. Also in Pamour pit are larger-scale en echelon sigmoid veins that are the product of west-over-east reverse movement. This orogen-parallel shortening is consistent with the kinematics of the kinks, and shows that vein growth occurred through D7 (Bateman, Ayer and Dubé 2003). The apparent continuity of D4 and D7 vein growth suggests that D7 was part of the major

Archaean deformation, and not some late event, unrelated to Archaean deformation. It is not known if these veins carried appreciable gold.

Photo 20. Quartz veins, Broulan pit. The veins that form extensional fracture arrays with respect to the major D4 fault-fill veins are in places themselves composed of en echelon vein arrays at the terminations of the first-order form extensional fracture arrays. The sense of shear implies east-over-west reverse shear. Looking southeast, location 03RJB091.

Late Strike Slip Faults

A suite of late, north-trending, strike-slip faults (Map P.3547–Revised), both left lateral and right lateral, crosscut both the Pamour and Hoyle Pond mafic belts. Maximum displacements of about 500 m (right lateral) are found on the Hallnor fault, and on an un-named fault on the south side of the Porcupine–Destor deformation zone (west of Bob's Lake). Otherwise, typical displacements of up to 50 m, both left lateral and right lateral, are distributed with no clear pattern along the length of the Timiskaming conglomerates. No sense of movement is dominant over the other, and total displacements for each movement sense appears equal (except that the 2 faults with 500 m displacement are both left lateral). Faults are brittle-ductile, with chlorite foliation only present within 10 cm of the fault plane. Subhorizontal striations confirm map-scale interpretation of strike slip. Since left-lateral and right-lateral strike-slip fault trends are bisected by the trend of S4, the strike-slip faults can be interpreted to have formed within the D4 stress field.

There is no correlation between gold and any strike-slip faulting. At Pamour pit, examination of historic level plans down to 165 m below surface (60 m (200 ft) level, 120 m (400 ft) level, and 180 m (600 ft) level shows that the alteration zones and the dip-slip faults are offset by these faults. These faults crosscut both the Timiskaming trough and the fault along its southern margin. Hence, this episode of faulting postdates gold mineralization, and is not important to it except as far as these faults dissect the ore zones.

Multiple Metamorphisms and Foliations

A foliation predating Timiskaming assemblage sedimentation in the Timmins gold camp has not previously been recognized or identified. However, evidence for such an early foliation is relatively widespread albeit not systematically interpreted in terms of regional folding. Folds interpreted regionally as D1 are commonly refolded and transposed by later deformation events, but where F1 fold trends have been discernible, they are typically northerly in orientation. Three examples include a broad anticline cored by the Kenogamissi Batholith (Ames et al. 1997); F1 folds with well-developed axial planar cleavages such as those observed in the Swayze belt (Heather 2001; Becker and Benn 2003); and northwest-trending folds in Deloro assemblage-aged iron formations in west-central Deloro Township (L.A.F. Hall, personal communication, 2004). These folds are cut by unfolded porphyry dykes which have been interpreted to be coeval with ca. 2690 Ma Krist formation volcanic units and syn-volcanic porphyry intrusions based on their identical geochemical characteristics. All these early folds have a well-developed axial planar fabric south of the Porcupine–Destor deformation zone.

Foliated clasts occur in Timiskaming assemblage sediments, with the internal foliation at a high angle to that of the enclosing conglomeratic sediments (Photo 21). There are several clasts observed of mafic composition, with a strong foliation internal to the clasts, that lies at a high angle to the S4 foliation in the enclosing Timiskaming assemblage sediments. This observation demonstrates that a strong foliation had been developed before erosion at the Timiskaming assemblage unconformity. The inference is that a greenschist grade foliation predates the deposition of Timiskaming assemblage rocks (Bleeker 1999), which are themselves foliated at greenschist grade. This has the important implication that Tisdale assemblage rocks were at a depth of ~10 km (Thompson 2004) when S2 foliation was acquired, ascended to the surface to be eroded prior to deposition of Timiskaming assemblage rocks, and went to a similar depth again to acquire S3 and S4. This process cannot have spanned much more than 10 Ma, and implies rapid rates of exhumation.

Photo 21. Mafic cobbles included in the basal conglomerate of the Timiskaming assemblage are outlined in both photos. In the close-up (left), the internal foliation of the pebble is shown truncated against the cobble edge. In the smaller-scale view (right), S4 foliation marked by flattened clasts lies at a high angle to the foliation internal to the clasts. Location 03RJB011, classic unconformity on ski trail, north of South Porcupine village.

Re-Os Geochronology of Timmins Gold-Molybdenite

Re-Os dating of molybdenite at the University of Alberta has provided a more direct method of determining the timing of molybdenite precipitation associated with gold deposition and thus could provide a more direct method to date gold mineralization than has the U-Pb zircon technique on the host rocks (Stein et al. 1998). A molybdenite selvedge to a quartz-dominated vein containing visible gold at the Dome mine provided a model age of 2670 ± 10 Ma, and a sample containing molybdenite and chalcopyrite in altered Pearl Lake porphyry gave a model age of 2661 ± 13 Ma for the age of the disseminated Cu-Au mineralizing event (Ayer et al. 2003). However, as this latter age had a large error and was therefore inconclusive, a second sample was taken from adjacent core in the same diamond-drill hole and was analysed as twin samples at the lab. Both of the second analyses are within the uncertainty of the first sample analysis. The weighted mean of the above analyses is 2672 ± 7 Ma, and this new date is the best indication of the age of the molybdenite and therefore the copper-gold mineralization in the Pearl Lake porphyry (Bateman et al. 2004). The value of the above Re-Os model ages overlap in error but in general supports the interpretation for an early disseminated Au-Cu event at McIntyre mine, followed by a later quartz-carbonate vein event at Dome mine.

Gold Mineralization: Kinematics and Timings

THE EASTERN ABITIBI SUBPROVINCE

The Abitibi greenstone belt hosts diverse styles of gold deposits showing various chronological relationships relative to deformation and metamorphism, and consequently were formed at different times and at different crustal levels (see Figure 2). These deposits are now juxtaposed along major crustal-scale faults such as the Porcupine–Destor and Larder Lake–Cadillac deformation zones (Robert and Poulsen 1997; Poulsen, Robert and Dubé 2000). Deposits that were formed before main-stage deformation include the LaRonde deposit and the Doyon mine located between Noranda and Val d'Or in the Doyon-Bousquet-LaRonde gold camp (Dubé et al. 2003). LaRonde is a giant pre-deformation Au-rich syn-volcanic volcanogenic massive sulphide deposit (Mercier-Langevin et al. 2004; Dubé et al. 2004) whereas Doyon is a world-class Au-Cu sulphide-rich vein-type deposit. The gold-bearing stockwork and sheeted veins at Doyon are deformed by the main foliation and mineralized veins in the West Zone are cut by pre-D2 deformation diorite dykes. These features suggest that the mineralization is pre- or early main-stage deformation. The Doyon deposit may be associated with the emplacement of a late magmatic phase (tonalite) of the multistage Mooshla pluton (Gosselin 1998; Galley, Pilote and Davis 2003). A pre-main stage deformation model has also been proposed for syenite-associated disseminated gold deposits (Robert 2001). The Sigma mine is a classic syn-deformation (orogenic) deposit (Robert and Brown 1986).

THE TIMMINS–PORCUPINE GOLD CAMP

Two key aspects in understanding gold mineralization are timing and kinematics. With these determined, it is possible to place a mineral deposit in the context of the district's deformation history, and to propose a structural model for its formation. It is also only then that predictions can be made: knowing the way a given deposit formed and the general structural history of the relevant district, loci of repeats of the critical combinations of stratigraphic and structural factors can be identified. The following is a distillation of published data on Timmins–Porcupine gold deposits relevant to this question. As indicated in this report, the geological setting of gold deposits in Timmins is highly complex and the timing relative

to deformation is commonly difficult to establish due to the complex structural evolution and the multiple generations of folds and foliations. However, the Timiskaming unconformity and the various porphyry intrusions combined with the detailed geochronological information available in the camp provide key chronological relationships that help to define the timing of the gold mineralization.

There have been suggestions that there are several relative timings for gold mineralization, and this is a particular line of enquiry here. The Cu-Au-Ag-Mo porphyry-style ore body hosted by the Pearl Lake porphyry at depth in the McIntyre mine has long been considered to be early (Mason and Melnik 1986). This early phase may be more widely developed that hitherto believed, as at Blueberry Hill near Dome mine (Gray and Hutchinson 2001). The presence of clasts of colloform-crustiform ankerite vein in the basal conglomerate of the Dome formation at Dome mine (Dubé, Williamson and Malo 2003) is good evidence for early hydrothermal alteration and low grade mineralization. Auriferous clasts found in the Timiskaming conglomerate at Pamour mine (Gray and Hutchinson 2001) have been interpreted as evidence for hydrothermal activity and mineralization predating the Timiskaming unconformity, however the timing of gold within the mineralized clasts has been disputed (Poulsen, Robert and Dubé 2000).

The Hollinger-McIntyre-Coniaurum Mines

The Hollinger-McIntyre deposit is the largest gold deposit in Canada. Mineralization is emplaced in south-facing mafic lavas of the Tisdale assemblage (Figure 3, Map P.3555). Early stage(s) of gold mineralization in the camp is indicated by the Cu-Au-Ag-Mo porphyry-style ore body hosted by the Pearl Lake porphyry (~2690 Ma) at depth in the McIntyre mine (Mason and Melnik 1986; Marmont and Corfu 1989). It also postdates an albitite dyke with an age of 2672 ± 1 Ma (see details above). Four stages are described (Burrows and Spooner 1986) comprising 1) chalcopyrite, hematite, molybdenite, anhydrite, pyrite, tourmaline, and ankerite; 2) bornite, chalcopyrite, albite; 3) sericite, pyrite; and 4) molybdenite, chalcopyrite, tetrahedrite. Stages 2 and 3 overprint the central anhydrite zone of stage 1. Overall, the Au:Ag ratio in the Cu-Au-Ag-Mo porphyry-style ore is about 1:5. Mineralization occurs as a series of lenses over 1200 vertical metres, plunging eastward parallel to the D5 constrictional lineation. The McIntyre Cu-Au-Ag-Mo mineralization is paragenetically early as it is cut by main-stage quartz-carbonate-Au veins.

Earlier components of the main stage mineralization consist of narrow ankerite-quartz veins that are crosscut by tourmaline and scheelite but little gold (Wood et al. 1986). Main-stage quartz-carbonate-Au veins comprise the major single concentration of gold ore (32 million ounces) in the Timmins–Porcupine camp. They crosscut veins that contain dominant quartz with subordinate ankerite-albite-scheelite-tourmaline-sulphides (sphalerite, chalcopyrite, pyrite, galena)-tellurides, and gold. Some early tourmaline veins show chocolate-tablet boudinage (Burrows et al. 1993), which cannot be an effect of late constriction. Wallrock alteration consists of sericite, ankerite, rutile, chlorite and sulphides. Veining is concentrated around the north and west of the Pearl Lake porphyry and along an east-northeast-trending belt of high strain. Maximum dimensions of the mineralized zone are 500 m x >5000 m length x 2400 m depth, with individual veins extending up to 300 m. The main stage Au veins cut the albitite dyke, the quartz-feldspar porphyry, and Cu-Au-Ag-Mo mineralization (Burrows et al. 1993; Rhys 2003). Vein geometries and kinematic indicators indicate vein formation during shear zone movement, with a sense of right lateral – oblique movement dominant over left lateral movement (Burrows et al. 1993; Rhys 2003). Other vein sets are confined within or between lithological units such as flows, and are controlled by competency contrasts (Burrows et al. 1993).

Vein arrays strike northeast and north-northeast. In the vein arrays, the main foliation (here enumerated S3) is rotated in the same manner as veins in the core of the array, and hence the shear is inferred to have been active during this deformation event (Burrows et al. 1993; Rhys 2003): D3. Veins

are in part strongly folded, boudinaged and transected by foliation (Rhys 2003), which is here interpreted as S4. A set of flat veins are also present, and were mined (Hall 1985). These flat veins splay off vertical veins and are probably a component of the same extensional fracture array.

The main-stage quartz-gold veins were interpreted (Mason and Melnik 1986) as the outermost zone of a porphyry-type hydrothermal system with a porphyry Cu core. This interpretation has not been accepted by other, later authors (Burrows et al. 1993).

These deposits represent the bulk of the gold mineralization in the Timmins district. However, a recent Re-Os molybdenite age of 2672 ± 7 Ma indicates that this stage of Cu-Au-Ag-Mo porphyry-style mineralization is not as early as originally thought (Mason and Melnik 1986), as it overlaps with the 2670 ± 10 Ma Re-Os age of molybdenite associated with an auriferous quartz vein at the Dome mine (Ayer et al. 2004), discussed above. This age, while having considerable uncertainty, is probably post-Timiskaming assemblage age. This early Cu-Au-Ag-Mo stage of mineralization could thus have formed early in the emplacement of the albitite dyke magmatic system, whereas the bulk of the quartz-carbonate gold veins post-date albitite dykes (Corfu et al. 1989). Dome mine contains comparable Cu-Au-Mo mineralization (Gray and Hutchinson 2001).

The Dome Mine

The Dome mine (Map P.3555) was the first deposit discovered in the Timmins–Porcupine camp. It consists of a complex assemblage of several vein types, some of which are found in both Timiskaming and Tisdale assemblage rocks. Ankerite(±quartz±tourmaline) veins extend over 500 m in strike, 900 m vertically, 2 m in width, and occur in arrays of sheeted veins subparallel to lithological layering (Pressacco 1999). They appear to occur exclusively in Tisdale assemblage volcanic rocks, and the presence of clasts of colloform-crustiform ankerite vein in the basal conglomerate of the Dome Formation at Dome mine (Dubé, Williamson and Malo 2003) suggests that these veins may predate Timiskaming assemblage sedimentation. Local millimetre-scale ankerite veinlets are injected into the basal conglomerate and suggest that ankerite veining outlasted the Timiskaming assemblage deposition. This suggests that the colloform-crustiform ankerite veins are pre- to syn-deposition of the conglomerate at the base of the Timiskaming unconformity. Steeply to moderately dipping quartz-tourmaline veins are well mineralized with gold. The relative timing of these 2 vein types is not clear, although small quartz-tourmaline veins are known to cut the ankerite veins (E. Barr, personal communication, 2003). At Aunor-Delnite mine (see below) the quartz-tourmaline veins form a younger crosscutting set. The most productive type of veins is the quartz veins hosted by the "dacite ore" and the sedimentary trough (Pressacco 1999). The dacite ore consists of intensely iron-carbonatized mafic lavas with arrays of gold-bearing quartz-ankerite veins that individually dip moderately to the northwest, and may comprise extensional vein arrays generated in both dip-slip and right-lateral shears. Distribution of dacite ore shows in places a spatial relationship to conglomerate-filled embayments in the Timiskaming assemblage unconformity. Porphyry ore, by definition, occurs in the Preston Porphyry and adjacent Tisdale assemblage mafic volcanics. It consists of quartz-ankerite-sulphide-gold veins that dip shallowly to the northwest, and so appear similar to dacite ore. "Sedimentary trough" ore is found in Timiskaming assemblage basal conglomerate and overlying slates (Pressacco 1999), and also extends into Tisdale assemblage rocks ("greenstone ore"), and is comprised of swarms of randomly oriented and locally folded quartz veins. Distribution is in part controlled by thickness of the conglomerate or irregularities in the unconformity surface. Arrays of gold-bearing moderately to shallowly dipping extensional quartz veins cut the ankerite veins at high angle. They are commonly better developed in the neck of the boudinaged ankerite veins and are consequently most probably contemporaneous with layer-parallel extension superimposed on these competent veins.

The quartz-fuchsite vein in the Dome mine is the highest grade part of the ore deposit (Moritz and Crocket 1991). It is a steeply southeast-dipping vein that strikes east-west parallel to lithological layering. The vein system is 500 x 500 x 3.5 m in extent, and it is emplaced into intensely carbonatized ultramafic volcanic rocks of the Tisdale assemblage, adjacent to greywackes of the Timiskaming assemblage to the north. It apparently does not occur in these sediments. Only subsidiary, associated quartz veining occurs in both Tisdale and Timiskaming assemblage rocks. It consists of both massive and discontinuous ribbon-textured quartz veins, which are coeval as they crosscut each other. The fuchsite is found in the laminae within ribbon veins. En echelon arrays of steeply dipping extension quartz veins indicate both left-lateral and right-lateral strike-slip movement. Timing of formation of the quartz-fuchsite vein is constrained by inclusions of foliated wall rock, serrated vein margins, folded quartz veins and crosscutting foliation (Moritz and Crocket 1990). The main foliation in the host rocks may be either S3 or S4 as described above, and cuts and postdates the quartz-fuchsite vein. Copper-Mo-Au mineralization is reported at Blueberry Hill (Gray and Hutchinson 2001), in close association with intrusive quartz-feldspar rocks. This form of mineralization is cut by a variety of quartz-gold veins.

Extensional quartz ladder veins also occur, crosscutting the ankerite, quartz-tourmaline, and ribbon quartz-fuchsite veins, some in association with boudinage of the quartz-fuchsite vein, and perpendicular to a slickenside striation that plunges steeply to the east. These observations imply that these veins were formed during D5 constrictional strain and near-vertical extension. They do not contain gold (Moritz and Crocket 1990; Pressacco 1999). A Pb-Pb age of 2266 ± 49 Ma (Worden, Cumming and Krstic 1995) may indicate a hydrothermal event, widespread in the Abitibi Subprovince. This event remobilized sulphides, and hence may have resulted in significant beneficiation of the ore. Thus, several episodes can be distinguished: the barren to low-grade ankerite veins are pre- to early-Timiskaming assemblage deposition; the quartz-fuchsite vein is possibly also of this age. Several styles of quartz-gold veins occur in both the sediments and volcanics, generally in arrays related to shears, but detailed kinematics and timings are not clear. Ladder and extension quartz veins date from D5 constrictional strain, but may not have introduced new gold.

The Aunor-Delnite and Buffalo-Ankerite Mines

The host rocks to these mines are pillowed mafic volcanics, which are enclosed within ultramafic lavas of the Tisdale assemblage Hersey formation. Veins comprise quartz-ankerite-pyrite-gold veins (5 mm to 5 m), contain some fuchsitic laminae, and have been compared to the ankerite veins at Dome mine (Brisbin 1997). Younger quartz-tourmaline-pyrite-gold veins crosscut and offset the quartz-ankerite veins. Individual veins strike east-northeast, and dip steeply to the north, subparallel to ore zones and to S3. Ore shoots plunge west at a shallow to moderate angle. Quartz-tourmaline veins occur in 2 apparent conjugate sets, the principal east-west set having right-lateral strike-slip offsets (Brisbin, Speidel and Mason 1987; Rhys 2003).

These 2 veins types are boudinaged and crosscut by a variety of quartz veins. Quartz-carbonate veining in the Buffalo-Ankerite pit extends across the Timiskaming unconformity into the sediments and conglomerates, where en echelon quartz-carbonate vein sets are found that indicate both northwest and southeast block up reverse movements (Photo 22). They crosscut S4 foliation, and may be akin in timing and kinematics to vein sets described below at Pamour mine. These may thus be syn- or late-D4. Some of these quartz veins carry gold adjacent to older veins, but do not everywhere contain gold, and so this gold may well be simply remobilized. They lie perpendicular to the host vein wall, and dip southwest perpendicular to the strong stretching lineation. Some are described as ladder veins, and are likely associated with D5 constriction.

Photo 22. En echelon quartz veins in Timiskaming assemblage conglomerate. Veins of this type crosscut ankerite veins in the mafic rocks. These veins indicate south block up reverse movement. Other veins in this mine are similar to the pre-Timiskaming ankerite veins at Dome mine. Location 04RJD0365, Buffalo-Ankerite pit, looking west.

The comparison of ankerite veins in the Delnite-Aunor-Buffalo-Ankerite-Vedron corridor with those at Dome mine suggest a pre-Timiskaming age for at least a component of the mineralization. Gold-bearing quartz veins and S2 foliation at Vedron are crosscut by S3 (see Photo 5) associated with the South Tisdale anticline. Hence, the Delnite-Aunor-Buffalo-Ankerite-Vedron mineralized corridor was likely originally a linear belt, later folded in F3. En echelon veins at Buffalo-Ankerite mine are younger still. These deposits may have formed in D2, with further mineralization in D4 post-Timiskaming assemblage sedimentation.

The Pamour Mine

At Pamour mine, 20 km east of Timmins (Figure 3, Map P.3547–Revised), the gold-bearing quartz-carbonate veins are mainly hosted by the Timiskaming sediments and in adjacent Tisdale (ultra)mafic volcanic rocks that lie to the north and below the Timiskaming unconformity. The major structures are the D4 syncline hosting the Timiskaming assemblage and the easterly extension of the F2 North Tisdale Anticline. F3 folds deform the sediments locally. Veins consist of quartz-albite-carbonate-gold± tourmaline and sulphides (pyrite-sphalerite±chalcopyrite±pyrrhotite ±arsenopyrite). Minor sericite occurs in the alteration halo. Three veining styles are recognized (Aitken 1990). Narrow veins (<1-3 m) hosted by the volcanics dip moderately north, more shallowly than the unconformity to the south. These veins crosscut stratigraphy, but are not fully developed in talc-chlorite schists. A set of veins that occur within the Timiskaming assemblage rocks are termed ‘TN’ veins (from Three Nations formation and lake). These dip steeply south, and converge slightly in strike eastward with the volcanic-hosted veins. These 2 veins types can extend for 500 m along dip and strike. These 2 vein types are associated with dip-slip fault movement (see Photo 10), consistent with D4 deformation, and are interpreted (Aitken 1990) as fault-fill veins. Quartz-pyrite(-other sulphides) extension fracture arrays occur to form bulk-minable ore, predominately in the Timiskaming assemblage sediments, and best within conglomerates. Where the volcanic-hosted veins approach the unconformity, they flatten in dip, and extension vein arrays appear in

the vein footwalls (Aitken 1990). Extension veins dip shallowly to the east-southeast and form shallowly east-plunging shoots. They are interpreted (Aitken 1990) as forming in extension fracture arrays associated with formation of the fault-fill veins.

The extension vein arrays crosscut S4 foliation, although they are locally crosscut (see Photo 10) and folded by this foliation. Strike-slip faults interpreted above as late in D4, crosscut and offset the ore bodies. Thus, Pamour ore formation is interpreted as syn-to late-D4 deformation (Bateman, Ayer and Dubé 2003). Several smaller mines in the area (Hallnor, Broulan, Hoyle, Bonetal) appear to exploit very similar deposits (Brisbin 1997). These deposits end around Pamour, and east of this point the dip of the unconformity is shallower. Perhaps this geometry, where volcanic-hosted veins and the unconformity dip at similar angles, prevents the intersection of the north-dipping volcanic-hosted veins with the unconformity, which is a prerequisite for the development of extension vein arrays.

The Hoyle Pond Mine

The Hoyle Pond mine lies 18 km northeast of Timmins (Figure 3, Map P.3547–Revised). It is a quartz vein-hosted gold deposit (Brisbin 1986; Pressacco 1999; Rhys 2003) hosted in folded Tisdale assemblage mafic-ultramafic volcanic rocks. This fold is interpreted here as the northernmost of the series of D2 thrust-related structures. Three vein types are recognized (Rhys 1999). The oldest veins, ribboned grey quartz veins (<3 m) with albite-tourmaline-hydromuscovite-carbonate-coarse gold, are folded and boudinaged in the main foliation (S3 or perhaps S4), and are folded around the map-scale fold (Figure 3, Map P.3547–Revised). Ribboned white quartz with folia of chlorite-muscovite-carbonate-pyrite-fine gold commonly dilate the older grey quartz veins, and splay off the grey vein footwalls as extension fracture arrays. Others of the set crosscut the grey veins and the map-scale fold. The white quartz veins may be deformed in the same event as the grey quartz veins, but to a lesser extent. They form oblique, right-lateral extension fracture arrays. Late extension quartz veins (a few centimetres thick, <4 m long) commonly occur in south-dipping extension fracture arrays, implying south block up reverse movement. Veins are localized within mafic volcanic rocks, or along their contacts.

The early vein distribution is complex, and has been folded in the main deformation interpreted as D3 in the area (Rhys 2003). Cross-cutting relationships with S3 foliation suggest a syn-D3 timing for the grey quartz and white quartz vein mineralization as a 2-stage early extensional fracture array (Rhys 1999). However, the axial trace of the major fold at Hoyle Pond mine lies at a high angle to other F3 folds such as the South Tisdale anticline and Porcupine syncline, yet parallels the F4 fold hosting Timiskaming assemblage sediments: the Hoyle Pond fold may therefore be F4, and hence it is possible that early veining is syn-D3 or at least pre-D4. The white quartz veins that are not folded at the map scale may be infill to fractures formed during late D3 shear after folding. Some veins parallel the axial surfaces of this F4 fold deforming the Porcupine and Tisdale assemblage (see Figure 3). The early mineralization at Hoyle Pond is thus most probably contemporaneous with D3, and later extension arrays with D4 deformation.

The Owl Creek Mine

The Owl Creek deposit (1.4 million ounces (Pressacco 1999)), northeast of Timmins and west of Hoyle Pond mine in the same northern belt of Tisdale assemblage mafic-ultramafic volcanic rocks, lies 4 km north of the Porcupine–Destor deformation zone (Map P.3547–Revised). It is a system of gold-bearing quartz-ankerite veins, lying in subvertical and subhorizontal orientations (Kingston 1987), emplaced into a sliver of Tisdale assemblage rocks along the contact with graphitic phyllite on the southern edge of this belt. This margin of the volcanic rocks marked by a graphitic phyllite is described as gouge material

(Coad et al. 1998) or a deformation zone characterized by dip-slip movement (Kingston 1987), and these faults strike parallel to lithological units. To the north and south of the Tisdale assemblage rocks are Porcupine assemblage greywackes (Coad et al. 1998; Pressacco 1999). Milled breccia and crack-seal vein textures suggest syn-deformation quartz vein formation (Coad et al. 1998). Cross-sections of gold-bearing veins (Coad et al. 1998; Pressacco 1999) suggest that veining was formed as relatively steep fault-fill veins (with wall-rock breccia fill) fringed by sets of subhorizontal or shallowly dipping arrays of extensional quartz veins. Veins are deformed by folding in shallowly dipping veins and boudinage of steeper veins (Brisbin 1986), and crosscut by 2 sets of left-lateral and right-lateral strike-slip faults (Brisbin and Pressacco 1999). By analogy with Pamour, these data may be interpreted as indicating syn-D4 ore formation, with late D4 folding and faulting of veins.

Conclusions and Implications

One new conclusion from this work is that a specific fabric (foliation or lineation) can be ascribed to 4 of the 5 major deformation events that affected the Timmins–Porcupine gold camp. D1 (no foliation) and D2-S2 predate the Timiskaming unconformity, whereas S3 and S4 postdate deposition of Timiskaming assemblage sediments. D5 constriction is a final component of this protracted orogeny. Other results include the identification of D1 extension, D2 south-over-north thrusting in the Porcupine–Destor deformation zone and the recognition of a stacked series of D2 thrust sheets north of the Porcupine–Destor deformation zone within the Timmins–Porcupine gold camp, with Tisdale assemblage lavas thrust over Porcupine assemblage sediments. The gold deposits lie in the hanging wall of these thrusts. Previous to identifying the stacked thrust sheets, these deposits appeared to lie in the footwall of the Porcupine–Destor deformation zone, a situation which conflicts with common observations for Archaean gold deposits elsewhere in the Abitibi Subprovince and the world generally (Robert 1990; Goldfarb, Groves and Gardoll 2001). D3 deformation is interpreted to represent oblique left-lateral transpressive deformation in the vicinity of the Porcupine–Destor deformation zone (Bleeker 1995). It is this event that opened the dilatation jog that was progressively filled with Timiskaming assemblage sediments. D4 showed an inversion to right-lateral strike-slip. These events were followed by intense D5 constrictional strain, especially in the area west of the flexure within the Porcupine–Destor deformation zone. Elsewhere in the Abitibi Subprovince, the Larder Lake–Cadillac deformation zone is interpreted as a zone of right-lateral transpression (Robert 1989). The Porcupine–Destor deformation zone went through a change in strike-slip movement similar to the Larder Lake–Cadillac deformation zone (Wilkinson, Cruden and Krogh 1999), where anticlockwise deviations of deformation zone trend underwent left-lateral motion. D2 (D3 in the scheme presented here for Timmins) had both left- and right-lateral strike-slip movement (within overall bulk shortening) along different parts of a curved Larder Lake–Cadillac deformation zone (Bleeker 1995; Wilkinson, Cruden and Krogh 1999). Their D3 event (D4 in Timmins) comprised right-lateral movement regardless of the variations in trend of the deformation zone. Data around Timmins do not allow for this more regional-scale interpretation.

Lesser components of hydrothermal and low-grade mineralization associated with extensive ankerite veining in the south (Dome, Aunor mines) predates the Timiskaming unconformity. The kinematic-tectonic setting is obscure, but may be related to D2 thrusting. Foliation identified as S3 was synchronous with extensional fracture arrays and quartz veining, and main-stage gold-quartz mineralization at Hollinger-McIntyre mines and in other deposits was early- to syn-D3. This stage was likely composite too, as the Cu-Au-Ag-Mo mineralization in the Pearl Lake porphyry is dated as being post-Timiskaming but is older than main-stage quartz-gold veins in Hollinger-McIntyre. The quartz veining was dominated by oblique (right-lateral-south block up) shear. D3 has been interpreted as left lateral, so these vein systems may represent antithetic R´ shear arrays. Late mineralization crosscuts S4 foliation with a minimum of deformation, as at Pamour mine. This was formed under north-south shortening, dip-slip

fault movement and related extensional fracture arrays. D5 constriction generated quartz ladder veins, but the evidence for introduction (rather than local remobilization) of additional gold is not conclusive.

This leads to the inference that some deposits hosted in the Tisdale and Timiskaming assemblage sediments comprise several distinguishable timings. The Cu-Au-Ag-Mo porphyry-style ore in the Pearl Lake porphyry in the McIntyre mine is considered to be early (Mason and Melnik 1986). Similar mineralization occurs at Blueberry Hill near Dome mine (Gray and Hutchinson 2001). Auriferous clasts found in the Timiskaming conglomerate at Pamour mine (Gray and Hutchinson 2001) have been interpreted as evidence for hydrothermal activity and mineralization predating the Timiskaming unconformity, but the timing of gold introduction in the clasts has been questioned (Poulsen, Robert and Dubé 2000). The presence of clasts of colloform-crustiform ankerite vein in the basal conglomerate of the Dome formation at Dome mine (Dubé, Williamson and Malo 2003) is better evidence for early hydrothermal low-grade mineralization. The post-Timiskaming deposits are likely to result from a single prolonged episode spanning 3 distinguishable but continuous deformation phases that may well represent 2 gold-bearing strain increments of a single large-scale protracted transpressive deformation and metallogenic event.

The protracted history of deformation, alteration and gold mineralization described in this report suggest a long-lived or multi-stage auriferous hydrothermal system, and indicates a plumbing system geometrically stable enough, and for long enough, to feed gold into a relatively small volume of rock throughout a period of transpressional deformation (Bateman, Hagemann et al. 2001). Diversity in timing emphasizes the need to consider the potential for diversity in style (veining, vein mineralogy, disseminated, sulfide-rich mineralization), alteration mineralogy (massive ankerite, sericite), sulphide and ore minerals (pyrite, tellurides) and metallic signature (Ag, Cu, Mo, W). Orogenic quartz-carbonate vein deposits are commonly spatially associated at the regional scale with Timiskaming-like regional unconformities and suggest an empirical relationship between large-scale greenstone quartz-carbonate gold deposits and regional unconformities (Hodgson 1993; Robert 2000; Dubé, Williamson and Malo 2003; Dubé et al. in press). In Timmins, geochronological results from the present study suggest a greater extent of Timiskaming assemblage sediments than previously recognized, since sediments previously assigned to the Porcupine assemblage contain young detrital zircons that suggest a Timiskaming assemblage age. Consequently, this expands the area that may contain large-scale gold deposits into areas previously not considered very prospective and hence secure guidance in seeking for hitherto unrecognized Timiskaming assemblage sediments – which clearly remain a first order key exploration target in the area.

Acknowledgements

D. Rhys gave a lot of time in discussing these ideas, and we thank him for his efforts and contributions. B. Atkinson, L. Hall and P. Thurston all gave valuable early help in coming to grips with Timmins geology. The Porcupine Joint Venture, Placer Dome Group gave generous access to a wide diversity of valuable data, and their geologists E. Barr, K. Green, G. Hall, S. Harding, B. MacRae, M. Nerup and A. Still all gave great assistance. The Resident Geologist's office, Ontario Ministry of Northern Development and Mines in Timmins, helped in a great many ways. The organizers and managers of the Discover Abitibi Initiative and of the Timmins Economic Development Corporation made the project possible. The Discover Abitibi Initiative is a regional, cluster economic development project based on scientific investigations of the western Abitibi greenstone belt. The initiative, centred on the Kirkland lake and Timmins mining camps, is directed by the local stakeholders. FedNor, Northern Ontario Heritage Corporation, municipalities and private sector investors have provided the funding for the Initiative.

References

Aitken, S.A. 1990. The Pamour One mine-site investigation, Timmins, Ontario; unpublished MSc thesis, Queen's University, Kingston, Ontario, 194p.

Ames, D.E., Bleeker, W., Heather, K.B. and Wodicka, N. 1997. Timmins to Sudbury transect: new insights into the regional geology and setting of mineral deposits; Geological Association of Canada, Field Trip Guidebook, B6, p.1-37.

Ayer, J.A., Amelin, Y., Corfu, F., Kamo, S.L., Ketchum, J.W.F., Kwok, K. and Trowell, N. 2002. Evolution of the southern Abitibi greenstone belt based on U-Pb geochronology: autochthonous volcanic construction followed by plutonism, regional deformation and sedimentation; Precambrian Research, v.115, p.63-95.

Ayer, J.A., Barr, E., Bleeker, W., Creaser, R.A., Hall, G., Ketchum, J.W.F., Powers, D., Salier, B., Still, A. and Trowell, N.F. 2003. Discover Abitibi. New geochronological results from the Timmins area: implications for the timing of late-tectonic stratigraphy, magmatism and gold mineralization; *in* Summary of Field Work and Other Activities 2003, Ontario Geological Survey, Open File Report 6120, p.33-1 to 33-11.

Ayer, J.A., Berger, B.R., Johns, G., Trowell, N., Born, P. and Mueller, W. 1999. Late Archean rock types and controls on gold mineralization in the southern Abitibi greenstone belt of Ontario; Geological Association of Canada–Mineralogical Association of Canada, Joint Annual Meeting, Sudbury 1999, Field Trip B3 Guidebook, 73p.

Ayer, J.A., Ketchum, J.W.F. and Trowell, N. 2002. New geochronological and neodymium isotopic results from the Abitibi greenstone belt, with emphasis on timing and implications of neorchean sedimentation and volcanism; *in* Summary of Field Work and Other Activities 2002, Ontario Geological Survey, Open File Report 6100, p.5-1 to 5-16.

Ayer, J.A., Thurston, P.C., Bateman, R.J., Dubé, B., Gibson, H.L., Hamilton, M.A., Hathway, B., Hocker, S., Houlé, M., Hudak, G., Ispolatov, V., Lafrance, B., Lesher, C.M., MacDonald, P.J., Peloquin, A.S., Piercey, S.J., Reed, L.E. and Thompson, P.H. 2005. Overview of results from the greenstone architecture project: Discover Abitibi Initiative; Ontario Geological Survey, Open File Report 6154.

Ayer, J.A., Thurston, P.C., Dubé, B., Gibson, H.L., Hudak, G., Lafrance, B., Lesher, C.M., Piercey, S.J., Reed, L.E. and Thompson, P.H. 2004. Discover Abitibi greenstone architecture project: overview of results and belt-scale implications; *in* Summary of Field Work and Other Activities 2004, Ontario Geological Survey, Open File Report 6145, p.37-1 to 37-15.

Ayer, J.A., Trowell, N.F. and Josey, S. 2004. Geological compilation of the Abitibi greenstone belt; Ontario Geological Survey, Miscellaneous Release–Data 143.

Bateman, R.J., Ayer, J.A., Barr, E., Dubé, B. and Hamilton, M.A. 2004. Discover Abitibi. Gold Subproject 1. Protracted structural evolution of the Timmins–Porcupine gold camp and the Porcupine–Destor deformation zone; *in* Summary of Field Work and Other Activities 2004, Ontario Geological Survey, Open File Report 6145, p.41-1 to 41-10.

Bateman, R.J., Ayer, J.A. and Dubé, B. 2003. Discover Abitibi. Gold Subproject 1. Structures and gold mineralization in the Pamour–Hoyle Pond portion of the eastern Timmins gold camp; *in* Summary of Field Work and Other Activities 2003, Ontario Geological Survey, Open File Report 6120, p.34-1 to 34-6.

Bateman, R.J., Costa, S., Swe, T. and Lambert, D. 2001. Archaean mafic magmatism in the Kalgoorlie area of the Yilgarn Craton, Western Australia: a geochemical and Nd isotopic study of the petrogenetic and tectonic evolution of a greenstone belt; Precambrian Research, v.108, p.75-112.

Bateman, R.J., Hagemann, S.G., McCuaig, T.C. and Swager, C.P. 2001. Protracted gold mineralization throughout Archaean orogenesis in the Kalgoorlie camp, Yilgarn Craton, Western Australia: structural, mineralogical, and geochemical evolution; *in* World-class gold camps and deposits in the eastern Yilgarn Craton, Western Australia, with special emphasis on the Eastern Goldfields Province, Fourth International Archaean Symposium, Geological Survey of Western Australia, Record, v.2001/17, p.63-98.

Becker, J.K. and Benn, K. 2003. The Neoarchean Rice Lake Batholith and its place in the tectonomagmatic evolution of the Swayze and Abitibi granite-greenstone belts, northeastern Ontario; Ontario Geological Survey Open File Report 6105, 42p.

Berger, B.R. 1998. Precambrian geology - Hoyle and Gowan townships; Ontario Geological Survey, Report 299, 49p.

Bleeker, W. 1995. Surface geology of the Porcupine camp; Geological Survey of Canada, Open File 3141, p.13-47.

———1997. Geology and mineral deposits of the Porcupine camp; Geological Association of Canada, Field Trip Guidebook, B6, p.10-37.

———1999. Structure, stratigraphy and primary setting of the Kidd Creek volcanogenic massive sulphide deposit: a semiquantitative reconstruction; *in* The giant Kidd Creek volcanogenic massive sulphide deposit, western Abitibi Subprovince, Canada, Society of Economic Geologists, Economic Geology Monograph 10, p.71-122.

Bleeker, W., Parrish, R.R. and Sager-Kinsman, S. 1999. High-precision U-Pb geochronology of the late Archean Kidd Creek deposit and surrounding Kidd volcanic complex; *in* The giant Kidd Creek volcanogenic massive sulphide deposit, western Abitibi Subprovince, Canada, Society of Economic Geologists, Economic Geology Monograph 10, p.43-69.

Born, P. 1995. A sedimentary basin analysis of the Abitibi greenstone belt in the Timmins area, northern Ontario, Canada; unpublished PhD thesis, Carleton University, Ottawa, Ontario, 489p.

Brisbin, D.I. 1986. Geology of the Owl Creek and Hoyle Pond gold mines, Hoyle Township, Ontario; unpublished MSc thesis, Queen's University, Kingston, Ontario, 47p.

———1997. Geological setting of gold deposits in the Porcupine gold camp, Timmins, Ontario; unpublished PhD thesis, Queen's University, Kingston, Ontario, 523p.

Brisbin, D.I. and Pressacco, R. 1999. World-class Archean vein gold deposits of the Porcupine camp, Timmins, Ontario; Geological Association of Canada–Mineralogical Association of Canada, Joint Annual Meeting, Sudbury 1999, Field Trip A3 Guidebook, 98p.

Brisbin, D.I., Speidel, F. and Mason, R. 1987. Grant 298B. Geology of the North Zone of the Delnite mine at Timmins, Ontario; Ontario Geological Survey, Miscellaneous Paper 136, p.224-229.

Buffam, B.S.W. 1948. Moneta Porcupine mine; *in* Structural Geology of Canadian Ore Deposits, Canadian Institute of Mining and Metallurgy, v.1, p.457-464.

Burrows, A.G. 1924. The Porcupine gold area; Ontario Department of Mines, Annual Report, v.33, pt.2, p.1-84.

———1911. The Porcupine gold area; Ontario Department of Mines, Annual Report, v.20, pt.2, p.3-33.

———1912. The Porcupine gold area (second report); Ontario Department of Mines, Annual Report, v.21, pt.1, p.205-249.

———1915. The Porcupine gold area (third report); Ontario Department of Mines, Annual Report, v.24, pt.3, p.1-57.

Burrows, D.R. and Spooner, E.T.C. 1986. The McIntyre Cu-Au deposit, Timmins, Ontario, Canada; *in* Proceedings of Gold '86: An International Symposium on the Geology of Gold, Konsult International, Toronto, p.23-39.

Burrows, D.R., Spooner, E.T.C., Wood, P.C.,and Jemielita, R.A. 1993. Structural controls on formation of the Hollinger-McIntyre Au quartz vein system in the Hollinger Shear Zone, Timmins, southern Abitibi greenstone belt, Ontario; Economic Geology, v.88, p.1643-1663.

Calvert, A.J. and Ludden, J.N. 1999. Archean continental assembly in the southeastern Superior Province of Canada; Tectonics, v.18, p.412-429.

Carlson, H.D. 1967. Geology of Ogden, Deloro and Shaw townships, District of Cochrane; Ontario Department of Mines, Open File Report 5012, 124p.

Chown, E.H., Harrap, R. and Mouksil, A. 2002. The role of granitic intrusions in the evolution of the Abitibi belt, Canada; Precambrian Research, v.115, p.291-310.

Coad, P.R., Brisbin, D.I., Labine, R.J. and Roussain, R. 1998. Geology of the Owl Creek gold mine, Timmins, Ontario; Canadian Institute of Mining and Metallurgy, Bulletin, v.7, p.271-286.

Corfu, F. 1993. The evolution of the southern Abitibi greenstone belt in light of precise U-Pb geochronology; Economic Geology, v.88, p.1323-1340.

Corfu, F., Krogh, T.E., Kwok, Y.Y. and Jensen, L.S. 1989. U-Pb zircon geochronology in the southwestern Abitibi greenstone belt, Superior Province; Canadian Journal of Earth Sciences, v.26, p.1747-1763.

Daigneault, R., Mueller, W. and Chown, E.H. 2002. Oblique Archean subduction: accretion and exhumation of an oceanic arc during dextral transpression, Southern Volcanic Zone, Abitibi Subprovince, Canada ; Precambrian Research, v.15, p.261-290.

Davies, J.F. 1977. Structural interpretations of the Timmins mining area, Ontario; Canadian Journal of Earth Sciences, v.14, p.1046-1053.

Davis, W.J., Lacroix, S., Gariepy, C. and Machado, N. 2000. Geochronology and radiogenic isotope geochemistry of plutonic rocks from the central Abitibi Subprovince: significance to the internal subdivision and plutono-tectonic evolution of the Abitibi belt; Canadian Journal of Earth Sciences, v.37, p.117-133.

Dimroth, E., Imreh, L., Goulet, N. and Rocheleau, M. 1983. Evolution of the south-central segment of the Archean Abitibi belt, Quebec, part II: Tectonic evolution and geomechanical model; Canadian Journal of Earth Sciences, v.20, p.1355-1373.

Dinel, E. and Fowler, A.D. 2004. Discover Abitibi. Preliminary results of the geology and geochemistry of the volcanic rocks hosting the Hoyle Pond mine, Timmins, Ontario; *in* Summary of Field Work and Other Activities 2004, Ontario Geological Survey, Open File Report 6145, p.46-1 to 46-4.

Dubé, B., Mercier-Langevin, P., Hannington, M.D., Davis, D.W. and Lafrance, B. 2004. Le gisement de sulfures massifs volcanogènes aurifères LaRonde, Abitibi, Québec: altération, minéralisation, genèse et implications pour l'exploration; Ministère des Ressources Naturelles, Faune et Parcs, Québec, v. MB 2004-03, p.1-112.

Dubé, B., Mercier-Langevin, P., Lafrance, B., Hannington, M.D., Moorhead, L., Davis, D.W. and Pilote, P. 2003. The Doyon-Bousquet-LaRonde Archean Au-rich VMS gold camp: the example of the world-class LaRonde deposit, Abitibi and its implications for exploration; Canadian Institute of Mining and Metallurgy, field conference abstracts, p.3-10.

Dubé, B., Williamson, K. and Malo, M. 2003. Gold mineralization within the Red Lake mine trend: example from the Cochenour-Willans mine area, Red Lake, Ontario, with new key information from the Red Lake mine and potential analogy with the Timmins camp; Geological Survey of Canada Current Research, v. 2003-C21, 15p. [available in electronic form only]

Dubé, B., Williamson, K., McNicoll, V.J., Malo, M., Skulski, T., Twomey, T. and Sanborn-Barrie, M. *in press*. Timing of gold mineralization in the Red Lake gold camp, northwestern Ontario, Canada: new constraints from U-Pb geochronology at the Goldcorp High-grade Zone, Red Lake mine and at the Madsen mine; Economic Geology.

Duff, D. 1986. Pamour No 1 mine; Gold '86, Excursion Guidebook, p.27-29.

Fan, J. and Kerrich, R. 1997. Geochemical characteristics of aluminum depleted and undepleted komatiites and HREE-enriched low-Ti tholeiites, western Abitibi greenstone belt: a heterogeneous mantle-plume-convergent margin environment; Geochimica et Cosmochimica Acta, v.61, p.4723-4744.

Feng, R. and Kerrich, R. 1990. Geochemistry of fine-grained clastic sediments in the Archaean Abitibi greenstone belt, Canada: Implications for provenance and tectonic setting; Geochimica et Cosmochimica Acta, v.54, p.1061-1081.

Ferguson, S.A., Buffam, B.S.W., Carter, O.F., Griffis, A.T., Holmes, T.C., Hurst, M.E., Jones, W.A., Lane, H.C. and Longley, C.S. 1968. Geology and ore deposits of Tisdale Township, District of Cochrane; Ontario Department of Mines, Geological Report 58, 177p.

Galley, A.G., Pilote, P. and Davis, D.W. 2003. Gold-related subvolcanic Mooshla intrusive complex, Bousquet Mining District, P.Q; *in* Ore Deposits at Depth, CIM 2003 Field Conference, Timmins, Ontario, Canadian Institute of Mining and Metallurgy, Abstract Volume, p. 16.

Goldfarb, R.J., Groves, D.I. and Gardoll, S.J. 2001. Orogenic gold and geologic time: a global synthesis; Ore Geology Reviews, v.18, p.1-75.

Gosselin, G. 1998. Veines de quartz aurifères précoces à la zone Ouest de la Mine Doyon, Canton de Bousquet, Preissac, Abitibi; unpublished Thèse de maîtrise, Université du Québec à Chicoutimi, 128p.

Gray, M.D. and Hutchinson, R.W. 2001. New evidence for multiple periods of gold emplacement in the Porcupine mining district, Timmins area, Ontario, Canada; Economic Geology, v.96, p.453-475.

Hagemann, S.G. and Brown, P.E. 1996. Geobarometry in Archean lode gold deposits; European Journal of Mineralogy, v.8, p.937-960.

Hagemann, S.G. and Cassidy, K.F. 2000. Archean orogenic lode gold deposits; SEG Reviews, v.13, p.9-68.

Hall, D.L. 1985. Flat veins at the Hollinger mine, Timmins, Ontario; unpublished MSc thesis, Queen's University, Kingston, Ontario, 92p.

Hall, L.A.F. and Smith, M.D. 2002. Precambrian geology of Denton and Carscallen townships, Timmins West area; Ontario Geological Survey, Open File Report 6093, 75p.

Heaman, L.M. 1988. A precise U-Pb zircon age for a Hearst dike; Geological Association of Canada, Abstracts, v.13, p.A53.

Heather, K. B. 2001. The geological evolution of the Archean Swayze greenstone belt, Superior Province, Canada; unpublished PhD thesis, Keele University, Keele, Staffordshire, UK.

Heather, K.B. and van Breeman, O. 1994. An interim report on geological, structural and geochronological investigations of granitoid rocks in the vicinity of the Swayze greenstone belt, southern Superior Province, Ontario; Geological Survey of Canada, Current Research, v.1995-C, p.1-10.

Hodgson, C.J. 1993. Mesothermal lode-gold deposits; Geological Association of Canada, Special Paper 40, p.635-678.

———1983. The structure and geological development of the Porcupine camp - a re-evaluation; Ontario Geological Survey, Miscellaneous Paper 110, p.211-225.

Hodgson, C.J., Hamilton, J. and Piroschco, D.W. 1990. Structural setting of gold deposits and the tectonic evolution of the Timmins-Kirkland Lake area, southwestern Abitibi greenstone belt; University of Western Australia Key Centre and University Extension Publication, v.24, p.101-120.

Holmes, T.C. 1968. Dome Mines Limited; *in* Geology and Ore Deposits of Tisdale Township, Ontario, Ontario Department of Mines, Geological Report 58, p.1-172.

———1944. Some porphyry-sediment contacts at the Dome mine, Ontario; Economic Geology, v.39, p.133-141.

Hurst, M.E. 1936. Recent studies in the Porcupine area; Canadian Institute of Mining and Metallurgy, v.39, p.448-458.

Jackson, J.A. 1994. Active tectonics of the Aegean region; Annual Review of Earth and Planetary Sciences, v.22, p.239-271.

Jackson, S.L. and Fyon, J.A. 1991. The western Abitibi Subprovince in Ontario; *in* Geology of Ontario, Ontario Geological Survey, Special Volume 4, Part 1, p.405-475.

Jones, M.I. 1992. Variolitic basalts: relations to Archean epigenetic gold deposits in the Abitibi greenstone belt; unpublished MSc thesis, University of Ottawa, Ottawa, Ontario.

Kerrich, R., Polat, A., Wyman, D.A. and Hollings, P.N. 1999. Trace element systematics of Mg to Fe tholeiitic basalt suites of the Superior Province: implications for Archaean mantle reservoirs and greenstone belt genesis; Lithos, v.46, p.163-187.

Kerrich, R., Wyman, D.A., Fan, J. and Bleeker, W. 1999. Boninite series: low Ti tholeiite associations from the 2.7 Ga Abitibi greenstone belt; Earth and Planetary Science Letters, v.164, p.303-316.

Kingston, D.M. 1987. Geology and geochemistry of the Owl Creek gold deposit, Timmins, Ontario; unpublished MSc thesis, Carleton University, Ottawa, 93p.

Kinkel, A.R. 1948. Buffalo Ankerite mine; *in* Structural Geology of Canadian Ore Deposits, Canadian Institute of Mining and Metallurgy, v.1, p.515-519.

Krogh, T.E., Corfu, F., Davis, D.W., Dunning, G.R., Heaman, L.M., Kamo, S.L., Machado, N., Greenough, J.D. and Nakamura, E. 1987. Precise U-Pb isotopic ages of diabase dikes and mafic to ultramafic rocks using trace amounts of baddeleyite and zircon; Geological Association of Canada, Special Paper 34, p.147-152.

Lahaye, Y., Barnes, S.J., Frick, L.R. and Lambert, D. 2001. Re-Os isotopic study of komatiitic volcanism and magmatic sulfide formation in the southern Abitibi greenstone belt, Ontario, Canada; Canadian Mineralogist, v.39, p.473-490.

MacDonald, P.J., Piercey, S.J. and Hamilton, M.A. 2005. An integrated study of intrusive rocks spatially associated with gold and base metal mineralization in Abitibi greenstone belt, Timmins area and Clifford Township: Discover Abitibi Initiative; Ontario Geological Survey, Open File Report 6160, 190p.

Manikyamba, C., Naqvi, S.M., Subba Rao, D.V., Ram Mohan, M., Khanna, T.C., Rao, T.G. and Reddy, G.L.N. 2005. Boninites from the Neoarchaean Gadwal Greenstone belt, Eastern Dharwar Craton, India: implications for Archaean subduction processes; Earth and Planetary Science Letters, v.230, p.65-83.

Marmont, S. and Corfu, F. 1989. Timing of gold introduction in the Late Archean tectonic framework of the Canadian Shield: evidence from U-Pb zircon geochronology of the Abitibi Subprovince; Economic Geology Monograph, v.6, p.101-111.

Mason, R. and Melnik, N. 1986. The anatomy of an Archean gold system – the McIntyre-Hollinger complex at Timmins, Ontario, Canada; *in* Proceedings of Gold '86: An International Symposium on the Geology of Gold, Konsult International, Toronto, p.40-55.

Mercier-Langevin, P., Dubé, B., Hannington, M.D., Davis, D.W. and Lafrance, B. 2004. Contexte géologique et structural des sulfures massifs volcanogènes aurifères du gisement LaRonde, Abitibi; Ministères des Resources naturelles de la faune et des parcs, v. ET 2003-03, 60p.

Moritz, R.P. and Crocket, J.H. 1990. Mechanics of formation of the gold-bearing quartz-fuchsite vein at the Dome mine, Timmins area, Ontario; Canadian Journal of Earth Sciences, v.27, p.1609-1620.

———1991. Hydrothermal wall-rock alteration and formation of the gold-bearing quartz-fuchsite vein at the Dome mine, Timmins area, Ontario, Canada; Economic Geology, v.86, p.620-643.

Mortensen, J.K. 1993. U-Pb geochronology of the eastern Abitibi Subprovince Part 2: Noranda–Kirkland Lake area; Canadian Journal of Earth Sciences, v.30, p.29-41.

Mueller, W., Daigneault, R., Mortensen, J.K. and Chown, E.H. 1996. Archean terrane docking: upper crustal collision tectonics, Abitibi greenstone belt, Quebec, Canada; Tectonophysics, v.265, p.127-150.

Neumayr, P., Hagemann, S.G. and Couture, J.F. 2000. Structural setting, textures, and timing of hydrothermal vein systems in the Val d'Or camp, Abitibi, Canada: implications for the evolution of transcrustal, second- and third-order fault zones and gold mineralisation; Canadian Journal of Earth Sciences, v.37, p.95-114.

Parks, W.A. 1900. Niven's base line, 1899; Ontario Department of Mines, Annual Report, v.9, p.125-142.

Piroschco, D.W. and Kettles, K. 1991. Structural geology of Tisdale and Whitney townships, Abitibi greenstone belt, District of Cochrane, northeastern Ontario; Ontario Geological Survey, Open File Report 5768, 115p

Poulsen, K.H., Robert, F. and Dubé, B. 2000. Geological classification of Canadian gold deposits; Geological Survey of Canada, Bulletin 540, 106p.

Powell, W.G., Carmichael, D.M. and Hodgson, C.J. 1995. Conditions and timing of metamorphism in the southern Abitibi greenstone belt, Quebec; Canadian Journal of Earth Sciences, v.32, p.787-805.

Powell, W.G., Hodgson, C.J., Hanes, J.A., Carmichael, D.M., McBride, S.L. and Farrar, E. 1995. $^{40}Ar/^{39}Ar$ geochronological evidence for multiple postmetamorphic hydrothermal events focussed along faults in the southern Abitibi greenstone belt; Canadian Journal of Earth Sciences, v.32, p.768-786.

Pressacco, R. 1999. Special project: Timmins ore deposit descriptions; Ontario Geological Survey, Open File Report 5985, 222p.

Price, P. and Bray, R.C.E. 1948. Pamour mine; Canadian Institute of Mining and Metallurgy, v.1, p.558-565.

Proudlove, D.C. and Hutchinson, R.W. 1989. Multiphase mineralization in concordant and discordant gold veins, Dome mine, South Porcupine, Ontario, Canada; Economic Geology Monograph, v.6, p.112-123.

Pyke, D.R. 1982. Geology of the Timmins area, District of Cochrane; Ontario Geological Survey, Report 219, 141p.

Rhys, D.A. 1999. Report on structural setting and controls on gold mineralization in the Porcupine mining camp, northern Ontario; unpublished company report for Kinross Gold Corporation.

———2003. Structural style and setting of gold deposits, Hollinger-McIntyre to Pamour, Porcupine mining camp; unpublished company report for PlacerDome (CLA).

Robert, F. 1989. Internal structure of the Cadillac tectonic zone southeast of Val d'Or, Abitibi belt, Quebec; Canadian Journal of Earth Sciences, v.26, p.2661-2690.

———2001. Syenite-associated disseminated gold deposits in the Abitibi greenstone belt, Canada; Mineralium Deposita, v.36, p.503-516.

———1990. Structural setting and control of gold-quartz veins of the Val D'Or area, southeastern Abitibi Subprovince; University of Western Australia Key Centre and University Extension Publication, v.24, p.167-209.

———2000. World-class greenstone gold deposits and their exploration; *in* 31st International Geological Congress, August 2000, Rio de Janeiro. Brasil, Vol. de Presentaciones, CD-ROM, doc. SG304e, 4 p.

Robert, F. and Brown, A.C. 1986. Archean gold-bearing quartz veins at the Sigma Mine, Abitibi greenstone belt, Quebec: Part II. Vein paragenesis and hydrothermal alteration; Economic Geology, v.81, p.593-616.

Robert, F. and Poulsen, K.H. 1997. World-class Archaean gold deposits in Canada: an overview; Australian Journal of Earth Sciences, v.44, p.329-351.

Robert, F., Poulsen, K.H. and Dubé, B. 1994. Structural analysis of lode gold deposits in deformed terranes; Geological Survey of Canada, Open File 2850.

Roberts, R.G. 1981. The volcanic-tectonic setting of gold deposits in the Timmins area, Ontario; Ontario Geological Survey, Miscellaneous Paper 97, p.16-28.

Rogers, D. 1986. Dome Mine; Gold '86 Excursion Guidebook, p.30-34.

Spooner, E.T.C., Bray, C.J., Wood, P.C., Burrows, D.R. and Callan, N.J. 1987. Au-quartz vein and Cu-Au-Ag-Mo-anhydrite mineralization, Hollinger McIntyre mines, Timmins, Ontario: δ13C values (McIntyre), fluid inclusion gas chemistry, pressure (depth) estimation, and H_2O-CO_2 phase separation as a precipitation and dilation mechanism; Ontario Geological Survey, Miscellaneous Paper 136.

Sproule, R.A., Lesher, C.M., Ayer, J.A. and Thurston, P.C. 2003. Geochemistry and metallogenesis of komatiitic rocks in the Abitibi greenstone belt, Ontario; Ontario Geological Survey, Open File Report 6073, 119p.

Sproule, R.A., Lesher, C.M., Ayer, J.A., Thurston, P.C. and Herzberg, C. 2002. Spatial and temporal variations in the geochemistry of komatiites and komatiitic basalts in the Abitibi greenstone belt; Precambrian Research, v.115, p.153-186.

Stein, H.J., Morgan, J.W., Markey, R.J. and Hannah, J.L. 1998. An introduction to Re-Os: what's in it for the mineral industry; Society of Economic Geologists, Newsletter, v.32, p.8-15.

Sun, S.S. and McDonough, W.F. 1989. Chemical and isotopic systematics of oceanic basalts: implications for mantle compositions and processes; Geological Society of London, Special Publication, v.42, p.313-345.

Thompson, P.H. 2003. Discover Abitibi. Metamorphic subproject. Metamorphism and its relationships to gold deposits in the Timmins–Kirkland Lake area, western Abitibi greenstone belt, Ontario: Report 1; *in* Summary of Field Work and Other Activities 2003, Ontario Geological Survey, Open File Report 6120, p.37-1 to 37-8.

———2004. Discover Abitibi. Metamorphic subproject. Metamorphic zones and gold exploration targets east of Timmins: interim report; *in* Summary of Field Work and Other Activities 2004, Ontario Geological Survey, Open File Report 6145, p.45-1 to 45-12.

Thurston, P.C. 2002. Autochthonous development of Superior Province greenstone belts?; Precambrian Research, v.115, p.11-36.

Wilkinson, L., Cruden, A.R. and Krogh, T.E. 1999. Timing and kinematics of post-Timiskaming deformation within the Larder Lake-Cadillac deformation zone, southwest Abitibi greenstone belt, Ontario, Canada; Canadian Journal of Earth Sciences, v.36, p.627-647.

Wood, P.C., Burrows, D.R., Thomas, A. and Spooner, E.T.C. 1986. The Hollinger–McIntyre Au-quartz vein system, Timmins, Ontario, Canada; geologic characteristics, fluid properties and light stable isotopes; *in* Proceedings of Gold '86: An International Symposium on the Geology of Gold, Konsult International, Toronto, p.56-79.

Worden, J.M., Cumming, G.L. and Krstic, D. 1995. The sequence of magmatic and mineralization events in the Abitibi greenstone belt: isotopic evidence from Taylor Township, Timmins area, northern Ontario, Canada; Canadian Journal of Earth Sciences, v.32, p.1221-1235.

Wyman, D.A. and Kerrich, R. 2002. Formation of Archean continental lithospheric roots: the role of mantle plumes; Geology, v.30, p.543-546.

Wyman, D.A., Kerrich, R. and Polat, A. 2002. Assembly of Archean cratonic mantle lithosphere and crust: plume-arc interaction in the Abitibi-Wawa subduction-accretion complex; Precambrian Research, v.115, p.37-62.

Appendix A

Table of Geochemical Data

Abbreviations:
GL-MNDM –Geoscience Laboratories, Ontario Ministry of Northern Development and Mines;
ActLab – Activation Laboratories Ltd (Ancaster, Ontario);
XRF – x-ray fluorescence;
IRC – infrared absorption;
ICP-MS – closed beaker solution, inductively coupled plasma mass spectrometry;
MS-AHT – acid solution with hydride generation, inductively coupled plasma mass spectrometry;
AAT-100 – atomic absorption spectrometry;
ICP-AES – closed beaker solution, inductively coupled plasma atomic emission spectrometry;
n.d. – not detected.

Station ID					04RJB0167	04RJB0152	04RJB0355
Sample number					04RJB0167_1_1	04RJB0152_1_1	04RJB0355_1_1
Township					Mountjoy	Tisdale	Tisdale
Easting	**UTM NAD83**				474313	476788	476214
Northing	**UTM NAD83**				5370055	5370678	5371157
Assemblage	**or formation**				Tisdale-Gold Centre	Tisdale-Gold Centre	Tisdale-Gold Centre
Rock Unit					basalt	Basalt	Basalt
Rock Type					pillows	pillows	flow
Rock Texture					amydaloidal		
	laboratory				ActLab	ActLab	ActLab
		method	units	d.l.			
SiO2		XRF	%	0.01	56.74	63.59	55.20
TiO2		XRF	%	0.01	1.46	1.18	1.41
Al2O3		XRF	%	0.01	11.37	9.97	12.45
Fe2O3		XRF	%	0.01	14.83	9.26	14.95
FeO		titrimetry	%	0.06			
MnO		XRF	%	0.01	0.236	0.113	0.200
MgO		XRF	%	0.01	2.28	1.98	2.95
CaO		XRF	%	0.01	3.87	5.33	6.44
K2O		XRF	%	0.01	0.08	0.28	0.41
Na2O		XRF	%	0.01	3.41	1.84	2.21
P2O5		XRF	%	0.01	0.51	0.44	0.51
Cr2O3		XRF	%	0.05	-0.01	-0.01	-0.01
LOI		XRF	%	0.05	5.39	5.76	3.12
Total			%		100.17	99.73	99.84
CO2	GL-MNDM	IRC	%	0.03	3.43		0.28
S	GL-MNDM	IRC	%	0.01	0.05		0.01
	laboratory				ActLab	ActLab	ActLab
Cr		XRF	ppm	4	40	22	40
Nb		XRF	ppm	2	10	3	11
Ni		XRF	ppm	2	4	5	13
V		XRF	ppm	4	32	31	42
Y		XRF	ppm	1	60	44	65
Zr		XRF	ppm	3	178	155	177
As	GL-MNDM	XRF	ppm	1			
Ba	GL-MNDM	XRF	ppm	25	19.57		85.11
Ga	GL-MNDM	XRF	ppm	2			
Pb	GL-MNDM	XRF	ppm	5			
Rb	GL-MNDM	XRF	ppm	2			
Sn	GL-MNDM	XRF	ppm	5			
Sr	GL-MNDM	XRF	ppm	2			
Ta	GL-MNDM	XRF	ppm	10			
Th	GL-MNDM	XRF	ppm	4			
Ce	GL-MNDM	ICP-MS	ppm	0.07	33.73		32.13
Cs	GL-MNDM	ICP-MS	ppm	0.007	0.108		4.524
Dy	GL-MNDM	ICP-MS	ppm	0.008	12.318		12.803
Er	GL-MNDM	ICP-MS	ppm	0.008	7.772		8.194
Eu	GL-MNDM	ICP-MS	ppm	0.005	2.706		3.201
Gd	GL-MNDM	ICP-MS	ppm	0.009	11.293		11.403
Hf	GL-MNDM	ICP-MS	ppm	0.1	5.4		5.4
Ho	GL-MNDM	ICP-MS	ppm	0.003	2.632		2.758
La	GL-MNDM	ICP-MS	ppm	0.02	12.1		11.72
Lu	GL-MNDM	ICP-MS	ppm	0.003	1.126		1.205
Nb	GL-MNDM	ICP-MS	ppm	0.2	8.5		8.4
Nd	GL-MNDM	ICP-MS	ppm	0.03	27.94		27.45
Pr	GL-MNDM	ICP-MS	ppm	0.006	5.418		5.18
Rb	GL-MNDM	ICP-MS	ppm	0.05	1.29		10.42
Sm	GL-MNDM	ICP-MS	ppm	0.01	8.75		8.6
Sr	GL-MNDM	ICP-MS	ppm	0.5	153.9		146.2
Ta	GL-MNDM	ICP-MS	ppm	0.17	0.5		0.5
Tb	GL-MNDM	ICP-MS	ppm	0.003	1.884		1.942
Th	GL-MNDM	ICP-MS	ppm	0.06	0.94		0.88
Tm	GL-MNDM	ICP-MS	ppm	0.003	1.135		1.201
U	GL-MNDM	ICP-MS	ppm	0.007	0.275		0.252
Y	GL-MNDM	ICP-MS	ppm	0.02	67.85		70.38
Yb	GL-MNDM	ICP-MS	ppm	0.01	7.38		7.76
Zr	GL-MNDM	ICP-MS	ppm	4	192.7		190.6
Bi	GL-MNDM	MS-AHT	ppm	0.05			
Sb	GL-MNDM	MS-AHT	ppm	0.1	0.12	N.D.	
Ag	GL-MNDM	AAT-100	ppm	2			
Be	GL-MNDM	ICP-AES	ppm	0.1	0.48		0.74
Cd	GL-MNDM	ICP-AES	ppm	2	N.D.	N.D.	
Co	GL-MNDM	ICP-AES	ppm	1	20		21
Cu	GL-MNDM	ICP-AES	ppm	3	16		13
Li	GL-MNDM	ICP-AES	ppm	1	8		9
Mo	GL-MNDM	ICP-AES	ppm	8	N.D.	N.D.	
Ni	GL-MNDM	ICP-AES	ppm	3	22		30
Sc	GL-MNDM	ICP-AES	ppm	0.3	24		25.4
Sr	GL-MNDM	ICP-AES	ppm	0.7	140		131.9
V	GL-MNDM	ICP-AES	ppm	0.6	27		33
W	GL-MNDM	ICP-AES	ppm	2	5	N.D.	
Zn	GL-MNDM	ICP-AES	ppm	2	152		125

Station ID	04RJB0533	04RJB0141	04RJB0143	04RJB0223	04RJB0256	04RJB0257
Sample number	04RJB0533	04RJB0141_2_1	04RJB0143_1_1	04RJB0223_1_1	04RJB0256_1_1	04RJB0257_1_1
Township	Tisdale	Tisdale	Tisdale	Tisdale	Mountjoy	Tisdale
Easting	480718	471609	472326	475071	475223	475223
Northing	5370692	5376167	5370851	5368999	5369131	5369131
Assemblage	Tisdale-Gold Centre	Porcupine	Porcupine	Porcupine	Tisdale-Vipond	Tisdale-Vipond
Rock Unit	Basalt	Clastic sediments	Clastic sediments	Clastic sediments	ultramafic flow	basalt
Rock Type	flow	sandstone	sandstone	greywacke	flow	massive
Rock Texture	aphanitic	bedded	medium grained	normal grading	schistose	
	ActLab	ActLab	ActLab	ActLab	ActLab	ActLab
SiO2	55.58	64.41	63.09	66.41	52.43	52.50
TiO2	1.44	0.62	0.56	0.53	1.58	1.57
Al2O3	10.87	16.04	16.91	15.49	13.02	12.97
Fe2O3	18.45	4.79	5.22	5.47	14.40	14.45
FeO						
MnO	0.142	0.057	0.067	0.064	0.152	0.155
MgO	2.99	1.94	3.25	2.81	6.45	6.48
CaO	3.71	3.13	1.88	1.42	4.03	4.28
K2O	0.12	1.85	1.83	1.87	1.24	1.19
Na2O	0.1	3.87	4.33	3.56	1.64	1.66
P2O5	0.68	0.21	0.18	0.14	0.15	0.15
Cr2O3	0	0.02	0.02	0.02	-0.01	-0.01
LOI	5.6073	2.26	2.61	2.77	4.13	4.21
Total	99.69	99.20	99.95	100.55	99.21	99.60
CO2	2.44				0.67	
S	0.05				0.05	
	ActLab	ActLab	ActLab	ActLab	ActLab	ActLab
Cr	37	133	142	173	28	18
Nb	7	15	5	5	5	4
Ni	1	53	57	73	25	30
V	28	104	108	111	388	391
Y	60	15	12	14	36	35
Zr	154	142	126	116	132	130
As						
Ba	33.97				385.89	
Ga						
Pb						
Rb						
Sn						
Sr						
Ta						
Th						
Ce	28.29				20.17	
Cs	0.257				0.491	
Dy	11.753				6.597	
Er	7.454				4.372	
Eu	2.564				1.825	
Gd	10.678				5.78	
Hf	4.7				4	
Ho	2.536				1.436	
La	9.84				7.86	
Lu	1.094				0.66	
Nb	7.8				5.7	
Nd	25.22				15.1	
Pr	4.619				2.995	
Rb	3.47				15.22	
Sm	7.89				4.44	
Sr	34.4				125.4	
Ta	0.46				0.34	
Tb	1.814				1.004	
Th	0.73				0.72	
Tm	1.077				0.657	
U	0.215				0.199	
Y	65.08				37.3	
Yb	7.08				4.35	
Zr	164.9				142.9	
Bi						
Sb	0.16				0.71	
Ag						
Be	0.31				0.3	
Cd	N.D.				N.D.	
Co	18				34	
Cu	9				28	
Li	55				21	
Mo	N.D.				N.D.	
Ni	19				43	
Sc	23.2				36.1	
Sr	29.4				111	
V	3.1				>320.0	
W	4				2	
Zn	122				65	

Station ID	04RJB0258	04RJB0259	04RJB0260	04RJB0275	04RJB0283	04RJB0230
Sample number	04RJB0258_1_1	04RJB0259_1_1	04RJB0260_1_1	04RJB0275_1_1	04RJB0283_1_1	04RJB0230_1_1
Township	Tisdale	Tisdale	Tisdale	Tisdale	Tisdale	Tisdale
Easting	475223	475223	475293	484391	484130	473666
Northing	5369131	5369197	5369410	5372121	5372714	5366081
Assemblage	Tisdale-Vipond	Porcupine	Tisdale-Vipond	Tisdale-Vipond	Tisdale-Vipond	Porcupine
Rock Unit	basalt	Clastic sediments	basalt	basalt	basalt	Clastic sediments
Rock Type	pillows	graphitic phyllite	massive	massive	pillows	siltstone
Rock Texture		laminated			variolitic	laminated
	ActLab	ActLab	ActLab	ActLab	ActLab	ActLab
SiO2	56.98	47.18	51.35	50.91	54.99	64.23
TiO2	1.43	1.34	1.46	1.45	1.14	0.56
Al2O3	14.18	13.31	12.95	13.79	13.96	15.98
Fe2O3	9.61	14.65	11.92	15.14	9.31	5.58
FeO						
MnO	0.166	0.256	0.188	0.203	0.189	0.058
MgO	4.14	5.28	5.19	4.75	4.34	2.70
CaO	5.58	7.43	7.46	8.95	8.13	1.53
K2O	0.08	0.58	0.05	0.16	0.14	2.42
Na2O	4.01	3.90	2.23	2.30	3.31	3.25
P2O5	0.13	0.12	0.13	0.16	0.12	0.16
Cr2O3	-0.01	0.01	-0.01	0.01	0.02	0.02
LOI	4.77	5.56	7.19	2.50	4.09	2.63
Total	101.06	99.62	100.10	100.32	99.74	99.12
CO2			3.92	0.25	2.23	
S			0.01	0.05	0.07	
	ActLab	ActLab	ActLab	ActLab	ActLab	ActLab
Cr	48	38	33	98	141	185
Nb	5	4	11	6	4	7
Ni	86	39	24	46	58	69
V	364	359	389	254	279	106
Y	36	38	36	32	35	14
Zr	114	107	109	86	111	128
As						
Ba			21.64	25.26	42.67	
Ga						
Pb						
Rb						
Sn						
Sr						
Ta						
Th						
Ce			18.05	15.39	17.32	
Cs			0.123	0.103	0.069	
Dy			7.072	5.836	6.59	
Er			4.601	3.752	4.283	
Eu			1.697	1.456	1.39	
Gd			6.012	5.045	5.583	
Hf			3.4	2.6	3.3	
Ho			1.527	1.245	1.415	
La			6.31	5.62	6.56	
Lu			0.697	0.568	0.629	
Nb			4.9	4	4.6	
Nd			15.09	12.77	14.17	
Pr			2.905	2.454	2.742	
Rb			0.43	2.19	2.29	
Sm			4.58	3.94	4.36	
Sr			318.9	206.2	134.3	
Ta			0.29	0.24	0.27	
Tb			1.041	0.854	0.997	
Th			0.61	0.52	0.59	
Tm			0.693	0.563	0.636	
U			0.171	0.131	0.156	
Y			39.84	32.38	37.76	
Yb			4.54	3.69	4.17	
Zr			121.3	91.3	117.2	
Bi						
Sb			0.36	0.11	0.1	
Ag						
Be			0.41	0.4	0.38	
Cd		N.D.		N.D.	N.D.	
Co			26	34	31	
Cu		N.D.		54	71	
Li			18	7	8	
Mo		N.D.		N.D.	N.D.	
Ni			40	55	61	
Sc			34.1	30.3	32	
Sr			277.9	185.1	119.8	
V			313.5	222.2	238.2	
W			2	N.D.	N.D.	
Zn			43	92	60	

Station ID	04RJB0374	04RJB0378	04RJB0301	04RJB0514	04RJB0527	04RJB-TW04-005
Sample number	04RJB0374_1_1	04RJB0378_1_1	04RJB0301_1_1	04RJB0514	04RJB0527	04RJB-TW04-005
Township	Tisdale	Tisdale	Tisdale	Tisdale	Tisdale	Ogden
Easting	481015	483427	480203	479108	477802	474553
Northing	5371765	5374452	5369636	5369815	5369775	5362785
Assemblage	Tisdale-Vipond	Tisdale-Vipond	Tisdale-Vipond	Tisdale-Vipond	Tisdale-Vipond	Tisdale-Vipond
Rock Unit	basalt	basalt	basalt	Basalt	Basalt	Basalt
Rock Type	pillows	pillow breccia	pillow breccia	pillows	pillows	flow breccia
Rock Texture			variolitic	variolitic	schistose	flattened clasts
	ActLab	ActLab	ActLab	ActLab	ActLab	ActLab
SiO2	54.31	53.88	54.02	50.19	61.8	58.29
TiO2	1.37	1.95	1.50	1	0.52	0.57
Al2O3	13.55	13.09	14.70	12.34	14.02	17.64
Fe2O3	12.69	12.79	11.37	10.01	9.22	4.95
FeO						
MnO	0.225	0.229	0.135	0.185	0.134	0.052
MgO	4.80	4.24	4.07	4.46	5.18	3.64
CaO	6.02	8.30	4.06	8.75	1.87	2.72
K2O	0.06	0.06	1.06	0.05	1.18	0.18
Na2O	3.24	2.15	2.91	3.15	0.87	7.59
P2O5	0.13	0.12	0.16	0.11	0.15	0.24
Cr2O3	-0.01	0.01	0.01	0.01	0.02	0.02
LOI	3.18	4.11	5.23	9.7293	5.0968	4.088
Total	99.56	100.93	99.22	99.98	100.06	99.98
CO2	0.88	1.9	2.34	6.64	1.45	2.29
S	0.01	0.02	0.07	0.12	0.99	N.D.
	ActLab	ActLab	ActLab	ActLab	ActLab	ActLab
Cr	36	35	63	135	142	158
Nb	4	1	0	4	0	4
Ni	43	54	80	59	58	70
V	344	489	390	283	146	110
Y	37	23	31	35	11	16
Zr	113	80	106	111	87	148
As						
Ba	24.26	30.25	177.35	7.98	161.05	216.37
Ga						
Pb						
Rb						
Sn						
Sr						
Ta						
Th						
Ce	18.8	10.46	11.83	17.59	12.34	55.38
Cs	0.094	0.151	0.815	0.042	0.739	0.163
Dy	7.056	4.491	6.349	6.638	0.66	2.68
Er	4.71	2.871	4.083	4.444	0.473	1.228
Eu	1.443	1.309	1.191	1.228	0.308	1.453
Gd	6.048	3.799	5.538	5.619	0.867	4.347
Hf	3.4	2.5	3.2	3.3	2.5	4
Ho	1.549	0.956	1.371	1.47	0.134	0.472
La	6.71	3.62	3.61	6.45	5.38	25.03
Lu	0.723	0.414	0.591	0.669	0.101	0.157
Nb	4.9	3.5	4.6	4.4	3.1	5
Nd	14.9	9.11	11.9	14.02	6.97	29.15
Pr	2.907	1.692	2.084	2.759	1.649	7.108
Rb	0.36	0.79	22.65	0.36	26.56	3.47
Sm	4.63	2.94	4.12	4.24	1.33	5.56
Sr	133.4	102.6	40.1	159	43.9	239.5
Ta	0.29	0.2	0.27	0.27	0.18	0.34
Tb	1.064	0.674	0.969	1	0.116	0.529
Th	0.62	0.36	0.32	0.56	1.25	3.69
Tm	0.709	0.422	0.599	0.669	0.082	0.165
U	0.165	0.107	0.144	0.149	0.446	1.117
Y	38.85	23.99	34.05	38.23	3.56	12.95
Yb	4.68	2.77	3.88	4.39	0.64	1.06
Zr	121.6	86.8	114.5	115.5	95	153.3
Bi						
Sb	0.12	0.09	0.06	0.5	0.58	0.86
Ag						
Be	0.46	0.27	0.38	0.27	0.23	0.91
Cd	N.D.	N.D.	N.D.	N.D.	N.D.	N.D.
Co	37	49	48	33	38	19
Cu	72	118	75	70	46	N.D.
Li	6	8	16	27	35	60
Mo	N.D.	N.D.	N.D.	N.D.	N.D.	N.D.
Ni	55	68	87	61	71	68
Sc	34.4	42.6	32.4	29.2	9.8	8.1
Sr	120.8	93.2	36.9	137.2	38.5	208.9
V	308.4	>320.0	312.3	200	109.3	81.1
W	N.D.	N.D.	N.D.	N.D.	6	N.D.
Zn	94	150	72	60	900	50

Station ID	04RJB0389	04RJB0166	04RJB0221	04RJB0222	04RJB0229	04RJB0370
Sample number	04RJB0389_1_1	04RJB0166_1_1	04RJB0221_1_1	04RJB0222_1_1	04RJB0229_1_1	04RJB0370_1_1
Township	Tisdale	Tisdale	Tisdale	Tisdale	Mountjoy	Tisdale
Easting	483043	480904	476793	476716	474726	481379
Northing	5372684	5370029	5367798	5367860	5367268	5370226
Assemblage	Tisdale-Central	Tisdale-Central	Tisdale-Central	Tisdale-Central	Tisdale-Central	Tisdale-Central
Rock Unit	basalt	basalt	basalt	basalt	basalt	basalt
Rock Type	pillows	basaltic komatiite	pillows	pillows	pillow breccia	flow
Rock Texture	flattened pillows	polysutured	variolitic	schistose	schistose	
	ActLab	ActLab	ActLab	ActLab	ActLab	ActLab
SiO2	50.47	48.09	45.95	52.11	47.21	46.25
TiO2	1.23	1.35	1.21	1.37	1.30	1.30
Al2O3	14.47	13.28	11.84	15.99	14.08	15.48
Fe2O3	11.32	15.25	13.20	7.92	9.91	12.85
FeO						
MnO	0.231	0.194	0.281	0.197	0.202	0.162
MgO	6.32	5.91	3.31	2.39	3.10	6.06
CaO	7.67	8.84	10.76	7.18	9.44	6.52
K2O	0.17	0.49	0.18	1.50	0.61	0.13
Na2O	3.45	2.22	1.77	3.80	2.85	3.80
P2O5	0.09	0.08	0.12	0.09	0.09	0.09
Cr2O3	0.02	0.02	0.01	0.02	0.01	0.02
LOI	4.55	3.88	11.14	7.74	9.93	7.24
Total	99.99	99.61	99.77	100.31	98.73	99.91
CO2	1.97		8.23		7.36	3.63
S	N.D.		0.14		0.2	0.02
	ActLab	ActLab	ActLab	ActLab	ActLab	ActLab
Cr	148	110	94	133	132	132
Nb	0	3	0	0	0	0
Ni	108	54	78	81	111	96
V	348	392	378	479	439	425
Y	23	22	22	20	20	20
Zr	58	51	50	54	56	57
As						
Ba	63.17		36.96		192.46	30.74
Ga						
Pb						
Rb						
Sn						
Sr						
Ta						
Th						
Ce	8.58		14.09		8.52	9.61
Cs	0.059		0.179		1.075	0.225
Dy	4.061		4.206		3.588	3.633
Er	2.688		2.764		2.375	2.279
Eu	0.873		0.893		0.777	0.842
Gd	3.429		3.566		3.013	3.188
Hf	1.7		1.5		1.8	1.7
Ho	0.884		0.914		0.778	0.776
La	3.1		5.9		3.11	3.44
Lu	0.4		0.42		0.353	0.348
Nb	2.3		2.2		2.5	2.3
Nd	7.56		9.68		7.24	7.64
Pr	1.4		2.046		1.385	1.496
Rb	1.87		3.2		20.03	1.82
Sm	2.5		2.75		2.26	2.44
Sr	58.4		63.2		102.2	64.2
Ta	N.D.		N.D.		N.D.	N.D.
Tb	0.606		0.639		0.532	0.548
Th	0.24		0.23		0.25	0.24
Tm	0.402		0.416		0.345	0.34
U	0.07		0.066		0.071	0.07
Y	23.45		23.64		20.23	20.74
Yb	2.62		2.69		2.3	2.24
Zr	57.6		53.1		62.6	59.3
Bi						
Sb	0.11		0.09		0.1	0.07
Ag						
Be	0.22		0.12		0.32	0.37
Cd	N.D.		N.D.		N.D.	N.D.
Co	46		44		58	51
Cu	68		84		122	143
Li	11		24		29	24
Mo	N.D.		N.D.		N.D.	N.D.
Ni	107		79		109	100
Sc	36		34.4		32	40.9
Sr	51		56		90.4	57.6
V	319		281.7		>320.0	>320.0
W	N.D.		N.D.		N.D.	N.D.
Zn	66		112		61	73

Station ID	04RJB0319	04RJB0390	04RJB0401	04RJB0447	04RJB0537	04RJB0437
Sample number	04RJB0319_1_1	04RJB0390_1_1	04RJB0401_1_1	04RJB0447	04RJB0537	04RJB0437
Township	Tisdale	Tisdale	Tisdale	Tisdale	Tisdale	Tisdale
Easting	479821	482992	482635	477362	481020	479729
Northing	5367598	5372553	5374512	5366760	5370352	5368272
Assemblage	Tisdale-Central	Tisdale-Central	Tisdale-Central	Tisdale-Central	Tisdale-Central	Tisdale-Central
Rock Unit	basalt	basalt	basalt	Basalt	Basalt	Basalt
Rock Type	massive	pillows	pillows	pillows	pillows	pillows
Rock Texture	amydaloidal	amydaloidal		variolitic	amygdaloidal	variolitic
	ActLab	ActLab	ActLab	ActLab	ActLab	ActLab
SiO2	44.69	49.77	45.30	52.49	47.66	49.03
TiO2	1.13	1.20	1.17	1.3	1.17	1.21
Al2O3	12.48	14.47	12.84	15.17	14.02	14.71
Fe2O3	13.37	11.83	12.82	13.06	10.96	14.29
FeO						
MnO	0.180	0.233	0.153	0.245	0.234	0.221
MgO	5.24	6.36	5.60	4.99	5.57	2.79
CaO	9.58	9.91	9.04	3.94	8.54	7.29
K2O	0.18	0.23	0.24	0.08	0.05	0.3
Na2O	2.52	1.89	2.38	3.71	2.99	1.94
P2O5	0.07	0.09	0.08	0.1	0.1	0.11
Cr2O3	0.01	0.02	0.01	0.01	0.02	0.02
LOI	10.84	4.04	10.17	5.4481	8.4637	8.5909
Total	100.29	100.05	99.80	100.54	99.78	100.50
CO2	7.36	1.52	6.95	2.28	5.1	5.82
S	0.03	0.03	0.13	0.01	0.01	0.33
	ActLab	ActLab	ActLab	ActLab	ActLab	ActLab
Cr	106	150	112	124	158	125
Nb	0	1	0	0	0	1
Ni	70	107	66	94	112	65
V	403	298	412	430	359	396
Y	17	22	19	17	24	25
Zr	44	55	46	60	55	73
As						
Ba	39.98	84.61	189.43	25.36	19	78.16
Ga						
Pb						
Rb						
Sn						
Sr						
Ta						
Th						
Ce	5.68	8.73	7.34	6.76	8.12	10.23
Cs	0.305	0.104	0.123	0.066	0.046	0.49
Dy	2.896	4.085	3.576	3.133	4	4.63
Er	1.927	2.719	2.382	2.119	2.653	3.081
Eu	0.634	0.889	0.602	1.295	0.887	0.963
Gd	2.416	3.48	2.982	2.606	3.341	3.885
Hf	1.3	1.7	1.7	1.8	1.6	2.2
Ho	0.635	0.899	0.782	0.689	0.863	1.019
La	2.04	3.42	2.64	2.37	2.96	3.65
Lu	0.312	0.411	0.365	0.312	0.381	0.468
Nb	1.8	2.2	2	2.3	2.2	3
Nd	5.11	7.7	6.45	5.63	7.26	8.97
Pr	0.917	1.43	1.181	1.049	1.331	1.676
Rb	3.07	5.22	3.83	1.12	0.26	7.38
Sm	1.7	2.53	2.12	1.87	2.35	2.88
Sr	137.2	119.1	77.6	54.1	103.4	86.4
Ta	N.D.	N.D.	N.D.	N.D.	N.D.	0.17
Tb	0.432	0.599	0.532	0.457	0.587	0.697
Th	0.18	0.25	0.2	0.24	0.22	0.3
Tm	0.287	0.406	0.358	0.311	0.391	0.469
U	0.047	0.069	0.073	0.073	0.066	0.086
Y	16.66	23.58	20.21	17.36	23.13	26.54
Yb	1.93	2.67	2.35	2.05	2.55	3.07
Zr	44.4	59.8	60.7	64.6	55.9	79
Bi						
Sb	0.48	0.19	0.17	1.12	0.26	0.42
Ag						
Be	0.17	0.21	0.14	0.26	0.27	0.22
Cd	N.D.	N.D.	N.D.	N.D.	N.D.	N.D.
Co	44	48	47	51	47	33
Cu	149	83	280	84	60	105
Li	24	12	19	18	16	22
Mo	N.D.	N.D.	N.D.	N.D.	N.D.	N.D.
Ni	80	114	76	97	110	73
Sc	35.1	36.3	35.7	27	34.3	28.6
Sr	118.7	104.7	68.8	46.7	90.5	75.3
V	309.1	312.4	318.8	305.8	293.9	286.6
W	N.D.	N.D.	3	N.D.	3	N.D.
Zn	73	62	50	90	72	67

Station ID	04RJB0523	04RJB0142	04RJB0147	04RJB0168	04RJB0150	04RJB0174
Sample number	04RJB0523	04RJB0142_1_1	04RJB0147_1_1	04RJB0168_1_1	04RJB0150_1_1	04RJB0174_1_1
Township	Tisdale	Tisdale	Mountjoy	Murphy	Tisdale	Tisdale
Easting	478966	474313	474691	481775	476126	483275
Northing	5370513	5370055	5370190	5376334	5370221	5375403
Assemblage	Tisdale-Central	Tisdale-Central	Tisdale-Central	Porcupine	Tisdale-Central	Tisdale-Central
Rock Unit	Basalt	Basalt	Basalt	clastic sediments	Basalt	Basalt
Rock Type	massive	pillow breccia	massive	sandstone	massive	pillows
Rock Texture	aphanitic		flattened pillows	crossbedded		flattened pillows
	ActLab	ActLab	ActLab	ActLab	ActLab	ActLab
SiO2	46.94	46.37	47.90	50.76	48.44	54.54
TiO2	0.59	0.58	0.78	0.83	0.72	1.23
Al2O3	13.25	11.10	14.06	13.97	11.43	14.44
Fe2O3	10.53	12.05	13.53	11.00	11.47	9.57
FeO						
MnO	0.176	0.200	0.317	0.160	0.340	0.225
MgO	6.81	12.65	6.36	9.02	4.52	5.16
CaO	9.61	9.92	10.03	5.27	10.01	6.36
K2O	0.05	0.18	0.26	3.54	0.52	0.24
Na2O	2.16	2.03	1.61	1.68	1.03	4.42
P2O5	0.05	0.05	0.06	0.06	0.06	0.11
Cr2O3	0.04	0.14	0.01	0.02	-0.01	0.01
LOI	9.3416	4.88	5.54	3.31	11.25	3.16
Total	99.55	100.15	100.46	99.62	99.78	99.46
CO2	5.58	1.76		0.22		
S	0.02	0.06		N.D.		
	ActLab	ActLab	ActLab	ActLab	ActLab	ActLab
Cr	316	998	109	172	58	82
Nb	0	0	0	0	0	2
Ni	79	367	65	83	77	363
V	244	213	259	318	278	380
Y	16	15	21	19	18	31
Zr	34	35	45	49	45	77
As						
Ba	13.69	47.96		650.04		
Ga						
Pb						
Rb						
Sn						
Sr						
Ta						
Th						
Ce	4.81	4.33		5.39		
Cs	0.094	0.098		0.655		
Dy	2.51	2.276		2.861		
Er	1.7	1.517		2.198		
Eu	0.515	0.428		0.456		
Gd	1.959	1.855		2.092		
Hf	1	0.9		1.4		
Ho	0.559	0.5		0.664		
La	1.75	1.7		1.97		
Lu	0.277	0.232		0.375		
Nb	1.2	1.2		1.8		
Nd	4.05	3.79		4.34		
Pr	0.792	0.713		0.858		
Rb	0.37	3.37		62.63		
Sm	1.41	1.35		1.5		
Sr	124.6	69.3		55.8		
Ta	N.D.	N.D.		N.D.		
Tb	0.358	0.343		0.399		
Th	0.15	0.14		0.24		
Tm	0.266	0.234		0.348		
U	0.038	0.036		0.059		
Y	14.78	13.16		17.39		
Yb	1.76	1.52		2.38		
Zr	35.2	31.2		49.7		
Bi						
Sb	0.09	0.1		0.08		
Ag						
Be	0.11	0.12		0.19		
Cd	N.D.	N.D.		N.D.		
Co	42	64		37		
Cu	82	67		22		
Li	9	25		22		
Mo	N.D.	N.D.		N.D.		
Ni	86	338		100		
Sc	34.8	31.1		38.5		
Sr	103.4	60.7		50.2		
V	201.9	191.9		281.1		
W	3	N.D.		N.D.		
Zn	51	68		42		

Station ID	04RJB0184	04RJB0262	04RJB0276	04RJB0287	04RJB0288	04RJB0285
Sample number	04RJB0184_1_1	04RJB0262_1_1	04RJB0276_1_1	04RJB0287_1_1	04RJB0288_1_1	04RJB0285_1_1
Township	Tisdale	Tisdale	Tisdale	Tisdale	Tisdale	Tisdale
Easting	478440	483483	484750	483879	483778	484059
Northing	5374375	5368978	5372128	5373152	5373307	5372922
Assemblage	Tisdale-Central	Tisdale-Central	Tisdale-Central	Tisdale-Central	Tisdale-Central	Tisdale-Central
Rock Unit	Basalt	Basalt	basalt	Basalt	Basalt	Basalt
Rock Type	basaltic komatiite	tuff	massive	pillows	pillows	pillows
Rock Texture	flattened pillows	laminated		variolitic	variolitic	variolitic
	ActLab	ActLab	ActLab	ActLab	ActLab	ActLab
SiO2	52.23	50.83	49.32	50.91	51.18	49.98
TiO2	0.79	0.96	0.68	0.68	0.71	0.84
Al2O3	13.86	14.19	15.67	14.39	13.22	13.71
Fe2O3	10.64	13.50	8.75	8.96	8.90	10.83
FeO						
MnO	0.224	0.133	0.157	0.213	0.215	0.264
MgO	6.38	6.87	8.13	5.52	5.61	4.92
CaO	9.59	4.76	12.49	11.53	11.98	11.72
K2O	0.16	0.76	0.58	0.07	0.07	0.06
Na2O	2.36	3.60	1.44	2.05	1.94	0.95
P2O5	0.07	0.08	0.05	0.05	0.07	0.07
Cr2O3	0.02	0.01	0.05	0.04	0.02	0.01
LOI	2.97	4.16	3.30	5.77	5.64	6.14
Total	99.29	99.85	100.62	100.18	99.55	99.50
CO2	0.81	1.44	0.96	3.78	3.45	3.54
S	0.03	0.02	0.03	0.02	0.02	0.02
	ActLab	ActLab	ActLab	ActLab	ActLab	ActLab
Cr	162	80	437	311	155	82
Nb	0	2	0	0	0	0
Ni	62	35	168	101	72	75
V	258	346	224	221	226	256
Y	22	24	17	16	17	18
Zr	47	60	40	41	43	45
As						
Ba	62.39	106.86	242.1	13.87	17.08	13.14
Ga						
Pb						
Rb						
Sn						
Sr						
Ta						
Th						
Ce	6.83	7.38	6.65	6.09	6.03	6.63
Cs	0.066	1.18	0.206	0.067	0.054	0.068
Dy	3.471	3.993	2.973	2.773	2.978	3.16
Er	2.359	2.758	1.985	1.868	2.004	2.089
Eu	0.707	0.708	0.664	0.61	0.667	0.673
Gd	2.76	3.255	2.504	2.274	2.414	2.613
Hf	1.4	1.8	1.3	1.3	1.3	1.4
Ho	0.767	0.888	0.66	0.609	0.651	0.69
La	2.51	2.58	2.43	2.24	2.22	2.49
Lu	0.36	0.418	0.296	0.285	0.309	0.314
Nb	1.7	2.1	1.9	1.6	1.6	1.9
Nd	6.01	6.53	5.63	4.99	5.16	5.66
Pr	1.114	1.214	1.078	0.986	0.973	1.082
Rb	3.37	18.29	17.72	0.54	0.93	0.82
Sm	2.01	2.23	1.86	1.65	1.7	1.88
Sr	69.5	157.9	127.7	100.8	69.5	97.4
Ta	N.D.	N.D.	N.D.	N.D.	N.D.	N.D.
Tb	0.502	0.585	0.447	0.407	0.438	0.466
Th	0.21	0.26	0.22	0.22	0.2	0.22
Tm	0.362	0.413	0.297	0.288	0.301	0.317
U	0.062	0.176	0.056	0.065	0.057	0.063
Y	20.18	23.52	17.7	15.61	17.37	18.67
Yb	2.35	2.74	1.95	1.9	1.96	2.08
Zr	48.6	63.8	46.9	44.3	43.3	50.1
Bi						
Sb	0.08	0.4	0.23	0.2	0.16	0.07
Ag						
Be	0.16	0.22	0.19	0.2	0.18	0.16
Cd	N.D.	N.D.	N.D.	N.D.	N.D.	N.D.
Co	41	41	48	43	40	42
Cu	89	58	63	84	86	99
Li	10	48	16	9	9	11
Mo	N.D.	N.D.	N.D.	N.D.	N.D.	N.D.
Ni	73	54	173	102	76	79
Sc	37.1	36.5	29.5	37.9	37.9	37.1
Sr	61.5	143.2	112.3	90	61.4	84.9
V	244.9	281.2	223.7	223.9	229.7	251.3
W	N.D.	N.D.	N.D.	3	N.D.	N.D.
Zn	62	50	50	51	43	54

Station ID	04RJB0300	04RJB0307	04RJB0353	04RJB0354	04RJB0366	04RJB0416
Sample number	04RJB0300_1_1	04RJB0307_1_1	04RJB0353_1_1	04RJB0354_1_1	04RJB0366_1_1	04RJB0416_1_1
Township	Tisdale	Tisdale	Tisdale	Tisdale	Deloro	Tisdale
Easting	480528	481513	475398	475610	480248	484767
Northing	5369627	5367826	5371238	5371148	5365051	5376059
Assemblage	Tisdale-Central	Tisdale-Central	Tisdale-Central	Tisdale-Central	Tisdale-Central	Tisdale-Central
Rock Unit	Basalt	Basalt	basalt	Basalt	basalt	basalt
Rock Type	flow breccia	pillows	massive	pillows	talc schist	massive
Rock Texture	flattened clasts	variolitic		flattened pillows	schistose	
	ActLab	ActLab	ActLab	ActLab	ActLab	ActLab
SiO2	47.94	45.13	52.15	52.09	51.89	52.62
TiO2	0.87	0.88	0.90	0.79	0.89	0.55
Al2O3	16.08	13.54	14.82	13.80	14.45	14.81
Fe2O3	8.34	10.81	11.37	11.10	8.70	12.35
FeO						
MnO	0.145	0.202	0.153	0.241	0.238	0.218
MgO	6.50	4.86	6.14	6.07	5.24	6.27
CaO	10.17	10.79	9.46	6.80	9.45	7.34
K2O	0.11	0.18	0.17	0.18	0.11	0.13
Na2O	2.73	0.89	2.51	2.09	4.02	2.90
P2O5	0.05	0.06	0.08	0.07	0.08	0.05
Cr2O3	0.06	0.04	0.03	0.01	0.01	-0.01
LOI	6.83	12.26	2.44	6.64	5.14	3.14
Total	99.82	99.64	100.22	99.88	100.22	100.37
CO2	3.66	8.38	0.27	3.32	3.09	0.73
S	0.02	N.D.	0.09	0.05	N.D.	0.01
	ActLab	ActLab	ActLab	ActLab	ActLab	ActLab
Cr	413	358	212	115	73	49
Nb	0	0	0	0	0	0
Ni	131	113	97	83	71	73
V	280	344	299	265	280	257
Y	19	18	23	19	19	20
Zr	53	50	56	52	51	35
As						
Ba	58.74	26.96	29.05	45.88	49.16	47.2
Ga						
Pb						
Rb						
Sn						
Sr						
Ta						
Th						
Ce	6.8	7.65	8.07	8.62	7.26	5.58
Cs	0.16	0.194	0.071	0.157	0.068	0.057
Dy	3.161	3.362	3.716	3.219	3.359	3.177
Er	2.073	2.186	2.666	2.173	2.197	2.962
Eu	0.683	0.736	0.864	0.768	0.759	0.508
Gd	2.667	2.809	2.958	2.66	2.75	1.916
Hf	1.7	1.5	1.7	1.5	4.6	1.1
Ho	0.686	0.74	0.862	0.723	0.735	0.825
La	2.4	2.75	2.97	3.31	2.61	2.2
Lu	0.32	0.338	0.416	0.331	0.318	0.583
Nb	2.3	2.2	2	1.9	2	1.4
Nd	5.82	6.45	6.48	6.71	6.21	3.98
Pr	1.103	1.226	1.245	1.339	1.148	0.827
Rb	1.37	2.94	2.3	4.07	0.97	1.16
Sm	1.91	2.18	2.15	2.02	2.02	1.23
Sr	102	87.5	65.4	101.3	97.6	112.4
Ta	N.D.	N.D.	N.D.	N.D.	N.D.	N.D.
Tb	0.477	0.503	0.533	0.476	0.486	0.403
Th	0.24	0.21	0.26	0.39	0.23	0.25
Tm	0.319	0.33	0.405	0.331	0.329	0.483
U	0.067	0.059	0.069	0.102	0.064	0.06
Y	17.9	19.14	22.89	18.82	19.01	22.09
Yb	2.12	2.18	2.74	2.16	2.1	3.52
Zr	59.9	50.6	59.9	53.4	188.4	38.5
Bi						
Sb	0.08	0.26	0.06	N.D.	0.08	0.1
Ag						
Be	0.23	0.22	0.21	0.2	0.17	0.11
Cd	N.D.	N.D.	N.D.	N.D.	N.D.	N.D.
Co	48	42	37	49	44	47
Cu	97	95	99	77	107	58
Li	13	68	12	19	14	16
Mo	N.D.	N.D.	N.D.	N.D.	N.D.	N.D.
Ni	119	104	107	93	77	84
Sc	30.7	30.2	39.4	34.6	39.2	>50.0
Sr	88.8	77	57.5	91.7	85.9	98.3
V	266.6	254.5	280.9	247.1	268.1	246.2
W	N.D.	3	N.D.	N.D.	2	N.D.
Zn	44	55	64	69	58	67

Station ID	04RJB0189	04RJB0400	04RJB0292	04RJB0151	04RJB0493	04RJB0495
Sample number	04RJB0189_1_1	04RJB0400_1_1	04RJB0292_1_1	04RJB0151	04RJB0493	04RJB0495
Township	Tisdale	Tisdale	Tisdale	Tisdale	Tisdale	Tisdale
Easting	483390	481782	482607	476771	478553	476403
Northing	5374176	5374152	5373545	5370718	5370568	5371695
Assemblage	Tisdale-Central	Tisdale-Central	Tisdale-Central	Tisdale-Central	Tisdale-Central	Tisdale-Central
Rock Unit	basalt	Basalt	Basalt	Basalt	Basalt	Basalt
Rock Type	massive	pillows	pillows	pillows	pillows	pillows
Rock Texture	brecciated	amygdaloidal	amygdaloidal		amygdaloidal	amygdaloidal
	ActLab	ActLab	ActLab	ActLab	ActLab	ActLab
SiO2	47.21	51.64	51.28	51.07	45.33	54.69
TiO2	0.90	0.95	0.72	0.73	0.73	1.02
Al2O3	14.30	14.83	14.20	13.99	12.3	11.67
Fe2O3	13.81	12.30	12.17	9.13	12.05	8.92
FeO						
MnO	0.216	0.238	0.167	0.274	0.278	0.227
MgO	8.56	6.73	8.36	4.96	5.77	3.35
CaO	10.26	6.11	7.99	13.1	10.39	10.27
K2O	0.21	0.21	0.07	0.07	0.04	0.12
Na2O	2.01	4.44	2.12	2.66	1.76	2.82
P2O5	0.07	0.08	0.06	0.06	0.06	0.09
Cr2O3	0.02	0.02	0.02	0.02	0.01	0.01
LOI	2.54	2.48	3.06	4.3507	11.7685	6.7878
Total	100.10	100.03	100.22	100.41	100.49	99.97
CO2			0.11		8.22	5.05
S			N.D.		0.08	0.04
	ActLab	ActLab	ActLab	ActLab	ActLab	ActLab
Cr	133	193	168	134	90	83
Nb	0	0	0	0	0	0
Ni	62	149	56	61	73	102
V	307	315	250	268	294	309
Y	22	24	17	17	18	29
Zr	52	60	42	46	44	65
As						
Ba			15.1		7.36	25.73
Ga						
Pb						
Rb						
Sn						
Sr						
Ta						
Th						
Ce			5.94		6.06	9.27
Cs			0.062		0.047	0.056
Dy			2.736		2.875	4.836
Er			1.917		1.969	3.447
Eu			0.586		0.593	0.83
Gd			2.177		2.205	3.692
Hf			1.3		1.2	1.9
Ho			0.612		0.636	1.116
La			2.23		2.26	3.4
Lu			0.301		0.297	0.533
Nb			1.6		1.6	2.3
Nd			4.89		5.11	7.72
Pr			0.968		0.974	1.499
Rb			0.2		0.42	2.3
Sm			1.6		1.62	2.6
Sr			105		62.8	62.1
Ta			N.D.		N.D.	N.D.
Tb			0.398		0.407	0.668
Th			0.19		0.16	0.3
Tm			0.291		0.295	0.523
U			0.052		0.054	0.079
Y			16.22		16.74	30.86
Yb			1.97		1.92	3.49
Zr			44.5		42.8	70.6
Bi						
Sb			0.06		0.77	N.D.
Ag						
Be			0.13		0.15	0.18
Cd			N.D.		N.D.	N.D.
Co			45		38	30
Cu			69		51	88
Li			10		9	11
Mo			N.D.		N.D.	N.D.
Ni			70		79	101
Sc			39.4		30.5	32.5
Sr			91.8		53.4	53.9
V			238		215.1	273.5
W			N.D.		N.D.	N.D.
Zn			66		66	50

Station ID	04RJB0501	04RJB0504	04RJB0505	04RJB0539	04RJB-TGP002	04RJB0146
Sample number	04RJB0501	04RJB0504	04RJB0505	04RJB0539	04RJB-TGP002	04RJB0146_1_1
Township	Tisdale	Tisdale	Tisdale	Deloro	Tisdale	Mountjoy
Easting	478151	477738	477719	476128	475920	474660
Northing	5370259	5369926	5370160	5364556	5369200	5370236
Assemblage	Tisdale-Central	Tisdale-Central	Tisdale-Central	Tisdale-Central	Tisdale-Central	Tisdale-Central
Rock Unit	Basalt	Basalt	Basalt	Basalt	Basalt	Basalt
Rock Type	pillows	pillows	pillows	flow breccia	pillows	pillows
Rock Texture	amygdaloidal	amygdaloidal	variolitic		brecciated	variolitic
	ActLab	ActLab	ActLab	ActLab	ActLab	ActLab
SiO2	48.09	45.37	47.45	43.55	49.28	49.17
TiO2	0.76	0.82	1.12	0.76	0.8	0.36
Al2O3	12.54	13.55	11.99	13.79	13.31	17.45
Fe2O3	10.3	13.38	10.5	16.43	8.92	9.36
FeO						
MnO	0.242	0.229	0.302	0.312	0.188	0.168
MgO	5.05	5.12	3.23	9.07	4.38	9.17
CaO	9.8	8.57	12.2	6.22	9.97	9.48
K2O	0.27	0.31	1.67	0.06	0.88	0.03
Na2O	2.42	1.65	0.12	0.83	1.96	0.42
P2O5	0.05	0.06	0.1	0.07	0.06	0.04
Cr2O3	0.01	0.01	0	0.01	0.01	0.03
LOI	10.7927	10.6255	11.7012	8.7376	10.7605	4.34
Total	100.32	99.69	100.38	99.84	100.52	100.02
CO2	7.86	6.92	8.59	4.7	7.7	0.11
S	0.25	0.01	0.23	0.84	0.01	0.02
	ActLab	ActLab	ActLab	ActLab	ActLab	ActLab
Cr	92	92	11	101	109	276
Nb	0	0	0	0	0	0
Ni	72	83	35	75	82	161
V	290	329	413	349	331	147
Y	17	20	25	21	18	15
Zr	43	48	75	47	46	28
As						
Ba	173.94	97.93	147.18	10.36	268.33	4.3
Ga						
Pb						
Rb						
Sn						
Sr						
Ta						
Th						
Ce	6.22	6.75	8.43	6.08	4.43	4.09
Cs	0.3	0.23	0.793	0.115	1.315	0.052
Dy	3.023	3.143	4.821	3.523	2.703	2.012
Er	2.113	2.135	3.31	2.405	1.811	1.759
Eu	0.64	0.553	1.053	0.575	0.395	0.341
Gd	2.402	2.425	4.013	2.612	1.966	1.315
Hf	1.3	1.3	2.3	1.4	1.4	0.8
Ho	0.671	0.709	1.072	0.781	0.597	0.525
La	2.29	2.46	2.82	2.14	1.53	1.59
Lu	0.325	0.345	0.516	0.392	0.276	0.339
Nb	1.6	1.8	3	1.8	1.7	1.1
Nd	5.24	5.55	7.81	5.22	3.8	2.98
Pr	1.02	1.057	1.43	0.98	0.721	0.618
Rb	9.83	8.27	53.81	1.4	26.56	0.17
Sm	1.66	1.78	2.79	1.73	1.29	0.95
Sr	91.8	67.9	38.6	34.8	113.9	145
Ta	N.D.	N.D.	0.19	N.D.	N.D.	N.D.
Tb	0.439	0.458	0.707	0.496	0.388	0.26
Th	0.18	0.2	0.33	0.23	0.18	0.15
Tm	0.315	0.333	0.495	0.374	0.277	0.299
U	0.055	0.061	0.084	0.078	0.05	0.037
Y	17.89	18.72	27.06	20.27	15.27	14.32
Yb	2.08	2.2	3.34	2.47	1.82	2.07
Zr	46	46.8	79.3	49.2	47.4	28.3
Bi						
Sb	0.65	0.24	0.37	1.18	0.14	0.46
Ag						
Be	0.16	0.14	0.22	0.15	0.16	0.12
Cd	N.D.	N.D.	N.D.	N.D.	N.D.	N.D.
Co	41	37	32	54	44	46
Cu	107	45	162	167	103	28
Li	8	16	15	38	28	21
Mo	N.D.	N.D.	N.D.	N.D.	N.D.	N.D.
Ni	78	85	42	86	79	144
Sc	34.6	36.2	34.5	38.2	32.7	37
Sr	79.5	58	33.7	29.7	95.7	127.4
V	223	249.3	298.2	250.2	239.9	152.2
W	N.D.	5	N.D.	3	N.D.	N.D.
Zn	57	109	57	143	49	43

Station ID	04RJB0173	04RJB0181	04RJB0183	04RJB0224	04RJB0254	04RJB0232	04RJB0349
Sample number	04RJB0173_1_1	04RJB0181_1_1	04RJB0183_1_1	04RJB0224_1_1	04RJB0254_1_1	04RJB0232_1_1	04RJB0349_1_1
Township	Tisdale	Tisdale	Tisdale	Deloro	Deloro	Mountjoy	Tisdale
Easting	483225	476221	478357	475571	480391	475060	475790
Northing	5375432	5377965	5375669	5364882	5365097	5366824	5372753
Assemblage	Tisdale-Central	Porcupine	Tisdale-Central	Tisdale-Central	Timiskaming	Tisdale-Central	Tisdale-Central
Rock Unit	Basalt	clastic sediments	Basalt	Basalt	Timiskaming	Basalt	Basalt
Rock Type	pillows	sandstone	pillows	pillows	conglomerate	pillows	pillows
Rock Texture	amygdaloidal	bedded	flattened pillows	schistose	flattened clasts	amygdaloidal	brecciated
	ActLab	ActLab	ActLab	ActLab	ActLab	ActLab	ActLab
SiO2	48.91	49.23	50.39	38.92	45.97	42.27	46.89
TiO2	0.60	0.41	0.52	0.47	0.30	1.00	0.39
Al2O3	16.57	18.26	17.84	8.82	15.53	10.15	18.24
Fe2O3	12.36	8.50	8.88	9.30	8.78	13.90	9.53
FeO							
MnO	0.217	0.133	0.176	0.201	0.152	0.309	0.164
MgO	6.41	7.63	7.84	8.69	7.96	4.31	10.44
CaO	8.11	4.01	9.00	11.27	4.93	13.02	7.77
K2O	0.08	0.07	0.07	0.30	0.49	0.04	0.05
Na2O	3.18	5.93	2.65	2.33	4.91	0.66	2.34
P2O5	0.06	0.04	0.06	0.05	0.03	0.10	0.04
Cr2O3	0.02	0.01	0.04	0.13	0.03	-0.01	0.03
LOI	3.54	5.47	3.28	18.77	10.04	13.53	4.37
Total	100.05	99.69	100.75	99.25	99.12	99.28	100.25
CO2			0.08	16	7.11		0.1
S			0.03	0.12	0.25		N.D.
	ActLab	ActLab	ActLab	ActLab	ActLab	ActLab	ActLab
Cr	182	158	169	1007	219	37	266
Nb	0	0	0	0	0	0	0
Ni	160	183	139	558	220	31	158
V	225	224	198	188	207	307	154
Y	26	16	20	13	15	30	16
Zr	46	32	39	36	23	85	29
As							
Ba			6.69	65.38	31.09		5.58
Ga							
Pb							
Rb							
Sn							
Sr							
Ta							
Th							
Ce			5.88	5.85	3.08		4.33
Cs			0.056	0.114	0.211		0.093
Dy			2.813	1.804	2.062		2.206
Er			2.397	1.231	1.897		1.874
Eu			0.562	0.417	0.25		0.487
Gd			1.95	1.594	1.167		1.45
Hf			1.1	1	0.6		0.8
Ho			0.703	0.404	0.544		0.549
La			2.34	2.34	1.24		1.7
Lu			0.426	0.183	0.351		0.37
Nb			1.5	1.2	0.7		1.1
Nd			4.34	4.03	2.35		3.38
Pr			0.877	0.837	0.475		0.669
Rb			0.28	4.24	5.95		0.22
Sm			1.36	1.24	0.77		1.01
Sr			47.7	74.6	46.6		48.3
Ta			N.D.	N.D.	N.D.		N.D.
Tb			0.38	0.279	0.251		0.293
Th			0.21	0.32	0.12		0.15
Tm			0.38	0.182	0.312		0.312
U			0.056	0.114	0.035		0.04
Y			19.06	10.8	14.73		15.09
Yb			2.65	1.19	2.18		2.23
Zr			39	37	22.7		29.2
Bi							
Sb			0.16	0.46	0.2		0.33
Ag							
Be			0.15	0.11	N.D.		0.1
Cd		N.D.		4	N.D.		N.D.
Co			43	49	48		46
Cu			38	60	39		38
Li			8	26	55		23
Mo		N.D.		N.D.	N.D.		N.D.
Ni			139	447	185		151
Sc			42.8	21.3	39.2		38.8
Sr			42.4	65.3	40.9		41.5
V			197	138.2	144.6		159.8
W		N.D.		N.D.	N.D.		N.D.
Zn			48	37	45		44

Station ID	04RJB0350	04RJB0345	04RJB0410	04RJB0352	04RJB0398	04RJB0472	04RJB0476
Sample number	04RJB0350_1_1	04RJB0345_1_1	04RJB0410_1_1	04RJB0352	04RJB0398	04RJB0472	04RJB0476
Township	Tisdale	Tisdale	Tisdale	Tisdale	Tisdale	Tisdale	Tisdale
Easting	475261	476137	479960	475309	480880	483359	483375
Northing	5372462	5373261	5374612	5372176	5373923	5375653	5376037
Assemblage	Tisdale-Central	Tisdale-Central	Tisdale-Central	Tisdale-Central	Tisdale-Central	Tisdale-Central	Tisdale-Central
Rock Unit	Basalt	Basalt	Basalt	Basalt	Basalt	Basalt	Basalt
Rock Type	pillows	pillows	pillows	pillows	pillows	pillows	pillows
Rock Texture	variolitic		variolitic	flattened pillows	amygdaloidal		schistose
	ActLab	ActLab	ActLab	ActLab	ActLab	ActLab	ActLab
SiO2	47.42	48.27	45.44	48.65	51.83	49.31	45.04
TiO2	0.35	0.36	0.30	0.49	0.53	0.49	0.29
Al2O3	16.80	17.16	19.77	16.44	14.84	16.48	18.39
Fe2O3	9.74	9.24	9.75	11.11	13.16	10.7	9.91
FeO							
MnO	0.183	0.181	0.178	0.191	0.232	0.164	0.169
MgO	9.94	9.46	9.36	8.57	6.56	8.27	11.38
CaO	7.94	8.03	8.03	10.51	6.92	9.17	8.1
K2O	0.08	0.07	0.07	0.09	1.18	0.07	0.05
Na2O	2.22	2.29	1.85	0.75	2.24	1.96	2.22
P2O5	0.04	0.04	0.03	0.05	0.05	0.05	0.03
Cr2O3	0.07	0.08	0.03	0.02	0	0.02	0.03
LOI	5.14	4.83	4.94	3.4805	2.5546	3.2604	4.5046
Total	99.92	100.01	99.75	100.35	100.10	99.94	100.11
CO2	1.23	0.98				0.13	0.05
S	0.04	0.01				0.03	N.D.
	ActLab	ActLab	ActLab	ActLab	ActLab	ActLab	ActLab
Cr	508	569	220	179	35	176	219
Nb	0	0	0	0	0	0	0
Ni	236	234	218	135	60	119	204
V	155	156	132	179	249	181	121
Y	16	15	15	20	24	19	14
Zr	29	27	23	37	39	38	24
As							
Ba	6.51	21.37				12.95	4.61
Ga							
Pb							
Rb							
Sn							
Sr							
Ta							
Th							
Ce	3.49	3.86				5.63	2.74
Cs	0.087	0.115				0.038	0.037
Dy	2.03	2.107				2.703	1.693
Er	1.813	1.89				2.29	1.592
Eu	0.461	0.231				0.455	0.215
Gd	1.274	1.329				1.855	0.981
Hf	0.7	0.8				1.1	0.7
Ho	0.525	0.544				0.669	0.44
La	1.3	1.58				2.2	1.06
Lu	0.352	0.352				0.42	0.316
Nb	1	1.2				1.6	0.8
Nd	2.6	2.76				4.1	2.22
Pr	0.531	0.571				0.836	0.437
Rb	0.32	1.38				0.65	0.18
Sm	0.8	0.9				1.3	0.67
Sr	38.8	26.8				43.7	38.2
Ta	N.D.	N.D.				N.D.	N.D.
Tb	0.257	0.268				0.363	0.213
Th	0.13	0.22				0.19	0.11
Tm	0.296	0.302				0.373	0.266
U	0.037	0.059				0.054	0.029
Y	14.35	14.84				18.33	11.75
Yb	2.13	2.18				2.61	1.9
Zr	25.9	29.2				37.7	23
Bi							
Sb	0.46	0.36				0.12	0.84
Ag							
Be	N.D.	N.D.				N.D.	N.D.
Cd	N.D.	N.D.				N.D.	N.D.
Co	52	49				43	53
Cu	32	11				31	17
Li	35	31				14	28
Mo	N.D.	N.D.				N.D.	N.D.
Ni	222	211				114	183
Sc	39.3	37.6				37	34
Sr	34	16.9				35.3	32.7
V	158.6	159.5				166.9	129.7
W	N.D.	N.D.				N.D.	N.D.
Zn	48	45				51	44

Station ID	04RJB0492	04RJB0500	04RJB0169	04RJB0170	04RJB0255	04RJB0344
Sample number	04RJB0492	04RJB0500	04RJB0169_1_1	04RJB0170_1_1	04RJB0255_1_1	04RJB0344_1_1
Township	Tisdale	Tisdale	Tisdale	Tisdale	Deloro	Tisdale
Easting	480110	477969	482873	482809	480284	476173
Northing	5371110	5370787	5375294	5375214	5365024	5373379
Assemblage	Tisdale-Central	Tisdale-Central	porphyry dyke	porphyry dyke	Tisdale-Hersey Lake	Tisdale-Hersey Lake
Rock Unit	Basalt	Basalt	porphyry dyke	porphyry dyke	ultramafic volcanic	ultramafic volcanic
Rock Type	massive	pillow breccia	quartz-feldspar	quartz-feldspar	basaltic komatiite	spinifex
Rock Texture		flattened pillows	porphyry	porphyry	sheared	polysutured
	ActLab	ActLab	ActLab	ActLab	ActLab	ActLab
SiO2	49.38	53.45	38.25	36.90	32.74	44.76
TiO2	1.14	1.02	0.27	0.40	0.30	0.35
Al2O3	12.95	12.02	3.69	6.74	4.18	4.80
Fe2O3	11.29	12.91	8.27	9.21	8.85	11.83
FeO						
MnO	0.126	0.141	0.131	0.184	0.166	0.184
MgO	3.43	4.59	17.80	15.78	17.78	24.56
CaO	9.05	5.87	6.96	10.44	9.50	6.86
K2O	1.02	0.31	0.02	0.03	0.02	0.05
Na2O	1.54	1.93	0.01	0.06	0.03	0.03
P2O5	0.1	0.1	0.02	0.03	0.03	0.03
Cr2O3	0.01	0.01	0.25	0.32	0.26	0.32
LOI	9.9545	7.6919	23.82	19.73	26.16	6.37
Total	99.99	100.04	99.49	99.83	100.01	100.14
CO2	7.01	4.68	20.3	14.6	22.8	0.22
S	0.07	0.07	0.02	0.02	0.01	0.01
	ActLab	ActLab	ActLab	ActLab	ActLab	ActLab
Cr	76	82	2110	2678	2172	2142
Nb	1	1	0	0	0	0
Ni	46	49	1386	1013	1367	1672
V	369	308	116	185	131	139
Y	24	27	9	11	8	10
Zr	85	102	15	23	18	18
As						
Ba	168.44	91.13	3.36	5.09	1.73	9.1
Ga						
Pb						
Rb						
Sn						
Sr						
Ta						
Th						
Ce	12.3	14.74	1.76	2.65	1.97	1.7
Cs	0.924	0.354	0.062	0.048	0.048	0.839
Dy	4.463	5.327	1.139	1.502	1.056	1.203
Er	3.018	3.531	0.69	0.943	0.635	0.717
Eu	0.957	1.11	0.148	0.512	0.225	0.181
Gd	3.867	4.626	0.979	1.251	0.905	1.071
Hf	2.6	3.1	0.5	0.7	0.5	0.7
Ho	0.988	1.143	0.239	0.311	0.214	0.252
La	4.43	5.36	0.58	0.97	0.69	0.57
Lu	0.478	0.546	0.088	0.132	0.082	0.091
Nb	3.6	4.2	0.4	0.6	0.6	0.5
Nd	9.8	11.43	1.76	2.36	1.81	1.82
Pr	1.9	2.243	0.31	0.439	0.339	0.33
Rb	26.84	8.3	0.33	0.23	0.17	2.04
Sm	3.06	3.53	0.68	0.86	0.62	0.72
Sr	76.1	85.6	28	28.6	94.7	8.8
Ta	0.21	0.25	N.D.	N.D.	N.D.	N.D.
Tb	0.68	0.804	0.174	0.231	0.158	0.188
Th	0.44	0.54	N.D.	N.D.	N.D.	N.D.
Tm	0.457	0.53	0.096	0.134	0.09	0.101
U	0.113	0.139	0.031	0.019	0.018	0.018
Y	25.19	29.16	6.2	8.36	5.83	6.35
Yb	3.11	3.56	0.59	0.86	0.58	0.62
Zr	93.6	108.2	17.1	23.6	16.2	22.1
Bi						
Sb	0.38	0.45	0.09	0.07	0.5	0.25
Ag						
Be	0.31	0.2	N.D.	N.D.	N.D.	N.D.
Cd	N.D.	N.D.	N.D.	N.D.	N.D.	N.D.
Co	34	37	75	80	71	99
Cu	41	73	59	125	12	7
Li	23	7	25	8	26	2
Mo	N.D.	N.D.	N.D.	N.D.	N.D.	N.D.
Ni	54	60	1031	769	962	1418
Sc	32.5	29.1	13.3	22.1	13.7	17.1
Sr	64.8	77.6	24.6	24.9	82.2	7.7
V	266.6	220.7	75.1	129.9	81.3	112.8
W	N.D.	N.D.	N.D.	N.D.	N.D.	N.D.
Zn	65	73	26	44	42	58

Station ID	04RJB0351	04RJB0405	04RJB0194	04RJB-TW04-010	04RJB-TW04-011
Sample number	04RJB0351_1_1	04RJB0405_1_1	04RJB0194	04RJB-TW04-010	04RJB-TW04-011
Township	Tisdale	Tisdale	Tisdale	Ogden	Ogden
Easting	475498	481488	481765	475092	472548
Northing	5372319	5374514	5373171	5362959	5362701
Assemblage	Tisdale-Hersey Lake	Tisdale-Hersey Lake	Porcupine	Krist	Tisdale-intermediate
Rock Unit	ultramafic volcanic	ultramafic volcanic	Clastic Sediments	Felsic Volcanic	Intermediate Volcanic
Rock Type	spinifex	basaltic komatiite	graphitic phyllite	lapilli tuff	pyroclastic breccia
Rock Texture	polysutured	cumulate	laminated	flattened clasts	porphyritic
	ActLab	ActLab	ActLab	ActLab	ActLab
SiO2	37.68	40.61	51.66	67.2	52.34
TiO2	0.38	0.35	0.78	0.34	1.81
Al2O3	5.16	4.78	15.02	16.51	14.11
Fe2O3	10.73	11.90	7.48	2.57	10.45
FeO					
MnO	0.196	0.182	0.164	0.031	0.118
MgO	23.12	29.14	5.1	1.91	5.62
CaO	11.16	3.35	8.91	1.47	5.99
K2O	0.04	0.04	0.91	1.74	0.23
Na2O	0.06	0.04	2.11	5.25	3.14
P2O5	0.03	0.03	0.06	0.12	0.14
Cr2O3	0.32	0.33	0.02	0	0.02
LOI	11.18	9.49	8.0427	2.7507	5.8684
Total	100.06	100.24	100.26	99.89	99.84
CO2	4.63			1.17	2.64
S	0.01			N.D.	0.01
	ActLab	ActLab	ActLab	ActLab	ActLab
Cr	2223	2037	128	30	187
Nb	0	0	0	2	8
Ni	1457	1815	57	46	135
V	132	119	226	32	178
Y	9	9	16	8	19
Zr	18	20	42	122	113
As					
Ba	7.72			412.05	94.29
Ga					
Pb					
Rb					
Sn					
Sr					
Ta					
Th					
Ce	1.86			43.69	20.44
Cs	0.507			0.807	0.309
Dy	1.092			0.996	3.66
Er	0.712			0.449	1.773
Eu	0.198			0.803	1.472
Gd	0.865			1.863	4.387
Hf	0.6			3.4	3.3
Ho	0.241			0.166	0.666
La	0.66			21.11	7.97
Lu	0.102			0.05	0.205
Nb	0.7			2.8	7.9
Nd	1.72			19.22	15.98
Pr	0.313			5.129	3.169
Rb	1.95			47.14	5.41
Sm	0.63			3.03	4.28
Sr	86.1			251.8	278.7
Ta	N.D.			N.D.	0.46
Tb	0.16			0.205	0.652
Th	N.D.			3.41	0.79
Tm	0.102			0.058	0.235
U	0.018			1.014	0.237
Y	5.94			4.73	17.24
Yb	0.65			0.37	1.44
Zr	19.5			129.9	122.3
Bi					
Sb	0.22			0.66	0.33
Ag					
Be	N.D.			0.68	0.53
Cd	N.D.		N.D.		N.D.
Co	90			9	34
Cu	34			13	37
Li	1			34	39
Mo	N.D.		N.D.		N.D.
Ni	1218			48	126
Sc	16.2			2.7	13.4
Sr	75.5			226	231.8
V	102.3			28.4	126.6
W	N.D.			6	N.D.
Zn	56			41	96

Station ID	04RJB404	04RJB289	04RJB392				
Sample number	04RJB404-1-1	04RJB289-1-1	04RJB392-1-1	04JAA-0003	04JAA-0009	04JAA-0010	04PCT-0062
Township	Tisdale	Tisdale	Tisdale	Tisdale	Tisdale	Whitney	Deloro
Easting	482000	482614	477664	484309	475920	491529	478510
Northing	5374500	5373634	5371321	5371290	5369210	5372949	5364034
Assemblage	Tisdale	Tisdale	Tisdale	Porcupine	Tisdale	porphyry dyke	Deloro
Rock Unit	Intermediate volcanic	basalt	basalt	Clastic Sediments	basalt	porphyry dyke	Intermediate
Rock Type	massive	massive	pillows	wacke	heterolithic breccia	albitite	lapilli tuff
Rock Texture							
	ActLab	ActLab	ActLab	OGS-GL	OGS-GL	OGS-GL	OGS-GL
SiO2	51.30	51.29	49.78	66.54	49.51	75.37	61.73
TiO2	1.17	0.65	0.95	0.57	1.20	0.07	0.94
Al2O3	16.83	14.28	14.73	14.71	12.34	13.63	19.75
Fe2O3	10.29	11.27	11.85	5.47	11.39	0.88	5.27
FeO							
MnO	0.166	0.187	0.280	0.066	0.219	0.020	0.053
MgO	5.76	8.44	6.04	2.88	3.61	0.38	1.25
CaO	8.73	8.87	9.13	1.64	9.58	0.70	1.12
K2O	0.14	0.41	0.16	2.05	1.16	0.33	2.29
Na2O	3.02	1.76	2.97	3.26	0.83	7.64	4.73
P2O5	0.07	0.05	0.08	0.15	0.22	0.05	0.15
Cr2O3	0.03	0.03	0.02	0.02	0.01	0.01	-0.01
LOI	2.61	2.83	4.19	2.88	9.91	1.03	3.02
Total	100.11	100.06	100.18	100.24	99.98	100.11	100.29
CO2							
S							
	ActLab	ActLab	ActLab	GL-MNDM	GL-MNDM	GL-MNDM	GL-MNDM
Cr	229	165	125	173	86	39	-8
Nb	1	-1	-1				
Ni	99	56	159				
V	337	235	285				
Y	16	17	23				
Zr	48	37	55				
As				12	-5	8	14
Ba				496	231	102	422
Ga				15	16	16	20
Pb							
Rb							
Sn							
Sr							
Ta							
Th							
Ce				55.15	14.66	6.9	45.65
Cs				4.685	1.59	0.195	1.139
Dy				2.414	5.926	0.27	4.209
Er				1.35	3.986	0.154	2.569
Eu				1.3	0.961	0.119	1.182
Gd				3.311	4.946	0.335	4.356
Hf				3.4	2.8	3	5.1
Ho				0.475	1.294	0.053	0.866
La				27.42	5.37	3.56	20.83
Lu				0.194	0.597	0.026	0.396
Nb				5	4.3	5.6	8.4
Nd				25.87	12.12	2.41	21.16
Pr				6.647	2.306	0.726	5.514
Rb				61.26	34.04	6.98	62.52
Sm				4.46	3.65	0.41	4.43
Sr				222.9	221.6	137.3	146.8
Ta				0.31	0.25	0.29	0.7
Tb				0.442	0.901	0.046	0.684
Th				4.53	0.53	2.61	4.38
Tm				0.199	0.594	0.023	0.387
U				1.207	0.18	5.431	1.202
Y				13.6	34.04	1.64	24.48
Yb				1.27	3.88	0.16	2.54
Zr				139.5	101.1	66.8	201.3
Bi							
Sb							
Ag							
Be							
Cd							
Co							
Cu							
Li							
Mo							
Ni							
Sc							
Sr							
V							
W							
Zn							

Station ID	03-0273-0001	03-0273-0002	03-0273-0003	03-0273-0004	03-0273-0005	03-0273-0006	03-0273-0007
Sample number	03RJB10894-2	03RJB10894-3	03RJB10894-6	03RJB18968-2	03RJB18968-4	03RJB18967-3	03RJB10889-4
Township	Hoyle	Hoyle	Hoyle	Whitney	Whitney	Whitney	Hoyle
Easting	489906	489906	489906	493570	493570	492548	489956
Northing	5,377,761	5,377,761	5,377,761	5,373,572	5,373,572	5,373,764	5,377,798
Assemblage	Tisdale	Tisdale	Tisdale	Deloro	Deloro	Deloro	Tisdale
Rock Unit	Basalt	Basalt	Basalt	Basalt	Basalt	komatiite	komatiite
Rock Type	massive	massive	massive	massive	massive	talc chlorite schist	talc chlorite schist
Rock Texture	fine grained	fine grained	fine grained	fine grained	fine grained	fine grained	fine grained
	OGS-GL	OGS-GL	OGS-GL	OGS-GL	OGS-GL	OGS-GL	OGS-GL
SiO2	41.65	49.99	46.62	48.8	48.13	38.58	39.75
TiO2	0.3	0.56	0.95	1.34	1.43	0.42	0.39
Al2O3	15.04	15.52	13.82	11.58	12.23	8.02	8.34
Fe2O3	10.77	10.16	8	14.06	14.67	11.01	12.33
FeO	9.01	8.11	6.32	9.22	10.22	8.51	10.23
MnO	0.34	0.18	0.17	0.29	0.29	0.17	0.18
MgO	6.18	5.16	4.29	6.62	7.47	20.21	17.1
CaO	9.54	5.92	8.55	13.54	12.09	8.26	8.53
K2O	1.01	0.69	0.55	0.15	0.63	3.36	0.00
Na2O	2.61	3.89	3.39	1	1.15	0.51	0.42
P2O5	0.03	0.04	0.06	0.1	0.1	0.04	0.03
Cr2O3							
LOI	12.96	8.12	13.28	3.18	2.13	7.84	11.92
Total	100.43	100.23	99.68	100.66	100.32	98.42	98.99
CO2	9.65	4.94	12.4	1.8	0.89	3.77	6.68
S	0.02	0.03	0.44	0.13	0.31	0	0
	GL-MNDM	GL-MNDM	GL-MNDM	GL-MNDM	GL-MNDM	GL-MNDM	GL-MNDM
Cr	760	386	36	859	809	2508	2836
Nb	0	0	0	3	4	0	0
Ni							
V							
Y	11	12	17	22	23	12	9
Zr	18	31	53	81	86	36	25
As	15	12	74	20	11	0	6
Ba	1024	385	107	108	327	441	0
Ga	10	12	14	17	17	10	10
Pb	0	0	0	0	0	0	0
Rb	24	15	15	3	16	129	0
Sn	0	0	0	0	0	0	0
Sr	86	92	71	252	323	165	22
Ta	0	0	0	0	0	0	0
Th	0	0	0	0	0	0	0
Ce	2.77	4.17	7.57	16.28	16.45	3.88	3.34
Cs	0.71	0.48	0.39	0.45	2.25	9.13	0.12
Dy	1.71	2.47	3.33	4.52	4.74	2.13	1.82
Er	1.42	1.81	2.09	2.59	2.81	1.4	1.12
Eu	0.32	0.52	0.82	1.4	1.56	0.56	0.26
Gd	1.13	1.77	2.85	4.52	4.87	1.8	1.47
Hf	0.6	1	1.6	2.3	2.6	1.2	0.8
Ho	0.44	0.59	0.76	0.96	0.99	0.47	0.4
La	1.08	1.4	2.81	5.91	5.96	1.41	1.26
Lu	0.28	0.31	0.31	0.37	0.38	0.24	0.17
Nb	0.7	1.3	2.2	4.9	5	1.1	0.8
Nd	2.18	3.52	6.54	13.34	13.94	3.52	2.9
Pr	0.43	0.7	1.23	2.63	2.76	0.67	0.54
Rb	25.74	17.25	16.24	3.49	16.85	132.75	0.42
Sm	0.78	1.15	2.11	3.8	4.1	1.22	1.12
Sr	93.9	104.2	82.4	275.1	329.9	172.6	21.9
Ta				0.32	0.34		
Tb	0.22	0.34	0.49	0.75	0.77	0.32	0.26
Th	0.1	0.12	0.25	0.37	0.39	0.11	0.1
Tm	0.23	0.29	0.32	0.38	0.39	0.22	0.17
U	0.06	0.07	0.07	0.11	0.14	0.04	0.03
Y	11.55	14.5	18.85	23.68	24.45	12.46	9.65
Yb	1.6	1.83	1.96	2.41	2.57	1.49	1.1
Zr	18.7	34.6	57.4	89.7	90.8	42.2	27.1
Bi	N.D.	N.D.	N.D.	N.D.	N.D.	N.D.	N.D.
Sb	0.81	0.88	0.24	1.82	1.79	0.41	0.18
Ag	4	4	3	4	4	3	3
Be	0.55	0.51	0.35	0.56	0.59	0.23	0.21
Cd							
Co	62	48	49	77	78	81	87
Cu	52	106	119	187	168	15	56
Li							
Mo	0	0	0	0	0	0	0
Ni	262	157	61	402	311	737	652
Sc	35.1	34.2	39	32	33.5	23.9	24.4
Sr	87.9	89.8	70	244.6	311.7	155.4	21.6
V	157.8	203.2	296.3	261.4	280.3	139.4	156.9
W	0	0	17	0	0	0	0
Zn	103	86	100	126	148	81	86

Station ID	03-0273-0008	03-0273-0009	03-0273-0010	03-0273-0011	03-0273-0012	03-0273-0013
Sample number	03RJB10889-5	03RJB10893-1	03RJB10893-3	03RJB10893-4	03RJB18969-1	03RJB18969-7
Township	Hoyle	Hoyle	Hoyle	Hoyle	Whitney	Whitney
Easting	489956	489936	489936	489936	494334	494334
Northing	5,377,798	5,377,739	5,377,739	5,377,739	5,372,956	5,372,956
Assemblage	Tisdale	Tisdale	Tisdale	Tisdale	Deloro	Deloro
Rock Unit	komatiite	komatiite	komatiite	komatiite	komatiite	komatiite
Rock Type	talc chlorite schist	talc chlorite schist	talc chlorite schist	talc chlorite schist	talc chlorite schist	talc chlorite schist
Rock Texture	fine grained	fine grained	fine grained	fine grained	fine grained	fine grained
	OGS-GL	OGS-GL	OGS-GL	OGS-GL	OGS-GL	OGS-GL
SiO2	40.38	42.69	46.04	50.53	44.39	39.17
TiO2	0.28	0.56	0.43	0.4	0.27	0.4
Al2O3	5.92	12.4	16.51	17	6.31	9.03
Fe2O3	11.19	9.52	10.06	9.2	11.15	11.74
FeO	9.18	7.72	8.5	6.43	8.99	9.59
MnO	0.17	0.19	0.24	0.18	0.18	0.12
MgO	21.74	5.53	7.45	7.84	22.3	25.84
CaO	8.48	12.62	6.77	7.82	8.26	2.75
K2O	0.00	0.05	1.51	0.03	0.00	0.13
Na2O	0.1	3.63	2.14	3.15	0.14	0.05
P2O5	0.02	0.03	0.04	0.04	0.02	0.01
Cr2O3						
LOI	11.6	13.28	9.59	4.53	6.15	9.64
Total	99.88	100.50	100.78	100.72	99.17	98.88
CO2	6.39	10.8	5.33	1.32	1.4	2.06
S	0	0.15	0.03	0.09	0.01	0
	GL-MNDM	GL-MNDM	GL-MNDM	GL-MNDM	GL-MNDM	GL-MNDM
Cr	2550	60	174	199	2698	3348
Nb	0	0	0	0	0	0
Ni						
V						
Y	7	15	15	14	7	2
Zr	15	34	30	28	16	19
As	6	17	22	0	0	0
Ba	0	86	784	0	0	0
Ga	8	13	12	11	8	13
Pb	0	7	0	0	0	0
Rb	0	0	37	0	0	12
Sn	0	0	0	0	0	0
Sr	35	144	80	83	27	65
Ta	0	0	0	0	0	0
Th	0	0	0	0	0	0
Ce	2.06	4.37	3.93	4.52	1.73	0.96
Cs	0.2	0.07	1.17	0.11	0.14	4.28
Dy	1.46	2.72	2.49	2.21	1.39	0.51
Er	0.87	1.91	2.12	1.88	0.86	0.34
Eu	0.24	0.52	0.33	0.41	0.15	0.08
Gd	1.14	2.27	1.57	1.5	1.04	0.41
Hf	0.5	1.1	0.9	0.9	0.5	0.6
Ho	0.31	0.62	0.66	0.55	0.29	0.11
La	0.75	1.6	1.49	1.71	0.91	0.43
Lu	0.12	0.31	0.4	0.37	0.12	0.05
Nb	0.5	1.2	1.3	1.3	0.4	0.8
Nd	2.09	4.01	3.24	3.23	1.47	0.75
Pr	0.36	0.73	0.6	0.7	0.28	0.16
Rb	0.08	0.83	36.93	0.49	0.16	11.46
Sm	0.78	1.37	1.07	1.11	0.67	0.27
Sr	36.8	150.8	88	90.6	26.1	63.9
Ta						
Tb	0.21	0.4	0.32	0.29	0.21	0.07
Th		0.14	0.13	0.15		0.08
Tm	0.12	0.3	0.36	0.32	0.12	0.05
U	0.02	0.04	0.04	0.04	0.03	0.05
Y	7.49	16.62	16.68	15.82	7.05	2.73
Yb	0.87	1.98	2.49	2.19	0.78	0.36
Zr	16.8	36.4	32.6	30.7	15.9	19.5
Bi	N.D.	N.D.	N.D.	N.D.	0.11	N.D.
Sb	0.15	1.79	0.51	2.19	0.11	0.19
Ag	4	4	4	3	3	3
Be	0.13	0.48	1.02	0.17	0.34	0.19
Cd						
Co	89	38	48	45	92	103
Cu	62	72	49	61	0	0
Li						
Mo	0	0	0	0	0	0
Ni	893	57	131	106	951	1080
Sc	17.3	33.3	37.1	36.2	22.4	25.8
Sr	35	141.8	79.6	80.7	26.8	64.5
V	116.2	224.6	171.9	171.8	122.1	140.7
W	2	3	5	0	0	0
Zn	79	83	80	69	93	85

Station ID	03-0273-0014	03-0273-0015	03-0273-0016	03-0273-0017	03-0273-0018	03-0273-0019
Sample number	03RJB5045-1	03RJB5045-2	03RJB5045-3	03RJB5410-1	03RJB5284-1	03RJB5284-2
Township	Hoyle	Hoyle	Hoyle	Hoyle	Hoyle	Hoyle
Easting	489909	489909	489909	490569	490822	490823
Northing	5,377,944	5,377,944	5,377,944	5,377,638	5,377,553	5,377,553
Assemblage	Tisdale	Tisdale	Tisdale	Tisdale	Tisdale	Tisdale
Rock Unit	komatiite	komatiite	komatiite	komatiite	komatiite	komatiite
Rock Type	talc chlorite schist	talc chlorite schist	talc chlorite schist	talc chlorite schist	talc chlorite schist	talc chlorite schist
Rock Texture	fine grained	fine grained	fine grained	fine grained	fine grained	fine grained
	OGS-GL	OGS-GL	OGS-GL	OGS-GL	OGS-GL	OGS-GL
SiO2	32.75	35	47.4	42.49	44.99	45.79
TiO2	0.28	0.33	0.45	0.55	0.47	0.31
Al2O3	5.02	5.45	14.17	8.64	7.74	5.52
Fe2O3	9.36	10.2	10.84	11.83	11.93	10.47
FeO	7.81	8.37	8.29	6.14	7.12	7.49
MnO	0.16	0.12	0.2	0.17	0.2	0.16
MgO	18.85	18.41	10	13.34	16.45	22.98
CaO	7.79	6.38	6.06	7.83	10.15	8.54
K2O	0.00	0.00	0.00	0.12	0.12	0.02
Na2O	0.03	0.05	4.94	3.04	1.43	0.15
P2O5	0.01	0.02	0.03	0.04	0.02	0.03
Cr2O3						
LOI	24.46	22.66	5.05	10.23	5.69	5.68
Total	98.71	98.62	99.14	98.28	99.19	99.65
CO2	21.3	19.9	1.84	5.05	1.59	0.22
S	0.03	0.11	0.01	0.2	0.06	0.03
	GL-MNDM	GL-MNDM	GL-MNDM	GL-MNDM	GL-MNDM	GL-MNDM
Cr	2492	3099	8	1969	2159	3013
Nb	0	0	0	2	0	0
Ni						
V						
Y	5	7	15	13	10	6
Zr	12	21	29	35	23	15
As	543	614	3	0	0	8
Ba	0	0	29	34	40	0
Ga	6	7	10	11	10	8
Pb	0	0	0	0	0	0
Rb	0	0	0	9	8	0
Sn	0	0	0	0	0	0
Sr	47	49	26	47	18	14
Ta	0	0	0	0	0	0
Th	0	0	0	0	0	0
Ce	1.73	4.72	5.12	15.48	2.71	1.65
Cs	0.06	0.05	0.07	6.16	4.79	2.36
Dy	1.11	1.43	2.49	2.97	1.69	1.32
Er	0.71	0.87	2	1.7	1.17	0.71
Eu	0.22	0.27	0.4	0.36	0.37	0.32
Gd	0.92	1.28	1.7	2.77	1.38	1.05
Hf	0.4	0.6	0.9	1.4	0.8	0.5
Ho	0.24	0.32	0.61	0.59	0.39	0.26
La	0.61	1.92	1.93	7.23	0.96	0.4
Lu	0.1	0.14	0.36	0.23	0.17	0.09
Nb	0.4	1.5	1.3	4	0.8	0.5
Nd	1.57	3.25	4.12	8.19	2.52	2.02
Pr	0.29	0.68	0.84	2.01	0.47	0.33
Rb	0.11	0.15	0.15	10	6.12	0.84
Sm	0.6	0.93	1.19	2.32	1.02	0.75
Sr	47.1	46.4	28.4	52.5	17	13.8
Ta				0.24		
Tb	0.17	0.22	0.33	0.47	0.27	0.2
Th		0.29	0.19	1.02	0.07	
Tm	0.1	0.14	0.33	0.23	0.17	0.1
U	0.01	0.07	0.05	0.77	0.02	0.01
Y	5.92	8.14	15.95	16.04	9.58	6.23
Yb	0.66	0.97	2.16	1.5	1.05	0.65
Zr	14	23.7	31.8	47.3	24.9	16.3
Bi	N.D.	0.16	N.D.	0.05	N.D.	N.D.
Sb	3.6	0.75	0.67	0.21	0.73	1.32
Ag	3	3	2	2	2	3
Be	0.15	0.26	0.23	1.27	0.17	0.13
Cd						
Co	81	81	62	86	81	99
Cu	44	36	44	56	114	0
Li						
Mo	0	0	0	0	0	0
Ni	942	807	268	610	589	1248
Sc	15.7	15.4	41.7	27.2	28.3	20.3
Sr	46.9	50.5	27.3	51.2	17.6	14.2
V	94.3	90.2	187.5	188	170.1	107
W	0	0	0	0	0	0
Zn	69	71	84	107	86	73

Station ID	03-0273-0020	03-0273-0021	03-0273-0022	03-0273-0023	03-0273-0024	03-0273-0025	03-0273-0029
Sample number	03RJB5422-1	03RJB5282-1	03RJB5282-2	03RJB5282-3	03RJB6025-3	03RJB6025-6	03RJB5698-1
Township	Hoyle	Hoyle	Hoyle	Hoyle	Hoyle	Hoyle	Hoyle
Easting	490323	490831	490831	490831	492912	492913	491437
Northing	5,377,762	5,377,807	5,377,807	5,377,807	5,377,540	5,377,540	5,377,394
Assemblage	Tisdale	Tisdale	Tisdale	Tisdale	Tisdale	Tisdale	Tisdale
Rock Unit	komatiite	komatiite	komatiite	komatiite	Basalt	Basalt	komatiite
Rock Type	talc chlorite schist	talc chlorite schist	talc chlorite schist	talc chlorite schist	pillow breccia	pillow breccia	talc chlorite schist
Rock Texture	fine grained	fine grained	fine grained	fine grained	fine grained	fine grained	fine grained
	OGS-GL	OGS-GL	OGS-GL	OGS-GL	OGS-GL	OGS-GL	OGS-GL
SiO2	39.92	42.48	36.13	38.45	42.14	46.71	42.31
TiO2	0.44	0.33	0.31	0.43	0.49	0.42	0.24
Al2O3	7.03	7.29	6.48	7.86	17.01	17.74	5.45
Fe2O3	12.81	11.15	9.84	12.66	9.4	9.32	10.43
FeO	10.21	8.3	8.11	10.29	7.89	7.65	8.62
MnO	0.16	0.17	0.19	0.15	0.2	0.23	0.12
MgO	20.76	23.07	20.32	21.87	7.27	6.89	23.13
CaO	6.48	8.54	8.51	6.31	7.01	7.29	4.93
K2O	0.00	0.00	0.00	0.00	0.27	0.37	0.00
Na2O	0.48	0.03	0.68	0.24	3.64	1.48	0.05
P2O5	0.03	0.02	0.01	0.02	0.05	0.04	0.02
Cr2O3							
LOI	10.92	5.9	16.51	10.34	12.47	10.41	12.28
Total	99.03	98.98	98.98	98.33	99.95	100.90	98.96
CO2	5.3	11.3	12.1	4.63	10.2	5.87	7.25
S	0.01	0.03	0.05	0.27	0.65	0.09	0
	GL-MNDM	GL-MNDM	GL-MNDM	GL-MNDM	GL-MNDM	GL-MNDM	GL-MNDM
Cr	3103	2670	2971	4500	206	180	2374
Nb	0	0	0	0	0	0	0
Ni							
V							
Y	8	5	6	8	18	14	4
Zr	20	14	15	21	34	30	10
As	4	13	7	2	94	23	3
Ba	0	0	0	0	35	53	0
Ga	10	8	7	11	12	10	8
Pb	0	0	0	0	0	0	0
Rb	0	0	0	0	7	8	0
Sn	0	0	0	0	0	0	0
Sr	29	36	38	37	85	61	34
Ta	0	0	0	0	0	0	0
Th	0	0	0	0	0	0	0
Ce	2.42	1.48	1.56	2.37	5.66	3.79	0.75
Cs	0.69	0.12	0.35	0.66	0.27	0.24	0.16
Dy	1.7	1.22	1.18	1.74	2.68	2.25	0.83
Er	0.97	0.79	0.83	1.07	2.26	1.88	0.6
Eu	0.14	0.21	0.17	0.42	0.41	0.34	0.11
Gd	1.32	0.93	0.92	1.41	1.81	1.36	0.71
Hf	0.7	0.5	0.5	0.7	1	0.9	0.3
Ho	0.35	0.26	0.27	0.37	0.7	0.56	0.2
La	0.83	0.54	0.6	0.75	2.3	1.38	0.24
Lu	0.13	0.12	0.12	0.15	0.41	0.38	0.08
Nb	0.8	0.4	0.4	0.9	1.5	1.3	0.4
Nd	2.22	1.38	1.43	2.43	4.37	2.97	0.82
Pr	0.41	0.25	0.27	0.43	0.89	0.59	0.15
Rb	0.19	0.09	0.07	0.14	7.16	7.69	0.17
Sm	0.79	0.55	0.59	0.98	1.33	0.96	0.42
Sr	29.6	38	38	39.2	89	62.8	34
Ta							
Tb	0.24	0.17	0.16	0.26	0.36	0.3	0.13
Th	0.06			0.09	0.21	0.11	
Tm	0.14	0.12	0.11	0.16	0.38	0.34	0.08
U	0.02	0.01	0.01	0.02	0.06	0.04	0.01
Y	9.28	6.51	6.63	8.93	18.53	14.9	4.92
Yb	0.87	0.8	0.77	1.04	2.53	2.28	0.56
Zr	22.3	17	15.9	25.3	37.3	31.9	11.2
Bi	N.D.	N.D.	N.D.	N.D.	N.D.	N.D.	N.D.
Sb	0.19	0.11	0.14	0.19	0.34	0.16	0.24
Ag	2	2	3	3	3	3	3
Be	0.19	0.13	0.11	0.15	0.34	0.18	0.1
Cd							
Co	105	82	93	124	47	45	79
Cu	71	41	57	84	42	51	16
Li							
Mo	0	0	0	0	0	0	0
Ni	1087	968	1046	1531	137	133	880
Sc	23.9	18.6	20.1	25.4	37.4	35.9	13.4
Sr	30	36.9	38.4	40	80	61.7	31.4
V	148.5	109.6	121.7	136.2	180.9	178.7	95.6
W	0	0	0	0	24	0	0
Zn	92	73	70	85	84	77	81

Station ID	03-0273-0030	03-0273-0034	03-0273-0035	03-0273-0036	03-0273-0037	03-0273-0038
Sample number	03RJB5698-2	03RJB18973-12	03RJB18973-17	03RJB18973-21	03RJB18974-3	03RJB18974-8
Township	Hoyle	Whitney	Whitney	Whitney	Whitney	Whitney
Easting	491437	492148	492148	492148	491388	491388
Northing	5,377,394	5,375,256	5,375,256	5,375,256	5,374,844	5,374,844
Assemblage	Tisdale	Tisdale	Tisdale	Tisdale	Tisdale	Tisdale
Rock Unit	komatiite	Basalt	Basalt	Basalt	komatiite	komatiite
Rock Type	talc chlorite schist	Basaltic komatiite	Basaltic komatiite	Basaltic komatiite	talc chlorite schist	talc chlorite schist
Rock Texture	fine grained	spinifex	spinifex	spinifex	fine grained	fine grained
	OGS-GL	OGS-GL	OGS-GL	OGS-GL	OGS-GL	OGS-GL
SiO2	37.08	29.78	42.52	42.11	33.43	38.82
TiO2	0.42	0.3	0.62	0.32	0.29	0.58
Al2O3	7.36	5.29	8.8	13.86	4.96	7.97
Fe2O3	11.93	9	15.03	8.86	8.98	10.39
FeO	9.9	7.37	11.81	7.02	7.44	8.41
MnO	0.14	0.18	0.34	0.16	0.17	0.19
MgO	20.67	14.84	11.13	8.16	16.98	13.71
CaO	6.31	14.31	12.21	11.78	9.91	7.64
K2O	0.00	0.00	0.13	0.68	0.00	0.00
Na2O	0.07	0.05	0.41	1.55	0.02	1.16
P2O5	0.02	0.02	0.04	0.03	0.02	0.04
Cr2O3						
LOI	14.45	24.42	7.88	12.46	23.98	18.39
Total	98.45	98.19	99.11	99.97	98.74	98.89
CO2	9.25	21.4	4.68	9	20.8	15.4
S	0.02	0.21	0.09	0.42	0.03	0.07
	GL-MNDM	GL-MNDM	GL-MNDM	GL-MNDM	GL-MNDM	GL-MNDM
Cr	3189	2770	2624	666	2537	1989
Nb	0	0	0	0	0	0
Ni						
V						
Y	7	5	13	11	6	14
Zr	18	16	31	21	13	31
As	4	78	4	18	216	318
Ba	0	0	58	154	0	0
Ga	9	7	12	8	6	10
Pb	0	0	0	0	0	0
Rb	0	0	3	13	0	0
Sn	0	0	0	0	0	0
Sr	36	91	33	37	51	34
Ta	0	0	0	0	0	0
Th	0	0	0	0	0	0
Ce	2.23	2.31	4.08	2.99	2.35	4.84
Cs	0.205	0.073	0.25	0.146	0.072	0.052
Dy	1.419	1.123	2.348	1.655	1.541	2.488
Er	0.901	0.725	1.521	1.403	0.974	1.732
Eu	0.203	0.259	0.46	0.226	0.322	0.449
Gd	1.143	0.925	1.96	1.056	1.247	1.918
Hf	0.6	0.5	0.9	0.6	0.5	1
Ho	0.308	0.239	0.516	0.412	0.33	0.557
La	0.75	0.86	1.39	1.18	0.82	1.71
Lu	0.117	0.1	0.223	0.27	0.12	0.261
Nb	0.6	0.7	1.3	0.9	0.5	1.2
Nd	2.2	2.07	3.98	2.32	2.22	4.16
Pr	0.395	0.391	0.72	0.473	0.421	0.793
Rb	0.33	0.28	2.99	15.09	0.39	0.24
Sm	0.78	0.67	1.42	0.72	0.8	1.42
Sr	38.6	100.3	35.2	40.4	57.3	38.4
Ta			0.19			0.18
Tb	0.209	0.164	0.354	0.213	0.229	0.362
Th		0.07	0.1	0.1		0.12
Tm	0.125	0.103	0.221	0.227	0.129	0.258
U	0.014	0.021	0.029	0.027	0.013	0.032
Y	8.26	6.58	13.18	11.7	9.2	15.2
Yb	0.81	0.67	1.44	1.63	0.83	1.72
Zr	21.5	17.8	30.7	23.1	16.4	34.8
Bi	N.D.	0.06	N.D.	N.D.	0.07	N.D.
Sb	0.2	0.2	0.5	0.15	1.09	1.65
Ag	2	3	3	3	2	0
Be	0.14	0.15	0.34	0.17	0.19	0.24
Cd						
Co	93	90	105	58	74	73
Cu	96	55	89	74	44	80
Li						
Mo	0	0	0	0	0	0
Ni	971	1007	611	376	887	726
Sc	22.1	17.5	32.1	29.5	16.4	25
Sr	34.7	92.5	33.1	37.4	52.1	34
V	144	107.9	203.2	140.6	103.5	189
W	0	0	0	0	0	0
Zn	84	72	113	69	62	82

Station ID	03-0273-0039	03-0273-0040	03-0273-0041	03-0273-0046	03-0273-0047	03-0273-0048	03-0273-0049
Sample number	03RJB18974-11	03RJB18974-13	03RJB18974-17	03RJB18966-15	03RJB18966-17	3RJB18971-1	03RJB18971-4
Township	Whitney	Whitney	Whitney	Whitney	Whitney	Whitney	Whitney
Easting	491388	491388	491388	492270	492270	493028	493028
Northing	5,374,844	5,374,844	5,374,844	5,374,290	5,374,290	5,372,884	5,372,884
Assemblage	Tisdale	Tisdale	Tisdale	Tisdale	Tisdale	Deloro	Deloro
Rock Unit	Basalt	Basalt	komatiite	komatiite	komatiite	Basalt	Basalt
Rock Type	Basaltic komatiite	Basaltic komatiite	talc chlorite schist	talc chlorite schist	talc chlorite schist	massive	massive
Rock Texture	brecciated	brecciated	fine grained	fine grained	fine grained	fine grained	fine grained
	OGS-GL	OGS-GL	OGS-GL	OGS-GL	OGS-GL	OGS-GL	OGS-GL
SiO2	49.62	38.99	36.97	43.99	41.62	51.36	49.66
TiO2	1.26	0.29	0.38	0.3	0.22	0.85	0.86
Al2O3	13.91	13.12	5.47	6.27	6.02	14.75	15.06
Fe2O3	9.83	8.56	10.23	10.28	9.97	11.73	13.08
FeO	7.89	7.06	8.98	8.28	6.22	8.53	8.79
MnO	0.2	0.16	0.14	0.15	0.16	0.27	0.18
MgO	4.67	8.35	23.1	24.64	25.11	6.8	7.36
CaO	6.27	10.27	6.24	6.09	7.99	9.57	10.26
K2O	0.13	0.4	0.00	0.52	0.07	0.09	0.21
Na2O	5.2	4.46	0.02	0.41	0.44	2.5	1.97
P2O5	0.09	0.02	0.02	0.01	0.01	0.07	0.06
Cr2O3							
LOI	9.55	15.07	16.77	6.47	7.96	3.32	2.44
Total	100.73	99.69	99.34	99.13	99.57	101.31	101.14
CO2	8.05	13.5	12.8	0.56	1.84	0.94	0.09
S	0.13	0.54	0.07	0.2	0.05	0.01	0.17
	GL-MNDM	GL-MNDM	GL-MNDM	GL-MNDM	GL-MNDM	GL-MNDM	GL-MNDM
Cr	118	646	3088	2944	2840	106	95
Nb	2	0	0	0	0	0	0
Ni							
V							
Y	32	10	6	5	8	19	19
Zr	75	19	16	15	15	46	48
As	28	89	43	3	0	0	0
Ba	57	89	0	0	0	35	62
Ga	17	9	8	7	7	14	16
Pb	0	0	0	0	0	0	0
Rb	0	6	0	28	3	2	4
Sn	0	0	0	0	0	0	0
Sr	51	74	40	58	92	72	117
Ta	0	0	0	0	0	0	0
Th	0	0	0	0	0	0	0
Ce	10.95	2.44	2.41	2.73	1.59	6.79	6.71
Cs	0.055	0.119	0.186	3.564	1.058	0.037	0.126
Dy	5.182	1.517	1.089	0.938	1.353	3.413	3.434
Er	3.713	1.318	0.669	0.565	0.919	2.39	2.393
Eu	0.948	0.203	0.251	0.233	0.236	0.713	0.723
Gd	4.014	0.968	0.952	0.797	1.04	2.738	2.722
Hf	2.2	0.6	0.5	0.4	0.5	1.4	1.5
Ho	1.188	0.378	0.228	0.193	0.305	0.778	0.776
La	4.02	0.94	0.86	1.16	0.59	2.44	2.42
Lu	0.572	0.245	0.089	0.082	0.143	0.364	0.388
Nb	2.9	0.8	0.6	0.7	0.4	1.7	1.9
Nd	8.94	1.96	>100.00	1.88	1.54	5.87	5.81
Pr	1.712	0.387	0.412	0.398	0.281	1.096	1.099
Rb	2	6.8	0.24	27.65	2.78	2.05	4.62
Sm	2.9	0.66	0.73	0.6	0.64	1.96	1.96
Sr	54.5	79.9	44.8	61	98.4	77.1	125.2
Ta	0.28					0.21	0.22
Tb	0.752	0.195	0.167	0.143	0.198	0.499	0.501
Th	0.33	0.08		0.16		0.2	0.2
Tm	0.554	0.21	0.094	0.081	0.136	0.358	0.368
U	0.087	0.022	0.012	0.073	0.011	0.052	0.054
Y	31.74	10.65	6.01	5.04	8.28	20.72	20.79
Yb	3.74	1.5	0.6	0.55	0.9	2.37	2.45
Zr	80	20.2	17.5	14.6	13.5	48	50.2
Bi	N.D.	0.11	N.D.	N.D.	N.D.	N.D.	N.D.
Sb	0.32	0.21	0.16	0.2	0.18	0.13	0.16
Ag	2	2	2	3	3	3	3
Be	0.38	0.18	0.13	0.62	0.12	0.34	0.33
Cd							
Co	45	49	99	89	98	46	47
Cu	148	41	72	23	40	93	135
Li							
Mo	0	0	0	0	0	0	0
Ni	149	255	1113	1064	1212	86	77
Sc	37.7	27.8	17.1	19.6	20.7	43.2	43.4
Sr	49.2	71.5	40.4	58.1	86.7	70	113.3
V	320	129.1	113.9	117	100.2	290.9	299.4
W	0	15	0	0	0	0	0
Zn	107	70	74	78	70	101	98

Station ID	03-0273-0050	03-0273-0052
Sample number	03RJB18971-7	03RJB18972-5
Township	Whitney	Whitney
Easting	493028	491548
Northing	5,372,884	5,372,704
Assemblage	Deloro	Deloro
Rock Unit	Basalt	Basalt
Rock Type	massive	massive
Rock Texture	fine grained	fine grained
	OGS-GL	OGS-GL
SiO2	49.7	44.59
TiO2	0.71	0.65
Al2O3	15.11	13.75
Fe2O3	11.82	9.83
FeO	8.12	7.85
MnO	0.17	0.2
MgO	8.45	9.39
CaO	10.8	8.76
K2O	0.32	0.07
Na2O	1.2	4.52
P2O5	0.05	0.06
Cr2O3		
LOI	2.79	8.9
Total	101.12	100.72
CO2	0.07	5.5
S	0.09	0.08
	GL-MNDM	GL-MNDM
Cr	319	1154
Nb	0	0
Ni		
V		
Y	16	13
Zr	38	34
As	0	13
Ba	83	0
Ga	15	15
Pb	0	0
Rb	9	0
Sn	0	0
Sr	98	52
Ta	0	0
Th	0	0
Ce	5.58	4.32
Cs	0.142	0.805
Dy	2.903	2.456
Er	2.057	1.684
Eu	0.615	0.543
Gd	2.318	1.981
Hf	1.2	1
Ho	0.65	0.54
La	1.98	1.59
Lu	0.319	0.259
Nb	1.4	1.3
Nd	4.81	3.82
Pr	0.916	0.708
Rb	8.37	1.25
Sm	1.64	1.38
Sr	102.4	55.1
Ta	0.2	0.18
Tb	0.427	0.367
Th	0.17	0.16
Tm	0.304	0.249
U	0.043	0.052
Y	17.61	14.13
Yb	2.03	1.64
Zr	39.3	35.9
Bi	N.D.	N.D.
Sb	0.11	N.D.
Ag	3	3
Be	0.28	0.28
Cd		
Co	48	58
Cu	118	116
Li		
Mo	0	0
Ni	116	307
Sc	40.5	36.1
Sr	96.1	50.1
V	254.3	223.6
W	0	0
Zn	126	73

Metric Conversion Table

Conversion from SI to Imperial			Conversion from Imperial to SI		
SI Unit	*Multiplied by*	*Gives*	*Imperial Unit*	*Multiplied by*	*Gives*
		LENGTH			
1 mm	0.039 37	inches	1 inch	**25.4**	mm
1 cm	0.393 70	inches	1 inch	**2.54**	cm
1 m	3.280 84	feet	1 foot	**0.304 8**	m
1 m	0.049 709	chains	1 chain	20.116 8	m
1 km	0.621 371	miles (statute)	1 mile (statute)	**1.609 344**	km
		AREA			
1 cm^2	0.155 0	square inches	1 square inch	**6.451 6**	cm^2
1 m^2	10.763 9	square feet	1 square foot	**0.092 903 04**	m^2
1 km^2	0.386 10	square miles	1 square mile	2.589 988	km^2
1 ha	2.471 054	acres	1 acre	0.404 685 6	ha
		VOLUME			
1 cm^3	0.061 023	cubic inches	1 cubic inch	**16.387 064**	cm^3
1 m^3	35.314 7	cubic feet	1 cubic foot	0.028 316 85	m^3
1 m^3	1.307 951	cubic yards	1 cubic yard	0.764 554 86	m^3
		CAPACITY			
1 L	1.759 755	pints	1 pint	0.568 261	L
1 L	0.879 877	quarts	1 quart	1.136 522	L
1 L	0.219 969	gallons	1 gallon	**4.546 090**	L
		MASS			
1 g	0.035 273 962	ounces (avdp)	1 ounce (avdp)	28.349 523	g
1 g	0.032 150 747	ounces (troy)	1 ounce (troy)	**31.103 476 8**	g
1 kg	2.204 622 6	pounds (avdp)	1 pound (avdp)	**0.453 592 37**	kg
1 kg	0.001 102 3	tons (short)	1 ton (short)	**907.184 74**	kg
1 t	1.102 311 3	tons (short)	1 ton (short)	**0.907 184 74**	t
1 kg	0.000 984 21	tons (long)	1 ton (long)	**1016.046 908 8**	kg
1 t	0.984 206 5	tons (long)	1 ton (long)	**1.016 046 90**	t
		CONCENTRATION			
1 g/t	0.029 166 6	ounce (troy)/ ton (short)	1 ounce (troy)/ ton (short)	34.285 714 2	g/t
1 g/t	0.583 333 33	pennyweights/ ton (short)	1 pennyweight/ ton (short)	1.714 285 7	g/t

OTHER USEFUL CONVERSION FACTORS

	Multiplied by	
1 ounce (troy) per ton (short)	31.103 477	grams per ton (short)
1 gram per ton (short)	0.032 151	ounces (troy) per ton (short)
1 ounce (troy) per ton (short)	20.0	pennyweights per ton (short)
1 pennyweight per ton (short)	0.05	ounces (troy) per ton (short)

Note: Conversion factors which are in bold type are exact. The conversion factors have been taken from or have been derived from factors given in the Metric Practice Guide for the Canadian Mining and Metallurgical Industries, published by the Mining Association of Canada in co-operation with the Coal Association of Canada.

ISSN 0826-9580
ISBN 0-7794-7791-X

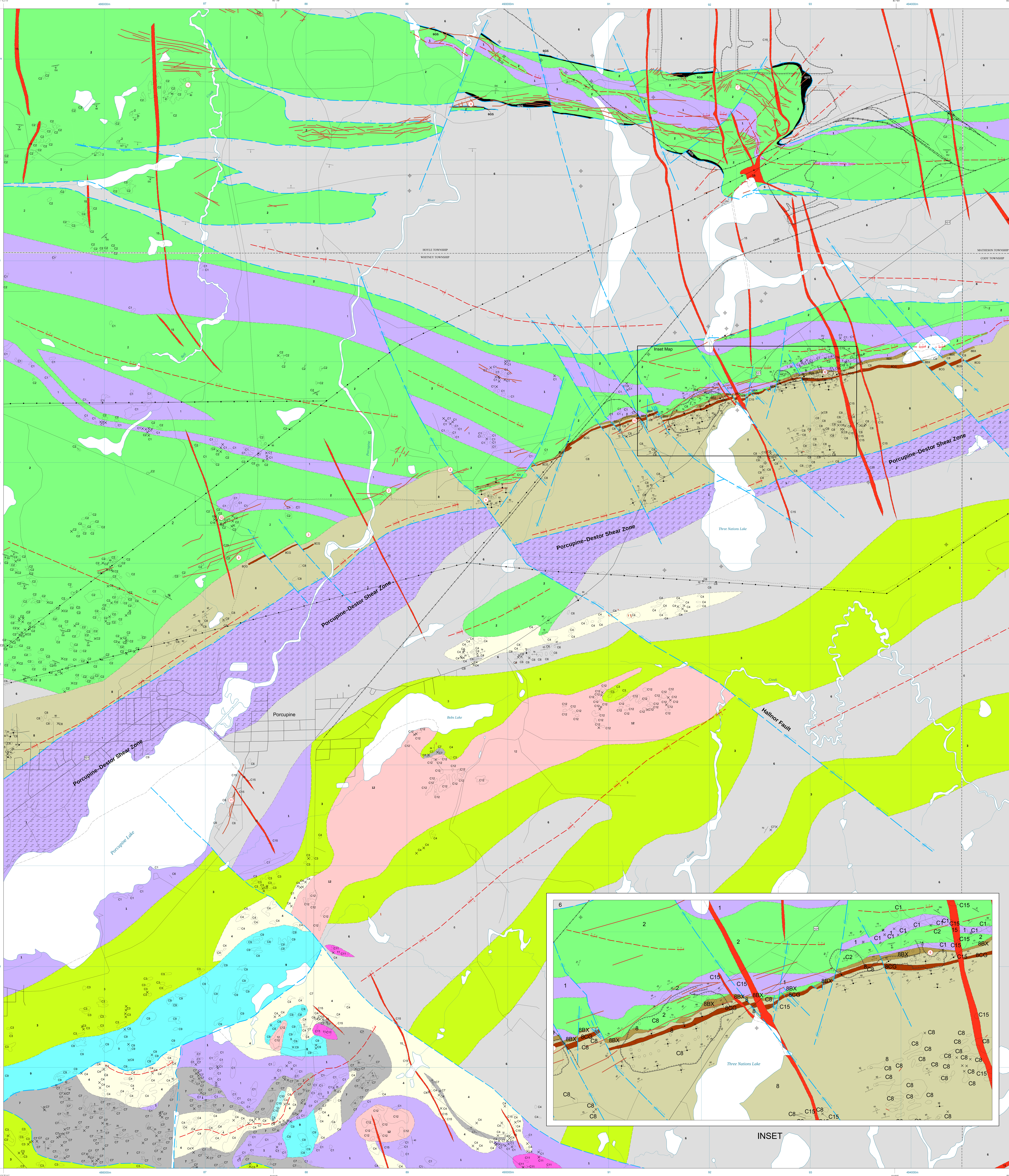

Ontario

Ontario Geological Survey

MAP P.3547—REVISED

PRECAMBRIAN GEOLOGY

PARTS OF WHITNEY AND HOYLE TOWNSHIPS

Scale 1:10 000

250 m 0 0.25 500 m

NTS Reference: 42 A/6, 11

This map is published with the permission of the Director, Ontario Geological Survey.

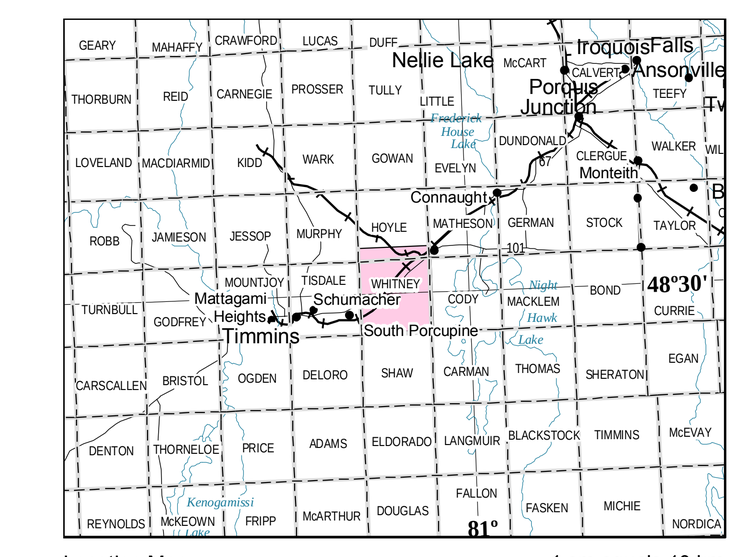

Location Map — 1 cm equals 10 km

This geologic map represents one of the products of the Greenstone Architecture Project of the Discover Abitibi Initiative, which was designed to stimulate mineral exploration in the Ontario portion of the Abitibi greenstone belt and has components that range from geophysical surveying to deposit-scale mapping (see Ayer et al. 2003). This map presents results from the first year of the Gold Subproject 1 study, as summarized in Bateman et al. 2004.

Cette carte géologique représente un des produits découlant du projet relatif à la ceinture de roches vertes architecturale, lequel s'inscrit dans le cadre de l'initiative *Découvrons l'Abitibi*, conçue pour stimuler l'exploration minérale dans la section ontarienne de la ceinture de roches vertes de l'Abitibi et constituée de diverses composantes, depuis les levés géophysiques jusqu'aux cartes à l'échelle du gisement (voir Ayer et al. 2003). Cette carte présente les résultats de la deuxième année de l'étude portant sur le sous-projet 1 relatif à l'or, résumée dans Bateman et al. 2004.

Ayer, J.A., Thurston, P.C., Dubé, B., Fowler, A.D., Gibson, H.L., Hudak, G., Lafrance, B., Lesher, C.M., Piercey, S.J., Reed, L.E. and Thompson, P.H. 2003. Overview of the Discover Abitibi Greenstone Architecture project: subprojects, goals and results; *in* Summary of Field Work and Other Activities 2003, Ontario Geological Survey, Open File Report 6120, p.32-1 to 32-12.

Bateman, R., Ayer, J.A. and Dubé, B. 2003. Discover Abitibi. Gold Subproject 1. Structures and gold mineralization in the Pamour–Hoyle Pond portion of the eastern Timmins gold camp; *in* Summary of Field Work and Other Activities 2003, Ontario Geological Survey, Open File Report 6120, p.34-1 to 34-6.

LEGEND[abcd]

PHANEROZOIC

CENOZOIC

QUATERNARY

PLEISTOCENE AND RECENT

UNCONFORMITY

PRECAMBRIAN

REGIONAL METAMORPHISM

PROTEROZOIC

15	**Diabase Dike (Matachewan Swarm)**

ARCHEAN

12	**Felsic to Intermediate Intrusive Rocks**
11	**Porphyry Intrusive Rocks**
10	**Mafic Intrusive Rocks**
9	**Ultramafic Intrusive Rocks**
8	**Timiskaming–Type Clastic Metasedimentary Rocks**
BX	Basal breccia
CG	Conglomerate
7	**Chemical Sedimentary Rocks**
6	**Clastic Sedmentary Rocks (Porcupine Assemblage)**
GS	Graphitic shale
4	**Felsic Volcaniclastic and Sedimentary Rocks**
3	**Intermediate Volcanic Rocks:** flows
2	**Mafic Volcanic Rocks:** flows
1	**Ultramafic Volcanic Rocks:** flows

[a] The rock unit codes for this legend were designed for use with a database of geoscience information related to the Discover Abitibi Initiative. Not all codes used in the database are shown in this legend.
[b] The letter "C" preceding a rock code denotes information compiled from previously published maps and reports.
[c] Lithology codes associated with diamond drill holes were derived from the author's logging of these drill cores.
[d] The placement of some contacts was based on interpretation of drill hole, surface and underground level plans made available by Porcupine Joint Venture.

SYMBOLS

- Geological contact, interpreted
- Area of bedrock outcrop
- Small bedrock outcrop
- Open pit mine
- Tailings pond
- Crossbedding, with facing, inclined
- Graded bedding, with facing, (inclined, overturned)
- Pillows, with facing, (inclined, trend, magnitude of dip uncertain)
- Sedimentary bedding, facing known from other than grading or crossbedding (inclined, magnitude of dip uncertain)
- Overturned sedimentary bedding, facing known from other than grading or crossbedding (inclined, magnitude of dip uncertain)
- Bedding, no facing (inclined, dip uncertain)
- Foliation, 3rd generation, (inclined, magnitude of dip uncertain)
- Foliation, 4th generation, inclined)
- Foliation, 5th generation, inclined
- Mine location, keyed to list
- Mapping location
- Logged diamond-drill hole
- Syncline, D2
- Anticline, inclined, D2
- Anticline, upright, D4
- Syncline, upright, D4
- Fault, thrust, D3 ball on downtown side
- Fault, extensional, D1, ball on downthrown side
- Fault, right lateral, D4
- Fault, left lateral, D4
- Fault, reverse, D2
- Fault, right lateral, inferred
- Fault
- Shear zone
- Quartz vein

MINE LOCATIONS

Map No.	Name	Status	Commodity
1.	Bell Creek Mine	past producer	Au
2.	Bonetal Mine	past producer	Au
3.	Bonwhit	past producer	Au
4.	Broulan Mine	past producer	Au
5.	Hallnor (Pamour No.2) Mine	past producer	Au
6.	Hoyle Mine	past producer	Au
7.	Hoyle Pond Mine	producing mine, Porcupine Joint Venture	Au
8.	Hugh-Pam mine	past producer	Au
9.	Owl Creek Mine	past producer	Au
10.	Pamour No.1 Mine	past producer	Au
11.	Porcupine Lake/Hunter Mine	past producer	Au
12.	Reef Mine	past producer	Au

SOURCES OF INFORMATION

Base map information data derived from the Ontario Land Information Warehouse, Land Information Ontario, Ontario Ministry of Natural Resources, scale 1:20 000. Universal Transverse Mercator (UTM) co-ordinates are in North American Datum 1983 (NAD 83), Zone 17.

Mineral deposit information derived from the Mineral Deposit Inventory (MDI2), maintained by the Ontario Geological Survey, Resident Geologist Program.

Berger, B.R. 1998. Precambrian geology, Hoyle township; Ontario Geological Survey, Map 2532, scale 1:20 000.

Ferguson, S.A. 1968. Geology and ore deposits of Tisdale Township, District of Cochrane; Ontario Department of Mines, Geological Report 58. Accompanied by Map 2075, scale 1:12 000.

Piroschco, D.W. and Kettles, K. 1990. Structural geology, Whitney Township; Ontario Geological Survey, Map 3172, scale 1:10 000.

Placer Dome (Porcupine Joint Venture) 2003. Helicopter magnetic survey, line spacing 100 m., sensor at 30 m., Whitney and Hoyle townships. Unpublished data.

Discover Abitibi 2003. Timmins GEOTEM electromagnetic survey (Abitibi Supergrid), line spacing 200 m., sensor altitude 120 m., Whitney and Hoyle townships. Unpublished data.

Magnetic declination approximately 11°7′ at the centre of the map area in 2003.

CREDITS

Geology and digital map preparation by R. Bateman, 2003.

Cartographic production by S. MacLean.

Geologic mapping and research supported by the Discover Abitibi Initiative under contract awarded to the Mineral Exploration Research Centre (MERC), Laurentian University, Sudbury, Ontario.

Contract management, project management by Robert Calhoun, Project Manager, Discover Abitibi Initiative.

Overall project management by Timmins Economic Development Corporation.

Porcupine Joint Venture made available their geological, geophysical, geochemical and drillhole databases.

L. Reed (consulting geophysicist) integrated data and generated custom plots of total magnetic field and first vertical derivatives of total magnetic field for Discover Abitibi.

Discover Abitibi Initiative
The Discover Abitibi Initiative is a regional, cluster economic development project based on geoscientific investigations of the western Abitibi greenstone belt. The initiative, centred on the Kirkland Lake and Timmins mining camps, will complete 19 projects developed and directed by the local stakeholders. FedNor, Northern Ontario Heritage Fund Corporation, municipalities and private sector investors have provided the funding for the initiative.

Initiative Découvrons l'Abitibi
L'initiative *Découvrons l'Abitibi* est un projet de développement économique régional dans une grappe d'industries, projet fondé sur des études géoscientifiques de la ceinture de roches vertes de l'Abitibi occidental. Cette initiative, centrée sur les zones minières de Kirkland Lake et de Timmins, mènera à bien 19 projets élaborés et dirigés par des intervenants locaux. FedNor, la Société de gestion du Fonds du patrimoine du Nord de l'Ontario, municipalités et des investisseurs du secteur privé ont fourni les fonds de cette initiative.

Bateman, R. 2004. Precambrian geology, parts of Whitney and Hoyle townships; Ontario Geological Survey, Preliminary Map P.3547—Revised, scale 1:10 000.

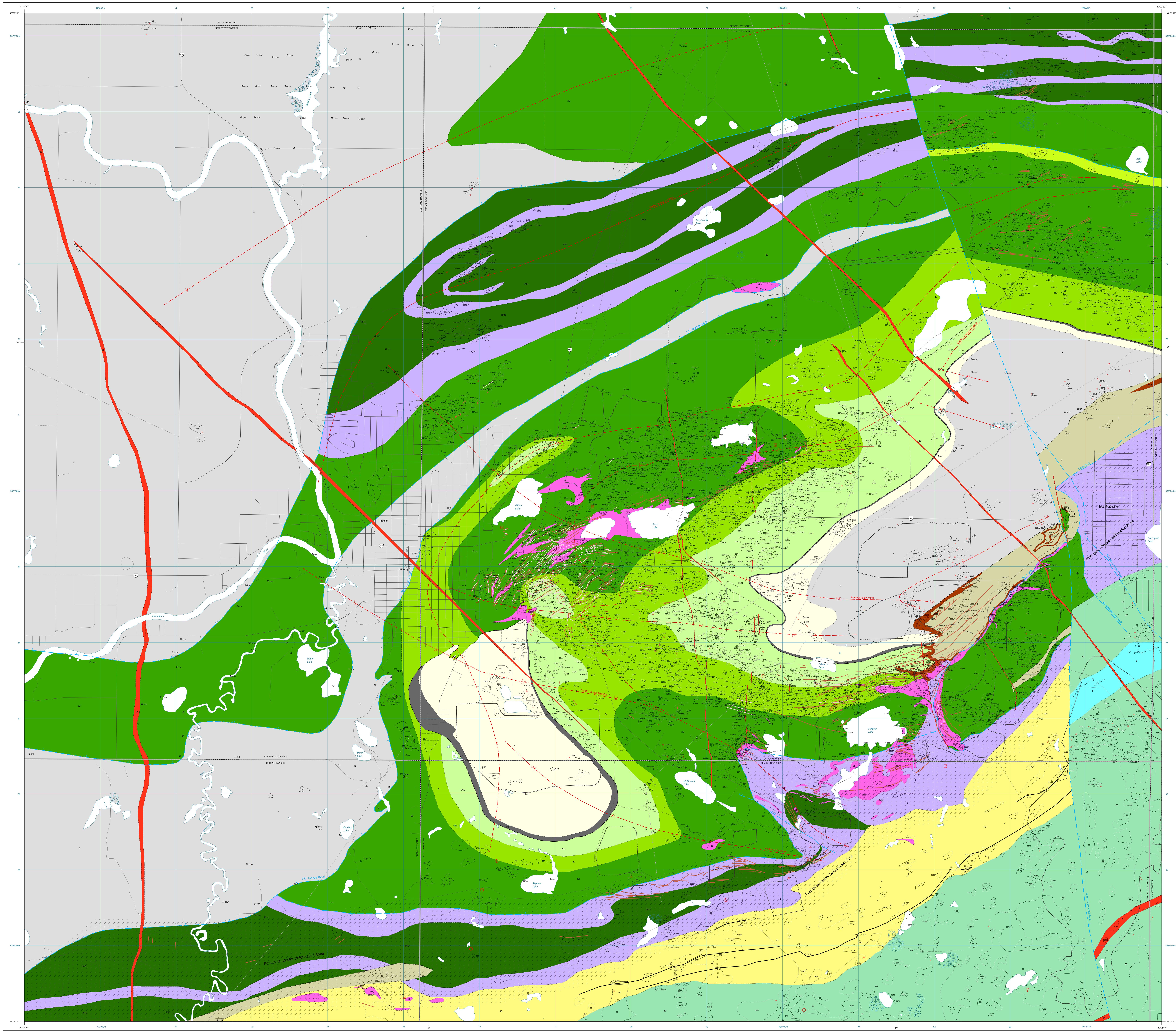

LEGEND[abc]

PHANEROZOIC
CENOZOIC
QUATERNARY
PLEISTOCENE AND RECENT
UNCONFORMITY

PRECAMBRIAN
PROTEROZOIC

- 15 **Diabase Dikes**

INTRUSIVE CONTACT

ARCHEAN

REGIONAL METAMORPHISM

- 11 **Quartz-Feldspar Porphyry Intrusive Rocks**
  - Porphyry dike
- 9 **Ultramafic Intrusive Rocks**

Timiskaming Assemblage

- 8 **Clastic Sedimentary Rocks**
  - CG Conglomerate

UNCONFORMITY

Porcupine Assemblage

- 6 **Clastic Sedimentary Rocks**
- 4 **Felsic Volcanic Rocks (Krist Formation)**

DISCONFORMITY

Tisdale Assemblage

- 3 **Intermediate Volcanic Rocks**
- 2 **Mafic Volcanic Rocks**
  - 2GC Gold Centre formation basalt
  - 2V Vipond formation basalt
  - 2C Central formation basalt
  - 2MG Magnesian basalt
  - 2GP Interflow graphitic sediment in basalt
- 1 **Komatiitic Rocks (Hersey Lake Formation)**

UNCONFORMITY

Deloro Assemblage

- 7 **Chemical Sedimentary Rocks**
  - Iron formation
- 4D **Felsic Sedimentary Rocks**
- 2D **Basalt**

a The rock unit codes for this legend were designed for use with a database of geoscience information related to the Discover Abitibi Initiative. Not all codes used in the database are shown in this legend.
b Lithology codes associated with diamond drill holes were derived from the author's logging of these drill cores.
c The placement of some contacts was based on interpretation of drill hole, surface and underground level plans made available by Porcupine Joint Venture.

EXPLANATION OF ROCK CODES

This map uses codes that are to be read from left to right.

①③
2PIamMA
②④

① The lithology code (2) identifies the main lithologic unit within a polygon or outcrop. Lithology codes correspond to units listed in LEGEND, above. The letters "C", "G" or "D" preceding a lithology code refer to, respectively, information compiled from previously published sources, information interpreted from geophysical data, and information derived from drill-hole logs.

② The primary rock type code (PI) identifies subdivisions of the main lithologic unit. Explanations of rock type codes are listed below under "Rock Type".

③ The texture code (am) supplies additional information about the texture of the rock. Explanations of texture codes are listed below under "Textural Description".

④ The secondary rock type code (MA), where present, identifies a second, less abundant lithologic unit and rock type within the polygon or outcrop. These codes are the same as those listed under LEGEND, "Rock Type" and, where applicable, "Textural Description".

Using the legend and the explanations listed below, therefore, 2PIamMA indicates a polygon or outcrop of mafic metavolcanic rock composed primarily of amygdaloidal pillowed flows, with subordinate massive flows.

2PIamMA

Rock Type

AG Argillite
BK Basaltic Komatiite
BX Breccia
CC Carbonate
CF Carbonate-Fuchsite Schist
CG Conglomerate
CH Chert
CS Chlorite Schist
DS Dike or Sill
FL Flow
FP Feldspar Porphyry
FX Flow Breccia
GW Greywacke
HY Hyaloclastite
IF Iron Formation
KO Komatiite
LT Lapilli Tuff
MA Massive
PI Pillows
PT Crystal Tuff
PX Pillow Breccia
RH Rhyolite
SP Spinifex
SS Sandstone
ST Siltstone
TC Talc-Chlorite Schist
TF Tuff
TS Talc Schist
TX Tuff Breccia
YX Pyroclastic Breccia
ZP Quartz-Feldspar Porphyry

Textural Description

am amygdaloidal
bd bedded
bx brecciated
cb cross bedded
cl clast supported
cu cumulate
ec elongated clasts
ep elongated pillows
fc flattened clasts
fp flattened pillows
fx fractured
lm laminated
mm monomictic
mx matrix supported
ng normal grading
pm polymictic
po porphyritic
ps polysutured
sc schistose
sh sheared
sx spinifex
va variolitic
ve vesicular

MINE LOCATIONS

Map No.	Name	Status	Commodity
1.	Ankerite (March) Mine	past producer	Au
2.	Aunor (Pamour #3) Mine	past producer	Au
3.	Buffalo Ankerite Mine	past producer	Au
4.	Coniaurum Mine	past producer	Au
5.	Crown Mine	past producer	Au
6.	Davidson–Tisdale Mine	past producer	Au
7.	Delnite Mine	past producer	Au
8.	Dome Mine, Porcupine Joint Venture	producing mine	Au
9.	Fuller Mine	past producer	Au
10.	Gillies Mine	past producer	Au
11.	Hollinger Mine	past producer	Au
12.	McIntyre Mine	past producer	Au, Cu, W
13.	Moneta Mine	past producer	Au,
14.	Naybob Mine	past producer	Au
15.	Paymaster Mine	past producer	Au
16.	Preston (New York) Mine	past producer	Au
17.	Preston Mine	past producer	Au
18.	Schumacher Mine	past producer	Au
19.	Tisdale–Ankerite Mine	past producer	Au
20.	Vipond Mine	past producer	Au

MINERAL OCCURRENCES

1. Allerston/Langmuir
2. Broulan Reef
3. Clucas Booker
4. Hydro claim
5. Placer 82-3
6. Placer 82-4
7. Placer 82-1
8. Powell

Ontario

Ontario Geological Survey

MAP P.3555

PRECAMBRIAN GEOLOGY

TISDALE TOWNSHIP AND PARTS OF DELORO, MOUNTJOY AND OGDEN TOWNSHIPS

Scale 1:10 000

250 m 0 250 500 m

NTS Reference: 42 A/6, 11

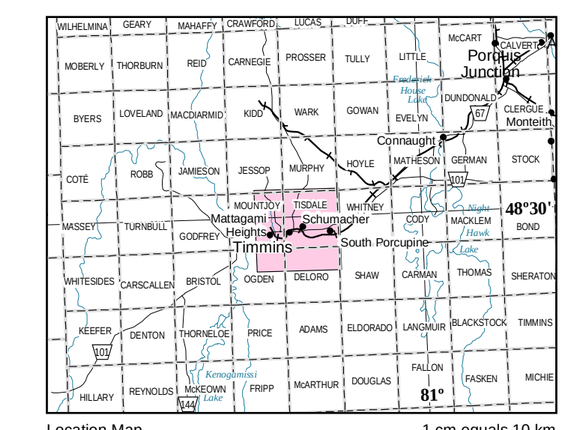

Location Map 1 cm equals 10 km

This geologic map represents one of the products of the Greenstone Architecture Project of the Discover Abitibi Initiative, which was designed to stimulate mineral exploration in the Ontario portion of the Abitibi greenstone belt and has components that range from geophysical surveying to deposit-scale mapping (*see* Ayer et al. 2003). This map presents results from the second year of the Gold Subproject 1 study, as summarized in Bateman et al. 2004.

Cette carte géologique représente un des produits découlant du projet relatif à la ceinture de roches vertes architecturale, lequel s'inscrit dans le cadre de l'initiative *Découvrons l'Abitibi*, conçue pour stimuler l'exploration minérale dans la section ontarienne de la ceinture de roches vertes de l'Abitibi et constituée de diverses composantes, depuis les levés géophysiques jusqu'aux cartes à l'échelle du gisement (voir Ayer et al. 2003). Cette carte présente les résultats de la deuxième année de l'étude portant sur le sous-projet 1 relatif à l'or, résumée dans Bateman et al. 2004.

Ayer, J.A., Thurston, P.C., Dubé, B., Fowler, A.D., Gibson, H.L., Hudak, G., Lafrance, B., Lesher, C.M., Piercey, S.J., Reed, L.E. and Thompson, P.H. 2003. Overview of the Discover Abitibi Greenstone Architecture project: subprojects, goals and results; *in* Summary of Field Work and Other Activities 2003, Ontario Geological Survey, Open File Report 6120, p.32-1 to 32-12.

Bateman, R., Ayer, J.A., Barr, E., Dubé, B. and Hamilton, M.A. 2004. Discover Abitibi. Gold Subproject 1. Protracted structural evolution of the Timmins–Porcupine gold camp and the Porcupine–Destor deformation zone; *in* Summary of Field Work and Other Activities 2004, Ontario Geological Survey, Open File Report 6145, p.41-1 to 41-10.

SYMBOLS

- Geologic contact (interpreted, observed)
- Area of bedrock outcrop (mapped by author, compiled)
- Small bedrock outcrop
- Constrictional lineation
- Foliation; fourth generation (inclined, magnitude of dip uncertain)
- Normal fault; third generation
- Foliation; third generation (inclined, magnitude of dip uncertain)
- Fold axis; third generation (anticline)
- Fold axis; third generation (syncline)
- Timiskaming basal unconformity
- Thrust fault; second generation
- Foliation; second generation (inclined, magnitude of dip uncertain)
- Fold axis; second generation (anticline)
- Fold axis; second generation (syncline)
- Intersection lineation; intersection of S_2 and S_3 fabrics
- Krist basal disconformity
- Extensional fault; first generation
- Dip-slip fault; unknown generation
- Strike-slip fault; unknown generation
- Porcupine–Destor deformation zone
- Tisdale basal unconformity
- Cross-bedding; facing known, dip not measured (overturned)
- Graded bedding; facing known (dip not measured, overturned)
- Bedding; facing known from other than grading or cross-bedding (inclined, dip not measured)
- Pillows; dip direction unknown (facing known, facing unknown)
- Bedding; facing unknown (inclined)
- Graded bedding; compiled, facing known (inclined, overturned, dip not measured)
- Bedding; compiled, facing known from other than grading or cross-bedding (inclined, overturned, dip not measured)
- Pillows; compiled[a], facing known, dip measured (inclined, overturned)
- Pillows; compiled[a], facing unknown (inclined)
- Bedding; compiled, facing unknown (inclined)
- Open pit
- Tailings and waste dump
- Sand and gravel pit
- Diamond drill-hole collar
- Quartz vein
- Mine location (keyed to list below)
- Mineral occurrence (keyed to list below)
- Township boundary
- Roads (primary, secondary, tertiary)

a Dip angles for pillowed flows in compiled data were measured by original author, but are not reproduced here.

SOURCES OF INFORMATION

Base map information derived from the Ontario Land Information Warehouse, Land Information Ontario, Ontario Ministry of Natural Resources, scale 1:20 000. Universal Transverse Mercator (UTM) co-ordinates are in North American Datum 1983 (NAD 83), Zone 17.

Mineral deposit information derived from the Mineral Deposit Inventory (MDI2), maintained by the Ontario Geological Survey, Resident Geologist Program.

Carlson, H.D. 1966. Geology of Ogden, Deloro and Shaw townships, District of Cochrane; Ontario Department of Mines, Open File Report 5012, 124p.

Ferguson, S.A. 1968. Geology and ore deposits of Tisdale Township, District of Cochrane; Ontario Department of Mines, Geological Report 58, 177p. Accompanied by Map 2075, scale 1:12 000.

Hall, L.A.F., MacDonald, C.A. and Dinel, E.R. 2003. Precambrian geology, Deloro Township; Ontario Geological Survey, Preliminary Map P.3528, scale 1:20 000.

Piroshco, D.W. and Kettles, K. 1991. Structural geology, Tisdale Township; Ontario Geological Survey, Preliminary Map P.3173, scale 1:10 000.

Discover Abitibi 2003. Timmins GEOTEM electromagnetic survey (Abitibi Supergrid), line spacing 200 m, sensor altitude 120 m, Tisdale Township. Unpublished data.

Magnetic declination approximately 10°58′W at the centre of the map area in 2004.

CREDITS

Geology and digital map preparation by R. Bateman, 2004.

Cartographic production by S. MacLean.

Geologic mapping and research supported by the Discover Abitibi Initiative under contract awarded to the Mineral Exploration Research Centre (MERC), Laurentian University, Sudbury, Ontario.

Contract management, project management by Robert Calhoun, Project Manager, Discover Abitibi Initiative.

Overall project management by Timmins Economic Development Corporation.

Porcupine Joint Venture made available their geological, geophysical, geochemical and drill-hole databases.

Laurie Reed (consulting geophysicist) integrated data and generated custom plots of total magnetic field and first vertical derivatives of total magnetic field for Discover Abitibi.

FedNor Canada

Ontario Northern Ontario Heritage Fund / Fonds du patrimoine du Nord de l'Ontario

Discover Abitibi — A project of innovation, cooperation and revitalization
Découvrons l' Abitibi — Un projet d' innovation, de coopération et de renouvellement

Discover Abitibi Initiative
The Discover Abitibi Initiative is a regional, cluster economic development project based on geoscientific investigations of the western Abitibi greenstone belt. The initiative, centred on the Kirkland Lake and Timmins mining camps, will complete 19 projects developed and directed by the local stakeholders. FedNor, Northern Ontario Heritage Fund Corporation, municipalities and private sector investors have provided the funding for the initiative.

Initiative Découvrons l'Abitibi
L'initiative *Découvrons l'Abitibi* est un projet de développement économique régional dans une grappe d'industries, projet fondé sur des études géoscientifiques de la ceinture de roches vertes de l'Abitibi occidental. Cette initiative, centrée sur les zones minières de Kirkland Lake et de Timmins, mènera à bien 19 projets élaborés et dirigés par des intervenants locaux. FedNor, la Société de gestion du Fonds du patrimoine du Nord de l'Ontario, municipalités et des investisseurs du secteur privé ont fourni les fonds de cette initiative.

Timmins

KIRKLAND LAKE
THE RIGHT ENVIRONMENT

Issued 2005.

Information from this publication may be quoted if credit is given. It is recommended that reference to this map be made in the following form:

Bateman, R. 2005. Precambrian geology of Tisdale Township and parts of Deloro, Mountjoy and Ogden townships; Ontario Geological Survey, Preliminary Map P.3555, scale 1:10 000.